

**Cardiomyocyte specific deletion of stromal cell derived  
factor-1 (SDF-1/CXCL12) protects the heart from  
hypertrophic and ischemic damage**

**Dissertation**

zur Erlangung des akademischen Grades

**doctor rerum naturalium (Dr. rer. nat.)**

Eingereicht im Fachbereich Biologie, Chemie, Pharmazie  
der Freien Universität Berlin

Vorgelegt von

**Santhosh Kumar Ghadge**

Geboren am 03.06.1980 in Narasannapeta (Indien)

Berlin, December 2010

Die vorliegende Arbeit wurde in der Abteilung für klinische kardiovaskuläre  
Forschung und in der Abteilung für Molekularbiologie von Hormonen im Herz-  
Kreislaufsystem des Max-Delbrück-Centrums für Molekulare Medizin in Berlin-Buch  
angefertigt

1. Gutachter: Prof. Dr. Udo Heinemann
2. Gutachter: Prof. Dr. Michael Bader

Disputation am 07.03.2011

---

1. Introduction.....	4
1.1. Congestive Heart Failure.....	4
1.1.1. Pathophysiology .....	4
1.1.2. Cardiac Remodeling and Compensatory Mechanisms.....	5
1.1.2.1. Frank- Starling Mechanism .....	6
1.1.2.2. Cardiac Hypertrophy .....	6
1.1.2.3. ECM Remodeling.....	7
1.1.2.4. Cell Death (Apoptosis).....	7
1.1.2.5. Neurohormonal System .....	8
1.2. Stem Cell Therapy in Heart Failure .....	8
1.2.1. Embryonic Stem Cells .....	9
1.2.2. Adults Stem Cells .....	9
1.3. Stem Cell Mechanisms and Paracrine Effects.....	11
1.4. Stem Cell Homing Factors and Mechanisms.....	13
1.5. SDF-1 and CXCR4 Axis in Stem Cell Homing & Mobilization .....	16
1.6. Biology of SDF-1.....	19
1.6.1. Chemokines.....	19
1.6.2. Molecular Structure of SDF-1 .....	21
1.6.3. CXCR4, a Receptor for SDF-1 .....	22
1.6.4. SDF-1/CXCR4 Axis and Cell Signaling .....	23
1.7. SDF-1 and Myocardial Infarctions .....	24
1.7.1. SDF-1/CXCR4 Axis and Therapeutic Applications in Myocardial Infarctions .....	25
1.7.2. Negative Implications of SDF-1 Therapy in MI .....	30
2. Objective of the Study .....	32
3. Materials and Methods.....	33
3.1. Materials .....	33
3.1.1. Chemicals and Reagents.....	33
3.1.2. Enzymes, Kits and Markers .....	34
3.1.3. Antibodies .....	35
3.1.4. Cloning Vectors (Plasmids and BAC) .....	36
3.1.5. Primers .....	36
3.1.6. Cell Lines .....	36
3.1.7. Bacterial Strains.....	37
3.1.8. Mouse and Rat Strains .....	37
3.1.9. Lab Equipment and Materials .....	37
3.2. Methods.....	39
3.2.1. Nucleic Acids .....	39
3.2.1.1. Isolation of Plasmid and BAC DNA – Rapid Alkaline Lysis Method.....	39
3.2.1.2. Maxi Preparation.....	39
3.2.1.3. Isolation of Genomic DNA From Tail Biopsies For PCR.....	40
3.2.1.4. Isolation of Genomic DNA From Tail and Tissues For Southern Blot.....	40
3.2.1.5. Isolation of Total RNA From Mouse Tissues .....	41
3.2.1.6. Measurement of the Nucleic Acid Concentration.....	41
3.2.1.7. Separation of DNA on Agarose Gel Electrophoresis .....	42
3.2.1.8. DNA Extraction From Agarose Gel .....	42
3.2.1.9. Restriction Digestion of DNA .....	42
3.2.1.10. Ligation of DNA Fragments.....	43
3.2.1.11. DNA Sequencing .....	43
3.2.1.12. Reverse Transcription (RT).....	43
3.2.1.13. Polymerase Chain Reaction (PCR) for Cloning and Genotyping.....	44
3.2.1.14. Southern Blot .....	47
3.2.1.14.1. Gel Electrophoresis and Blotting.....	47

Table of contents

3.2.1.14.2.	Probe Labeling .....	47
3.2.1.14.3.	Hybridization .....	48
3.2.1.15.	Real-Time-PCR Quantification (TaqMan®-PCR).....	49
3.2.2.	Western Blot .....	50
3.2.2.1.	Protein Isolation from Tissues.....	50
3.2.2.2.	Measurement of Protein Concentration .....	51
3.2.2.3.	SDS-Polyacrylamide Gel Electrophoresis (SDS-PAGE).....	51
3.2.2.4.	Blotting of Proteins.....	52
3.2.3.	Bacterial Cell Culture .....	52
3.2.3.1.	Preparation of Electro Competent Cells.....	52
3.2.3.2.	DNA Transformation in Competent Bacterial Cells.....	53
3.2.3.3.	Homologous Recombination in Bacteria (Gap Repair) .....	54
3.2.4.	Cell Culture .....	55
3.2.4.1.	Preparation of Feeder Cells .....	55
3.2.4.2.	ES Cell Culture and Electroporation .....	55
3.2.5.	Animal Experiments & Breeding .....	57
3.2.5.1.	Animals .....	57
3.2.5.2.	Generation of SDF-1 Transgenic Rat .....	57
3.2.5.3.	Generation of SDF-1 Chimeras .....	58
3.2.5.4.	Echocardiography .....	58
3.2.5.5.	Angiotensin-II Infusion in Mice .....	59
3.2.5.6.	Cold Organ Preparation and Collection .....	60
3.2.5.7.	Electrocardiogram.....	60
3.2.5.8.	Permanent LCA Ligation.....	60
3.2.5.9.	Cardiac MRI.....	61
3.2.5.10.	Histological Methods.....	61
3.2.5.10.1.	Tissue Fixation, Embedding and Sectioning .....	61
3.2.5.10.2.	Hematoxylin and Eosin (H&E) Staining.....	62
3.2.5.10.3.	Masson-Goldner Trichrome Staining .....	62
3.2.5.10.4.	Sirius Red Staining.....	62
3.2.5.10.5.	Cryosections .....	62
3.2.5.10.6.	Immunofluorescence Staining on Cryosections .....	63
4.	Results .....	64
4.1.	Generation of the SDF-1 $\alpha$ Transgenic Rat .....	64
4.1.1.	Cloning of DNA Construct for the Overexpression of SDF-1 $\alpha$ in Rat Heart....	64
4.2.	Expression Analysis of SDF-1 $\alpha$ in the Transgenic Rat Heart .....	65
4.3.	Generation of the Conditional SDF-1 Knockout (KO) Vector.....	65
4.3.1.	Construction of the Cre-LoxP Vector .....	65
4.4.	Gene Targeting in ES Cells .....	67
4.5.	Generation of the Complete SDF-1 KO Mice .....	68
4.6.	Generation of the Cardiomyocyte Specific SDF-1 KO (cKO) Mice.....	69
4.7.	Expression Analysis of Cardiac SDF-1 Levels in cKO Mice .....	71
4.8.	Characterization of Basal Cardiovascular Physiology of the SDF-1 cKO Mice .....	71
4.8.1.	Echocardiography Characterization of Cardiac Function.....	72
4.8.2.	Cardiac Morphology and Histology of SDF-1 cKO Mice .....	73
4.9.	Cardiac Function and Morphology of SDF-1 cKO Mice in Ang-II Induced Cardiac Hypertrophy.....	75
4.9.1.	Echocardiography Characterization of Cardiac Function in Cardiac Hypertrophy .....	75
4.9.2.	Cardiac Morphology and Histology in Cardiac Hypertrophy .....	76
4.9.3.	Histological Analysis of Cardiac Fibrosis in Cardiac Hypertrophy .....	77
4.9.4.	Gene Expression Analysis in Cardiac Hypertrophy .....	78
4.9.4.1.	SDF-1 Expression in Cardiac Hypertrophy .....	78
4.9.4.2.	Expression of ANP and BNP as Markers of Cardiac Hypertrophy.....	79
4.9.4.3.	Expression of Fibrosis Markers in Cardiac Hypertrophy .....	80



## Table of contents

---

4.10.	Characterization of Cardiac Function and Morphology of SDF-1 cKO Mice in Myocardial Infarction (MI).....	81
4.10.1.	Echocardiography Characterization of Cardiac Function in MI.....	82
4.10.2.	Cardiac MRI Characterization of Cardiac Function in MI.....	83
4.10.3.	Histological Analysis in MI .....	85
4.10.4.	Gene Expression Analysis in MI .....	86
4.10.5.	Analysis of Inflammatory Cell Infiltration in MI .....	88
5.	Discussion.....	89
5.1.	Role of SDF-1 in Embryonic Development.....	89
5.2.	Cardiac SDF-1 in Cardiac Function.....	90
5.3.	SDF-1 and its Pathological Role in Cardiac Hypertrophy.....	91
5.4.	SDF-1 and its Pathological Role in Myocardial Infarction.....	93
6.	Summary/ Zusammenfassung.....	97
6.1.	Summary .....	97
6.2.	Zusammenfassung.....	98
7.	References.....	100
8.	Appendix .....	111
8.1.	Abbreviations.....	111
9.	Curriculum Vitae.....	114
10.	Acknowledgements .....	116
11.	Eidesstattliche Erklärung.....	118

## 1. Introduction

### 1.1. Congestive Heart Failure

Heart Failure (HF) is a very common and complex clinical disorder in which hearts are unable to pump sufficient amount of blood to meet body's need due to abnormal cardiac structure and function. The typical symptoms of heart failure patients are shortness of breath, fatigue, chest pain, pulmonary congestion, and edema. HF is an age related problem with a prevalence of 2% in adult population and with an increasing rate of 6-10% and 10-20% over the age of 65 to 75 years. It is a global and a major concern of industrialized countries. In USA 5 million patients from all ages are suffering from heart failure, and over 550,000 new cases are diagnosed every year. The estimated costs for HF patients in 2005 were approximately 29.8 billion dollars. The annual costs of 2.9 billion dollars on drugs for treatment, accounted as 1-2% a major expenditure of national medical costs. Similarly in European countries there are 15 million patients with a prevalence of 2-3% increasing sharply over the age of 75 years. Despite the recent advances in medical treatment and better prognosis, morbidity and mortality rates remain still high. It becomes life threatening since 60-70% patients die within 5 years and also future generations are in risk of developing heart failure one in five over the age 40 ([McMurray et al. 2005](#); [Dickstein et al. 2008](#); [Hunt et al. 2009](#)).

#### 1.1.1. Pathophysiology

The syndrome of heart failure is majorly resulting from coronary artery disease, cardiomyopathies, and abnormalities of the pericardium and cardiac valves leading to left ventricular (LV) myocardial damage, systolic and diastolic dysfunction. Coronary artery diseases and dilated cardiomyopathies are the far most common cause for HF comprising of 60-70%. Hypertension, valvular diseases, obesity, diabetes, and others account for 30-40% ([Cowie et al. 1999](#); [Fox et al. 2001](#); [Baldasseroni et al. 2002](#)).

The left ventricular systolic dysfunction and chronic heart failure is a progressive disorder with complex cellular mechanisms (Fig.1). The left ventricular dysfunction is initiated with an insult or cardiac stress that undergoes modifications in cellular

metabolism and left ventricular structure leading to cardiac hypertrophy, fibrosis, and enlarged chambers. The altered left ventricular geometry with increased hemodynamic overload is part of the cardiac remodeling process. Although, cardiac remodeling is an adaptive response to compensate the cardiac dysfunction, in long term, cardiac remodeling results in cardiomyocyte death and maladaptive changes of surviving myocytes and extracellular matrix. Thus, prolonged remodeling has adverse effects on cardiac function and eventually leads to progression of cardiac decompensation and heart failure (Delgado et al. 1999).

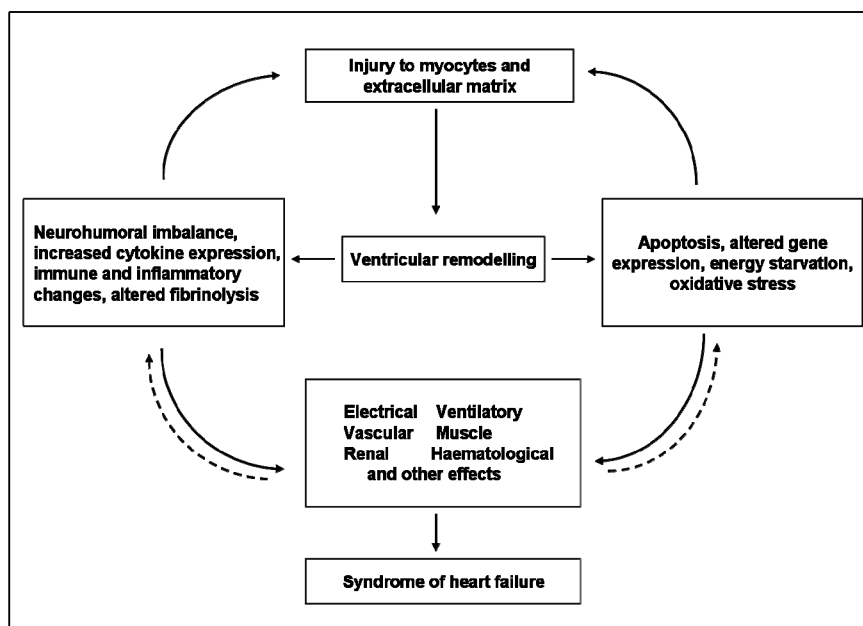


**Fig.1: Pathophysiology of heart failure due to left-ventricular systolic dysfunction.**  
(McMurray et al. 2005)

### 1.1.2. Cardiac Remodeling and Compensatory Mechanisms

Cardiac remodeling begins with progression of cardiovascular disease such as myocardial infarction, hypertension, valvular heart diseases and dilated cardiomyopathy. Regardless of the pathological cause, the progression of cardiac remodeling in heart failure is regulated by various compensatory mechanisms which exist at different cellular levels such as the Frank-Starling mechanism, myocardial hypertrophy, extracellular matrix remodeling (ECM), cell death (apoptosis) and the neurohormonal system.

### **1.1.2.1. Frank- Starling Mechanism**

The Frank Starling mechanism is a primary compensation to regulate the impaired cardiac output which is directly reflected by stroke volume and enddiastolic volumes of left ventricle. In chronic heart failure an increased afterload induces stress in the left ventricular and reduces cardiomyocyte shortening, contractility and its inability to expel sufficient amount of blood from the left ventricle. This leads to a reduction of stroke volume and the elevation of enddiastolic volumes (preload). To partially compensate, the Frank Starling mechanism is activated by chronically extended sarcomeric length and increases cardiac contractility and thereby stroke volume. The sustained abnormal stroke volume has adverse effects on cardiac structure and function, which leads to development of heart failure and decompensation ([Brilla et al. 1994](#); [Shiels et al. 2008](#)).

### **1.1.2.2. Cardiac Hypertrophy**

Cardiac hypertrophy is an adaptive cellular response to increased mechanical stress and volume overload of the left ventricle. Cardiac hypertrophy is defined by an increase in cell mass and thickness of the myocardium without change in cardiomyocyte turnover. It is accompanied by activation of immediate early genes and re-expression of fetal genes like myosin heavy chains, the natriuretic peptides (ANP; BNP) and  $\alpha$ -actinin. This leads to the growth of cardiomyocytes and alteration of sarcomeric organization to compensate for contractile properties ([Barry et al. 2008](#)). Cardiac hypertrophy can be either physiological (adaptive) or pathological (maladaptive) and regulated by different molecular mechanisms. The physiological hypertrophy is reversible and not detrimental. Under pathological conditions of pressure overload induced concentric hypertrophy, left ventricular wall thickness is increased to adjust to the wall stress and to maintain normal chamber diameters. In volume overload induced eccentric hypertrophy, left ventricular wall thickness moderately increases with dilated chambers. The disease progression is characterized by left ventricular dilation, and afterload increase which results in the development of heart failure ([Zelis et al. 1991](#); [Frey et al. 2003](#); [Gupta et al. 2007](#)).

### **1.1.2.3. ECM Remodeling**

Extracellular matrix is mainly composed of a collagen network. This scaffold acts as structural support to cardiomyocytes for generating force and passive stiffness. In heart failure extensive myocardial loss and hypertrophy of viable cardiomyocytes are not sufficient to maintain contractile function. Myocardium becomes replaced by scar tissue from proliferated cardiac fibroblasts. The cardiac fibrosis begins with marked changes in gene expression of extracellular components such as collagen Type-I, collagen Type-III, and fibronectins in ECM. The cardiac fibroblasts proliferate into myofibroblasts under stimulation of various growth factors and cytokines, such as ANG II, TGF- $\beta$ 1, IGF-1, and TNF- $\alpha$ . This results in increased synthesis of collagen and secretion into the perivascular and interstitial spaces. Collagen content can be degraded by the activity of extracellular proteinases including matrix metalloproteinases (MMPs) and serine proteinases. Thus, an imbalance in the ratio of MMPs and tissue inhibitor of metalloproteinases (TIMPs) regulates ECM collagen remodeling (synthesis and degradation), which contributes to systolic dysfunction, LV dilation and finally to progression of heart failure ([Zamilpa et al. ; Boluyt et al. 2000;](#) [Berk et al. 2007](#)).

### **1.1.2.4. Cell Death (Apoptosis)**

Among the multiple etiological key factors, myocyte death by apoptosis and necrosis is involved in cardiac remodeling and progression of LV hypertrophy to heart failure. Studies in end stage heart failure patients and animal models with myocardial infarctions reported cardiomyocyte apoptotic rates of 2-12%. The apoptotic pathways are regulated by caspases, which are involved in proteolytic cleavage of cellular substrates leading to cell death. Apoptosis signaling pathways are regulated through intrinsic and extrinsic pathways under hypoxic and oxidative stress. Intrinsic apoptotic pathways are mitochondrial dependent through release of cytochrome-c and apaf1 complex and downstream activation of caspase-9 and caspase-3. This finally results in DNA fragmentation and cell death. These pathways are further regulated by anti-apoptotic bcl-2 and pro-apoptotic proteins Bax and caspase inhibitors. The extrinsic pathway is an alternative pathway regulated via death receptor activation such as

Fas receptor or Tumor necrosis factor receptor (TNFR) family and caspase-8 ([Kang et al. 2000](#); [van Empel et al. 2005](#)).

#### **1.1.2.5. Neurohormonal System**

The progression of LV heart failure is accompanied by activation of neurohormonal mechanisms to compensate the decrease in cardiac output and hemodynamic imbalance. Though initially it has a compensatory role to enhance cardiac contractility, continuous progression has adverse effects on cardiac remodeling and function. The neurohormonal system is mainly activated through molecular mechanisms such as the renin angiotensin-aldosterone system (RAAS) and the sympathetic nervous system. These pathways results in release of various hormones and neurotransmitters including renin, angiotensin-II, norepinephrine, aldosterone, natriuretic peptides, vasopressin, and endothelins into systemic circulation and tissues. This rise in vasoactive molecules leads to vasoconstriction, endothelial dysfunction, and fluid retention, and also has direct effects on cardiomyocyte hypertrophy, apoptosis and finally progression to chronic heart failure ([Pool 1998](#); [Jackson et al. 2000](#)).

#### **1.2. Stem Cell Therapy in Heart Failure**

The advancement in understanding the pathophysiological mechanisms of LV remodeling allowed designing therapeutic approaches including pharmacological medications and invasive surgical interventions. However, despite of significant improvement in prognosis of heart failure, the mortality rate remains still high. This is due to variability and limitations of conventional therapies in replacing the cardiomyocyte loss. Over the last decade, a new era of regenerative cell therapy arose as a promising tool for the treatment of ischemic cardiac diseases. The concept of stem cell therapy and its potential in myocardial regeneration has emerged in treating patients with cardiac failure ([Leri et al. 2005](#); [Anversa et al. 2006](#); [Dimmeler et al. 2008](#)). Several investigations challenge the old notion of adult heart as terminally differentiated organ and fractions of cardiomyocytes could enter post mitotic cell divisions following myocardial infarctions and in end stage heart failure patients ([Anversa et al. 1998](#); [Kajstura et al. 1998](#); [Beltrami et al. 2001](#)). Extensive studies characterized the various populations of exogenous and endogenous

progenitor or stem cells for applications in regenerative medicine (Fig.2). These studies evaluated the possibilities of using different types of stem cells such as embryonic stem cells (ESCs) and tissue specific or adult stem cells (ASCs) to regenerate and restore a functional myocardium in myocardial infarction.

### **1.2.1. Embryonic Stem Cells**

Embryonic stem cells are pluripotent stem cells isolated from inner cell mass of the blastocyst at 4-5 days post fertilization. ES cells are self renewing and proliferative indefinitely and have capability to differentiate into all three primary germ layers: ectoderm, endoderm, and mesoderm. They have great potential to develop in vitro into all cells types including cardiomyocytes (Maltsev et al. 1993) with cardiomyocyte structural, functional and electrophysiological properties (Kehat et al. 2001). Although ES cells are promising donor cells for cardiac regeneration and have significant importance in clinical application there are limitations and concerns over their safety. This is due to their tumorigenic potential, and other challenges, like immunorejection and ethical issues.

### **1.2.2. Adults Stem Cells**

Numerous studies over the last decade have shown adult stem cell plasticity and transdifferentiation to different cell lineages other than the source of origin (Horwitz 2003; Grove et al. 2004). Adult stem cells from various cell types have been widely used for clinical studies, such as bone marrow derived stem cells (BMSCs), circulating endothelial progenitor cells (EPC) and cardiac stem cells (CSCs) (Dimmeler et al. 2008). Bone marrow-derived stem cells (BMSCs) had remarkable success in animal and preliminary clinical studies with significantly improved cardiac function and regeneration (Orlic et al. 2001; Strauer et al. 2002; Fernandez-Aviles et al. 2004; Kajstura et al. 2005). Bone marrow (BM) contains heterogeneous populations of stem or progenitor cells apart from differentiated cells, including hematopoietic stem or progenitor cells (HSCs or HPCs) (Shizuru et al. 2005) mesenchymal stem cells (MSCs) (Pittenger et al. 2004) and multipotent adult progenitor cells (MAPCs) (Jiang et al. 2002). Several clinical studies have shown positive outcomes with the application of all different cell types of bone marrow in restoring the ischemic tissue and preserving the impaired cardiac function. Despite of

plasticity of bone marrow derived stem cells in cardiac repair, the controversy exists over stem cell transdifferentiation and acquiring cardiomyocyte cell lineage in recovering functional myocardium (Balsam et al. 2004; Murry et al. 2004).

Another source of progenitor cells isolated in peripheral blood (PB) are circulating progenitor cells or endothelial progenitor cells (EPCs), which have also shown therapeutic potential in neovascularization and proangiogenic effects after myocardial infarction. EPCs are characterized by expression of cell surface hematopoietic stem cell markers, CD34<sup>+</sup>, CD133<sup>+</sup> and endothelial markers, such as VEGFR-2. Several animal studies with peripheral blood isolation and ex-vivo cultivation of EPCs and infusion of the cells showed improved neovascularization with preserved cardiac function and attenuated cardiac remodeling (Kawamoto et al. 2001; Kocher et al. 2001). Though, there are questions and concern about identification of proper EPCs from a heterogeneous population of peripheral mononuclear blood cells and its reliability in in-vivo conditions.

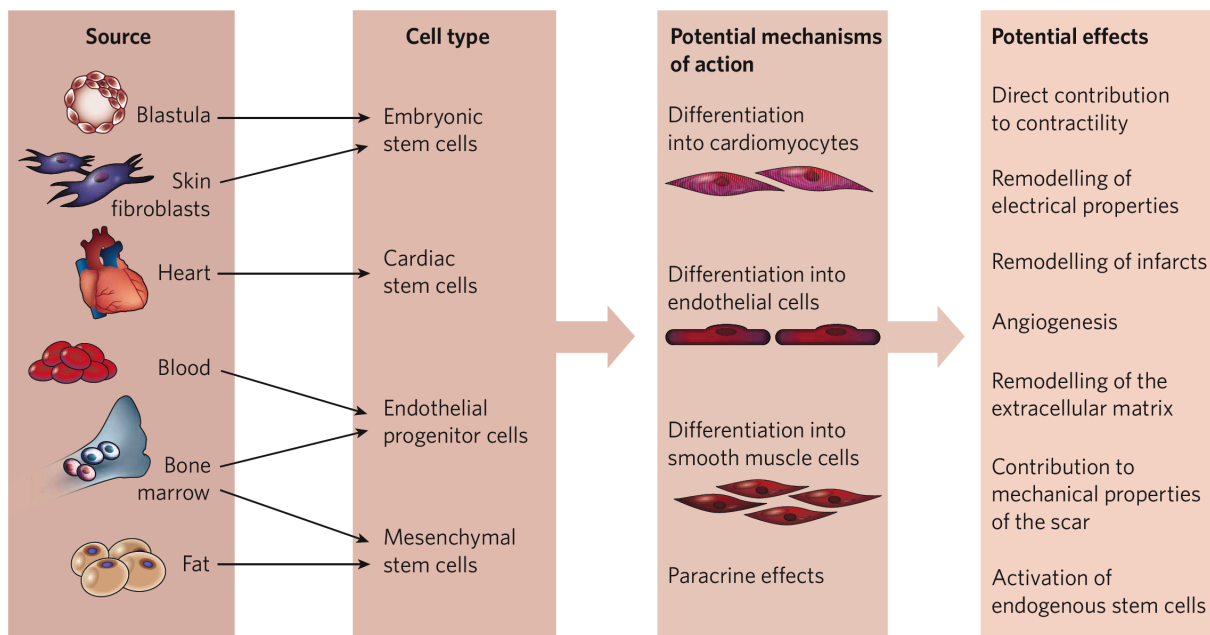


**Fig.2: Many cell types and mechanisms have been proposed for cardiac therapy.**

Stem cells and progenitor cells can be isolated from either autologous or allogeneic sources. Different types of stem cells and progenitor cells have been shown to improve cardiac function through various mechanisms, including the formation of new myocytes, endothelial cells and vascular smooth muscle cells, as well as through paracrine effects (Segers et al. 2008).



Recent studies also showed the existence of organ specific cardiac stem cells (CSCs) in the adult heart and their ability to reconstitute functional myocardium following myocardial infarction. Different populations of cardiac stem cells were identified and isolated from recipient hearts that express stem cell related antigens such as c-kit, Sca-1, MDR1, side population cells (SP) and isl1+ cardiac progenitor cells ([Hierlihy et al. 2002](#); [Beltrami et al. 2003](#); [Oh et al. 2003](#); [Laugwitz et al. 2005](#)). The cardiac stem cells have self renewing, clonogenic and multipotent nature, enabling differentiation to cardiomyocytes and vascular cells including endothelial, and smooth muscle cells. Although cardiac stem cells were isolated from local niches of heart, it is still unclear which cellular mechanisms maintain the CSC pool. There are studies showing the bone marrow origin for CSCs. Questions remain whether these cells are mobilized after injury or stably remain within the selective niches of heart ([Mouquet et al. 2005](#); [Fazel et al. 2006](#)).

Overall clinical applications of different types of adult stem cells have been characterized and showed improved cardiac function after myocardial infarction. But several fundamental questions remained to be addressed such as which cell type(s) are beneficial for cardiac regeneration therapy. What is the suitable time point, optimal dose and route of delivery. Furthermore, understanding the molecular mechanisms that regulates the cardiomyocyte turnover and effect of cytokines and growth factors in stem cell proliferation and mobilization to the sites of injury will be crucial for the development of optimal stem-cell based therapies for cardiac regeneration.

### **1.3. Stem Cell Mechanisms and Paracrine Effects**

Several studies showed that transplanted bone marrow derived stem cells and CSC are able to home to the ischemic heart and promote myocardial regeneration and neoangiogenesis. Though the mechanisms are not fully understood, different mechanisms were proposed including that adult stem cells could transdifferentiate to vascular and cardiac lineages (Fig.3). Mouse models of myocardial infarction following different cell transplantation studies showed that the cells engraft to the infarcted region of the heart, are stably integrated, differentiate into cardiomyocytes, and restore cardiac function ([Tomita et al. 1999](#); [Kawamoto et al. 2001](#); [Orlic et al. 2001](#); [Beltrami et al. 2003](#)). However, there are several studies with negative results which question the concept of cell transdifferentiation of both endogenous and bone

marrow derived stem cells. Later on, other studies proposed that cell-cell fusion could be another possible mechanism for incorporation of transplanted stem cells into recipient cardiomyocytes (Alvarez-Dolado et al. 2003; Nygren et al. 2004). But cell fusion is a rare event with low frequency and it was debated over the possibility of cell fusion in myocardial regeneration (Kajstura et al. 2005). Thus, transdifferentiation and cell fusion mechanisms are quite unlikely to explain the improved cardiac function through neovascularization and cardiac regeneration. There are studies showing that alternative paracrine and autocrine mechanisms (Fig.3) are involved after cells home to ischemic tissues or are injected into infarcted hearts. They secrete various signals such as cytokines, chemokines and angiogenic growth factors which stimulate the local microenvironment and enhance cardiomyocyte survival, neovascularization and cardiac regeneration (Kinnaid et al. 2004; Gneccchi et al. 2005).

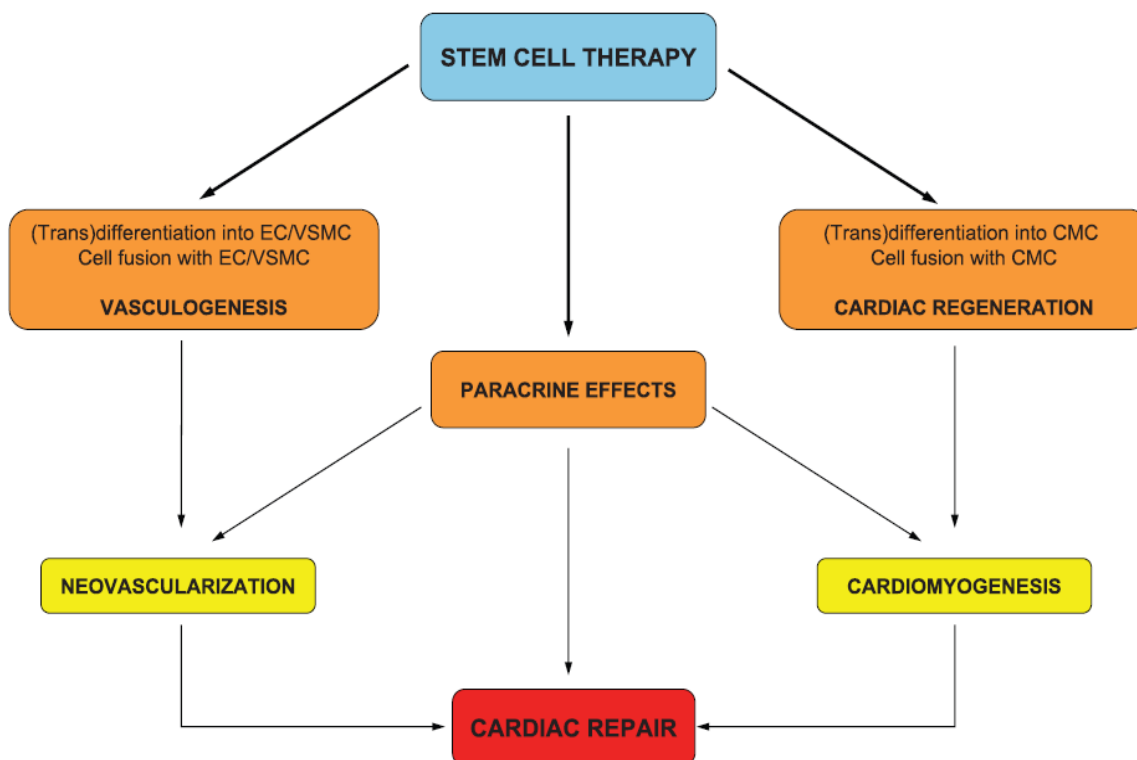


**Fig.3: Proposed mechanisms of adult stem cell action in cardiac repair.**

*Transdifferentiation and cell fusion of transplanted stem cells lead to cardiac regeneration and vasculogenesis. Paracrine effects can positively influence many processes, among them cardiomyogenesis and neovascularization. Cardiac regeneration, vasculogenesis, and paracrine effects lead to cardiac repair (Gneccchi et al. 2008).*

#### 1.4. Stem Cell Homing Factors and Mechanisms

Cell homing is considered to be one of the most important mechanisms and a prerequisite for cell survival, proliferation, mobilization and differentiation of hematopoietic (HPCs) or tissue specific progenitor cells in the bone marrow (Papayannopoulou 2004). The bone marrow "stem cell niche" is defined as a local microenvironment that contains different population of cells such as stromal cells, osteoblasts, endothelial cells and fibroblasts, which regulate the homing processes but also induce the mobilization of stem cells to the sites of injury or inflammation (Lapidot et al. 2005). The stem cell mobilization process is initiated by inflammation or injury in tissues which releases various signaling molecules. These molecules include cytokines – granulocyte colony stimulating factor (G-CSF), granulocyte macrophage colony stimulating factors (GM-CSF), stem cell factor (SCF), interleukins (IL-7,IL-12, IL-3) as well as chemokines like stromal cell derived factor-1 (SDF-1), IL-8, macrophage inflammatory protein-1 alpha (Mip-1 $\alpha$ ), growth related oncogene beta (GRO- $\beta$ ) and growth factors like vascular endothelial growth factor (VEGF), hepatocyte and insulin like growth factor (HGF, IGF). Its is also possible to induce stem cell mobilization through chemotherapeutic agents such as cyclophosphamide (Cy) and paclitaxel.

Stem cell mobilization is a coordinated, multistep process in which secreted chemokine and cytokine factors induce the proteolysis enzymes such as elastase, cathepsin G, proteinase 3, CD26, and various matrix metalloproteinases (MMPs 2/9) in bone marrow. These molecules degrade the extracellular matrix, cell adhesion molecules (VLA-4 and P/E selectins), cytokines and chemokines leading to the proliferation and mobilization of stem cells from bone marrow into the circulation via transendothelial migration (Fig.4) (Papayannopoulou 2000; Vaday et al. 2000; Cottler-Fox et al. 2003). Due to the expression of homing receptors and cell adhesion proteins like integrins on these mobilized cells, they are able to recruit to the site of injury and differentiate into appropriate lineages. The alternative hypothesis is that under steady state conditions a constant number of tissue specific circulating progenitor cells are maintained in the PB. They increase in number after stress or injury and are also released from bone marrow into the blood and recruited to various organs depending on an SDF-1 concentration gradient (Kucia, Ratajczak, et al. 2004). Despite of the clinical importance of stem cell mobilization the

environmental cues and secreted factors are still unclear as well as the mechanisms behind mobilization and homing of bone marrow stem cells to injured tissues. There are several ligand receptor interactions involved in bone marrow stem cell trafficking and homing pathways.

Stem cell factor (SCF) is a hematopoietic cytokine also known as c-kit receptor ligand or mast cell growth factor. It has diverse functions such as stem cell migration, early haematopoiesis and germ cell development. SCF is used as a potent agent particularly in combination with G-CSF for the mobilization of HPCs from bone marrow to peripheral blood ([Menendez et al. 2002](#)). In mice and primates treatment with an antibody against VLA-4/VCAM-1 signaling leads to down regulations c-kit expression in bone marrow cells strengthening the possibility of an integrin/cytokine cross talk for stem cell mobilization ([Papayannopoulou et al. 1993](#); [Papayannopoulou et al. 1998](#)). Another study with a genetic mouse model showed that the stem cell mobilization from bone marrow requires MMP-9 mediated release of c-kit ligand and chemokine factors SDF-1 $\alpha$ , VEGF and G-CSF, which regulate the MMP-9 expression in bone marrow ([Heissig et al. 2002](#)).

G-CSF is the most commonly used cytokine to mobilize cells from bone marrow after chemotherapy for harvesting by leukapheresis and has wider clinical application. The G-CSF is used alone or in combination with chemotherapy agents like cyclophosphamide (Cy) for 5-6 days to achieve adequate mobilization ([To et al. 1997](#)). It has been shown that G-CSF and Cy treatment induce hematopoietic stem or progenitor cell proliferation in the bone marrow before its mobilization into peripheral blood ([Morrison et al. 1997](#)). In addition to that, a combination of cytokine SCF with G-CSF treatment increases the mobilization of long term repopulating hematopoietic stem cells or progenitor cells in mice and larger mammals ([Verfaillie 2002](#)). However, stem cell mobilization by G-CSF seems rather complicated and their mechanisms are unclear. Earlier studies from Levesque *et al.* showed that bone marrow HPC mobilization by G-CSF and SCF or Cy is due to increased expression of neutrophil elastase and cathepsin G proteases ([Levesque et al. 2001](#); [Levesque et al. 2002](#); [Levesque et al. 2003](#)). Thereby disrupting vascular cell adhesion molecule-1 (VCAM-1) and other mobilizing factors c-kit, SDF-1/CXCR4 in bone marrow releases the progenitor cells. From these studies, proteolytic enzyme secretion was positively correlated with stem cell egress and the hematopoietic stem or progenitor cell mobilization process. A further surprising study with protease deficient genetic

mouse models showed that G-CSF treatment showed no significant difference in HPC mobilization but showed SDF-1 protein reduction in bone marrow, implying that SDF-1 mediated stem cell mobilization is a common process in several mouse models (Levesque et al. 2004).

The angiogenic factor VEGF has been shown to promote mobilization of HPCs, and EPCs facilitating postnatal angiogenesis and hematopoiesis (Asahara et al. 1997). Using adenoviral gene delivery, VEGF overexpression into plasma induces a very rapid mobilization of HPCs and EPCs, suggesting that VEGF induction promotes EPCs mobilization and neovascularization of ischemic tissues (Rafii et al. 2002). A recent study by Pitchford *et al.* treating mice with VEGF alone or in combination with G-CSF and CXCR4 inhibitor AMD3000 has shown enhanced stem cell proliferation and differential mobilization of HPCs to EPCs from bone marrow to blood (Pitchford et al. 2009).

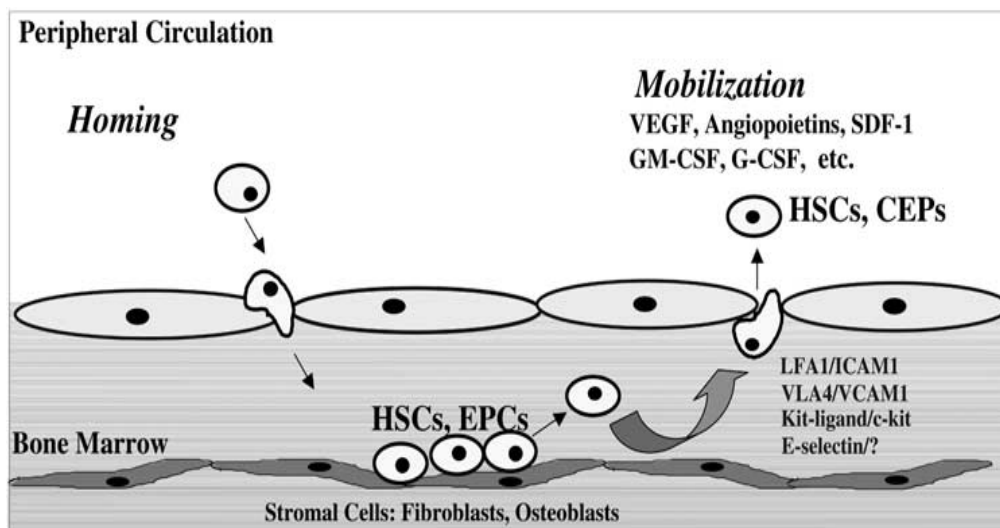


**Fig.4: Trafficking of stem cells is regulated through sequential interaction with chemokines and adhesion molecules.** Homing of stem cells to the BM is dependent on specific chemokines and adhesion molecules expressed within the BM microenvironment. Similarly, chemokine-induced mobilization of stem cells is mediated through interaction with E-selectin followed by firm adhesion mediated by VLA4 and LFA1 integrins. Chemokines orchestrate this process by increasing the motility of stem cells, releasing them from the harness of extracellular matrix and stromal cells, as well as providing directional cues for the stem cells to exit the BM (Rafii et al. 2002).

### 1.5. SDF-1 and CXCR4 Axis in Stem Cell Homing & Mobilization

Chemokine induced hematopoietic stem cell proliferation, mobilization and potential mechanisms have also been explored and a number of chemokines such as monocyte chemoattractant protein-1 (MCP-1), MIP-1 $\alpha$ , Gro $\beta$ , SDF-1, and others have been extensively studied ([Pelus et al. 2002](#)). Subsequently, numerous studies showed that SDF-1(CXCL12) is the most potent chemoattractant signal for mobilizing mature and immature HPCs from BM to PB as part of host defence and repair mechanisms. SDF-1 is expressed in many tissues including BM stromal and endothelial cells and thereby anchors stem cells to endosteal osteoblasts via binding to its receptor CXCR4. Cottler-Fox and Lapidot *et al.* reviewed the essential role of SDF-1/CXCR-4 axis in regulating stem cell homing, repopulation and mobilization under steady state homeostasis and in response to stress signals (Fig.5) ([Lapidot et al. 2002](#); [Cottler-Fox et al. 2003](#)).

Gene knock out studies with SDF-1/CXCR4 mouse models revealed that the lack of SDF-1 and its receptor CXCR-4 showed embryonic lethality with multiple developmental defects including impaired bone marrow myelopoiesis suggesting that SDF-CXCR4 axis has an important role in stem cell homing to bone marrow and haematopoiesis during embryonic development ([Nagasawa, Hirota, et al. 1996](#); [Ma et al. 1998](#); [Zou et al. 1998](#)). Preclinical studies in immunodeficient NOD/SCID mice and B2m null (beta 2 microglobulin) NOD/SCID mice that received serial transplants with enriched human CD34+, severe combined immunodeficient (SCID) repopulating cells (SRCs), and SCID leukemia initiating cells (SLICs) showed that homing to the BM is dependent on the interaction of cell surface human CXCR4 and murine BM stromal and endothelial SDF-1 ([Spiegel et al. 2004](#); [Tavor et al. 2004](#)). When CXCR4 deficient fetal liver cells were transplanted into wild type lethally irradiated mice, they homed and engrafted but displayed abnormal myeloid and lymphoid progenitor cell repopulation in BM. However, another study also showed an impaired reconstituting ability of serially transplanted CXCR4<sup>null</sup> cells derived from primary transplant recipients into secondary recipients, indicating the importance of SDF-1/CXCR4 axis for stem cell homing to BM ([Kawabata et al. 1999](#); [Ma et al. 1999](#)). In line with this, the transplantation of BM-derived hematopoietic progenitor cells (HPCs) expressing a genetically modified SDF-1-intrakine (an engineered form of SDF-1 $\alpha$  inhibitor) by



using a retroviral expression vector could suppress the CXCR4 activity *in vivo* and lead to defective lymphopoiesis and myelopoiesis (Onai et al. 2000).

Nevertheless, many reports proposed that SDF-1 is the most potent chemoattractive signal and that the disruption of the BM SDF-1/CXCR4 signaling is the central molecular mechanism for mobilizing immature and mature stem and progenitor cells into peripheral blood in response to stress signals as part of the host defence and repair mechanisms. Disrupting the bone marrow SDF-1/CXCR4 signaling by using methionine-SDF-1 $\beta$  analog leads to prolonged desensitization and downregulation of CXCR4 activity. Similarly, the treatment with pertussis toxins which suppress the G protein coupled receptor CXCR-4 function on HPCs in BM, eventually results in translocation of stem cells from BM to PB (Shen et al. 2001; Papayannopoulou et al. 2003). In addition to that, the serial administration of the selective CXCR4 antagonist AMD3100 in healthy human volunteers was able to cause rapid mobilization of HPCs into the peripheral blood further indicating that the inhibition of BM SDF-1/CXCR4 signaling leads to significant mobilization (Liles et al. 2003).

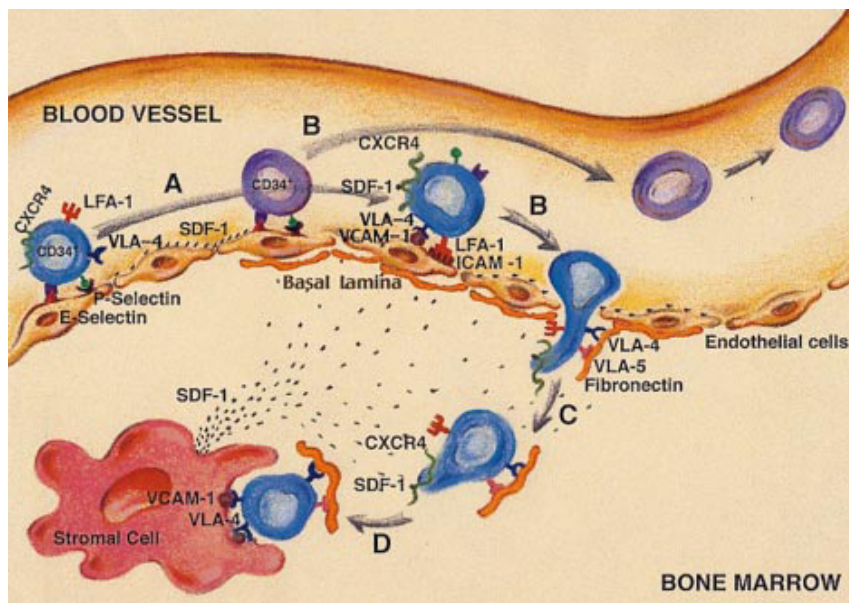


**Fig.5: SDF-1/CXCR4 interactions and other regulators of stem cell homing** (a) Stem cell rolling interactions on constitutively expressed endothelial E and P selectins. Following rolling, CXCR4<sup>+</sup> stem cells (blue cells) are activated by SDF-1, which is secreted from bone marrow endothelial cells and triggers LFA-1/ICAM-1 and VLA-4/VCAM-1 interactions, supporting firm adhesion to endothelial cells. (b) Cells that do not express sufficient levels of CXCR4 (purple) will detach from the endothelial layer and return to the blood stream. (c) The arrested human CXCR4<sup>+</sup> stem cells, in response to SDF-1, will extravasate and migrate through the underlying basal lamina ECM using VLA-4 and VLA-5 integrin receptors to FN. (d) Migrating stem cells will eventually reach the "stem cell niches," which consist of stromal cells that present the proper set of adhesion molecules (e.g. VCAM-1 and FN), SDF-1, and growth stimulatory factors (Peled et al. 2000).

In support to this view, mice and primates treated with sulfated polysaccharides reported a rapid increase of SDF-1 levels in plasma and decreased levels in BM (Sweeney et al. 2002). On the other hand, data from Hattori *et al.* demonstrated that the modulation of SDF-1 expression through overexpression of the chemokine (AdSDF-1) in the plasma leads to induced mobilization of hematopoietic stem and progenitor cells (HSCs and HPCs) into peripheral circulation (Hattori et al. 2001). This also suggests that changes in SDF-1 gradients influence the number of circulating stem and progenitor cells (Sweeney et al. 2002). Another surprising study reported that HSCs selectively mobilize in response to SDF-1 but not to other chemokine signaling implicating the crucial role of the SDF-1/CXCR4 interaction in stem cell homing and adult BM hematopoiesis (Wright et al. 2002).

Several studies also investigated whether the SDF-1/CXCR4 interaction plays a major role in G-CSF induced stem cell mobilization. A study from Petit *et al.* showed a reduction of BM SDF-1 levels and an increase in CXCR4 receptor expression followed by stem cell egress as result of G-CSF treatment (Petit et al. 2002). In detail, they described the transient upregulation of BM SDF-1 followed by the gradual degradation of the chemokine during G-CSF stimulation. This decrease of SDF-1 protein levels in the BM results from the activity of proteolytic proteins such as elastase, cathepsin G, CD26/dipeptidylpeptidase IV (DPPIV) and matrix metalloproteinases 2 and 9 (MMP 2/9). These proteins are capable of cleaving SDF-1 at its NH<sub>2</sub> terminus thereby generating an inactive truncated protein. Accordingly, the inhibition of these proteolytic molecules or the application of neutralizing SDF-1 and CXCR4 antibodies prevents G-CSF-induced stem cell mobilization, suggesting that BM SDF-1 degradation is essential for stem cell egress after G-CSF induction.

Previous studies from Levesque *et al.* further showed that the degradation of SDF-1 in BM correlates with the accumulation of serine proteases and is critical for G-CSF- and cyclophosphamide-induced stem cell mobilization (Levesque et al. 2001; Levesque et al. 2003). These findings further indicate that BM SDF-1 degradation is essential for stem cell egress into the circulation. Moreover, an activating CXCR4 mutation in patients was shown to cause a syndrome of warts, hypogammaglobulinemia, immunodeficiency and myelokathexis (WHIM) (Hernandez et al. 2003). This disease is characterized by failing neutrophil egress from BM as well as B-cell lymphopenia emphasizing the importance of the SDF-1/CXCR4 axis for



the regulation of homing and retention of stem and progenitor cells in the BM, but also their mobilization into peripheral blood.

Taken together, many studies suggest that the interaction between SDF-1 and CXCR4 has a significant role in regulating the homing and proliferation of stem cells in the BM under homeostatic conditions. Accordingly, the disruption of the BM SDF-1/CXCR4 signaling under stress-induced conditions is necessary to induce the mobilization of stem cells into the circulation. In parallel, the local elevation of SDF-1 levels in the inflamed or injured organ is capable of recruiting the mobilized cells to the site of injury where they can support tissue repair and regeneration. However, stem cell mobilization is a complex process with different mobilization pathways and multiple interactions between chemokines, cytokines, proteolytic enzymes and cell adhesion molecules. Underlying mechanisms and order of orchestrating events remain elusive. A better understanding of the molecular mechanisms of SDF-1/CXCR4 interactions in stem cell mobilization protocols by manipulating these pathways can lead to improved stem cell transplantation therapies, particularly in clinical applications.

## **1.6. Biology of SDF-1**

### **1.6.1. Chemokines**

Chemokines or chemoattractant cytokines are a large family of small secreted proteins (with a molecular weight of approximately 8-14 kDa) that share 20-90% of structural homology (Luster 1998; Charo et al. 2006). In the past years, over 50 chemokines and 20 receptors have been discovered and their multifunctional characteristics in recruiting leukocytes to basal and inflamed tissue have been thoroughly studied. They are classified into 4 subfamilies on the basis of the relative position of two N-terminal cysteine residues which form disulfide bridges together with two other cysteine residues (Fig.6). They are termed as C-X-C ( $\alpha$ ), C-C ( $\beta$ ), C ( $\gamma$  or lymphotactin) and C-X<sub>3</sub>-C ( $\delta$  or fractalkine) and similarly the nomenclature of receptor uses C-X-C, C-C, C, C-X<sub>3</sub>-C followed by R (receptor) (Murphy et al. 2000). The  $\alpha$  and  $\beta$  family molecules are most extensively characterized regarding their functions. C-X-C or  $\alpha$  chemokines have one amino acid separating the first two cysteine residues. They are further subdivided into two groups, ELR<sup>+</sup> and ELR<sup>-</sup>, depending on the presence of the sequence glutamic acid–leucine–arginine near the N-terminal sequence of the molecule. ELR<sup>+</sup> chemokines (e.g. Interleukin-8 (IL-8 or

CXCL8) and growth-related oncogene-alpha (GRO $\alpha$  or CXCL1)) are characterized by the ability to attract neutrophils to sites of inflammation, whereas ELR<sup>-</sup> chemokines (e.g. SDF-1/CXCL12 and platelet factor 4 (PF-4 or CXCL4)), are capable of recruiting lymphocytes and monocytes. The C-C or  $\beta$  chemokines (e.g. monocyte chemoattractant protein-1 (MCP-1 or CCL2), macrophage inflammatory protein-1 (MIP-1 $\alpha$  or CCL3, MIP-1 $\beta$  or CCL4), eotaxin (CCL11) and RANTES (CCL5)) have two adjacent cysteine residues and they attract monocytes, basophils, dendritic cells and memory T cells. The third chemokine subfamily, lymphactin, has only two cysteine residues and fractalkine presenting the fourth group has three amino acids separating the first two cysteines.

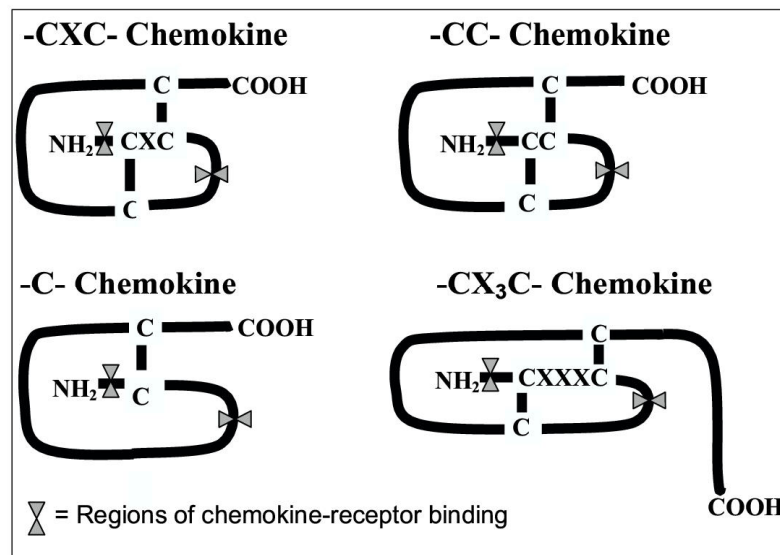


**Fig.6: Schematic representation of the four chemokine families (Townson et al. 2003).**

Chemokine receptors belong to the family of G protein-coupled receptors and are expressed on various populations of leukocytes. Chemokine binding to their specific receptors on the surface of the target cells initiates downstream signaling cascades resulting in leukocyte migration and activation. Although, chemokine and chemokines receptors has specific interactions within the family, some chemokines exhibit overlapping effects with many receptors, similarly receptors bind to many chemokines (Townson et al. 2003; Ratajczak et al. 2006). However, chemokine receptors are also expressed on other cell types such as endothelial and epithelial

cells, neurons, astrocytes, and cardiomyocytes, suggesting that chemokines have diverse functions apart from triggering immune responses.

### 1.6.2. Molecular Structure of SDF-1

SDF-1 or CXCL12, also known as Pre-B-cell growth stimulating factor (PBSF), is a member of the C-X-C chemokine subfamily and was initially isolated from murine bone marrow stromal cells (Nagasawa, Nakajima, et al. 1996). The constitutive and inducible expression of this chemokine has been reported in several tissues such as BM, heart, liver, kidney, thymus, spleen, skeletal muscle, and brain (Nagasawa, Nakajima, et al. 1996; Ratajczak et al. 2006). The analysis of the genomic structure of SDF-1 in human and mouse revealed two isoforms, SDF-1 $\alpha$  and SDF-1 $\beta$ , which are encoded by a single gene and result from alternative splicing (De La Luz Sierra et al. 2004).

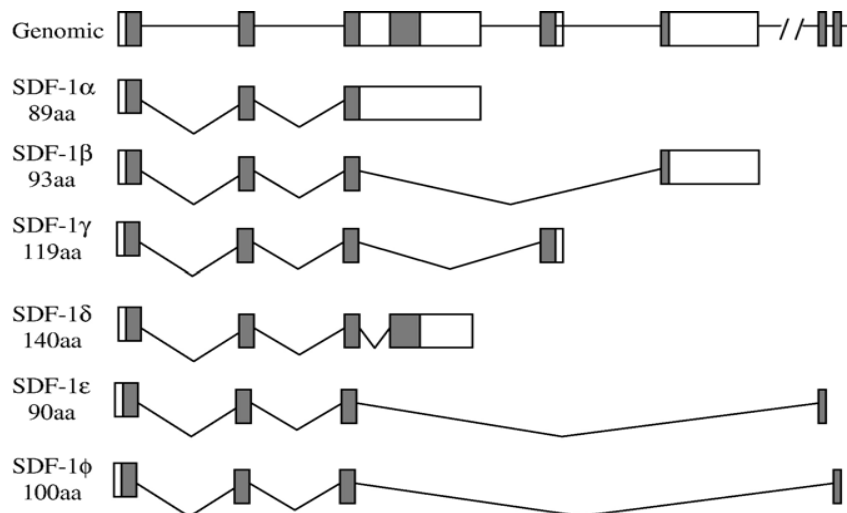


**Fig.7: Predicted human SDF-1 splice variants (Yu et al. 2006).**

The functional diversity and differential proteolytic processing abilities of these two isoforms are well investigated and characterized. SDF-1 $\alpha$  comprises 3 exons and encodes a protein of 89 amino acids whereas SDF-1 $\beta$  consists of 4 exons and encodes a protein of 93 amino acids. Both isoforms are highly similar regarding their sequences with the only difference of 4 additional amino acids at the C-terminus of SDF-1 $\beta$ . Unlike other chemokines of the C-X-C subfamily, that display clustered genes, SDF-1 has been mapped to a unique chromosomal localization and shows a highly conserved sequence between various species, suggesting unique biological

---

functions among the chemokine family (Shirozu et al. 1995). Gleichmann *et al.* later identified another splicing variant named SDF-1 $\gamma$  in adult rat brain, heart and lung with strongest expression observed in heart (Gleichmann et al. 2000). A recent study reported the existence of three additional human splice variants, SDF-1 $\delta$ , SDF-1 $\epsilon$ , SDF-1 $\zeta$ , in different tissues by RT-PCR analyses (Yu et al. 2006). Functional studies revealed differences of these isoforms in their ability to stimulate cell migration. However, future investigations are required to understand the functional diversity of these SDF-1 variants.

### 1.6.3. CXCR4, a Receptor for SDF-1

CXCR4 belongs to a large family of seven-transmembrane spanning, G protein-coupled receptors and specifically binds the sole ligand SDF-1. Unlike other chemokines, SDF-1 had originally been shown to bind exclusively to its receptor CXCR4 further emphasizing the unique biological role of this chemokine. Meanwhile, several studies showed that SDF-1 also binds another G protein-coupled receptor, CXCR7 or RDC1, making it even more complex to understand the biological role of SDF-1 and the significance of this CXCR7 receptor in the regulation of cellular trafficking and embryonic development (Balabanian et al. 2005; Sierro et al. 2007).

CXCR4 is widely expressed on many cell types including CD34<sup>+</sup> hematopoietic progenitor cells, lymphocytes, monocytes and non hematopoietic cells like endothelial and epithelial cells. A number of studies described the essential role of SDF-1/CXCR4 axis in hematopoiesis, organogenesis, vascularization, and immune response. In addition to that, CXCR4 expression also correlated with pathological diseases such as HIV, cancer and WHIM syndrome. CXCR4 was initially discovered as an orphan receptor called fusin or LESTR. Later it was identified as a coreceptor for T-tropic HIV entry into CD4<sup>+</sup>-expressing cells and number of studies focused on the role of CXCR4 in pathogenesis of HIV and identified it as a potential target in treating the disease (Murdoch 2000; Lusso 2006). In addition to that, CXCR4 is also widely expressed on several hematopoietic and non hematopoietic malignant cells and plays an essential role in metastasizing of the CXCR4<sup>+</sup> cells to SDF-1 secreting organs and promotes tumor angiogenesis, cell survival and proliferation of neoplastic cells (Burger et al. 2006).

#### 1.6.4. SDF-1/CXCR4 Axis and Cell Signaling

It is known from several studies that the interaction between SDF-1 and CXCR4 exerts multiple downstream signaling pathways in targeting cells which regulate various biological effects related to cell motility, chemotactic responses, cell adhesion and gene transcription (Kucia, Jankowski, et al. 2004; Wong et al. 2008). Thereby, SDF-1 binding to CXCR4 stabilizes homo- or hetero-dimerization of the receptor and enhances the G protein-coupled receptor activation (Percherancier et al. 2005). Activation of G $\alpha$ i protein pathways by the CXCR4 receptor leads to regulation of several signaling cascades including inactivation of adenylyl cyclase, activation of proline-rich kinase 2, Rho GTPase, the MAPK p42/44-ELK-1 and the PI3K-AKT-NF- $\kappa$ B axes, Crk and Crk-L, focal adhesion kinase (FAK), p130<sup>Cas</sup> and paxillin as well as phospholipase C (PLC), protein kinase C (PKC) and calcium release. It was also demonstrated that CXCR4 is able to activate the Jak/STAT pathway by transphosphorylation in a G $\alpha$ i-independent manner (Vila-Coro et al. 1999; Kucia, Jankowski, et al. 2004; Busillo et al. 2007; Wong et al. 2008). The second SDF-1 receptor, CXCR7, might also activate MAPK, PI3K and Jak/STAT pathways thereby regulating stem/progenitor cell migration (Gao et al. 2009).

Following the receptor activation, signal termination by arrestins (arrestin-2 and 3) plays a vital role in uncoupling the receptor from further activation and regulating the CXCR4/Gi signaling as a process of desensitization, internalization (Busillo et al. 2007). This process is initiated by the rapid phosphorylation of the cytoplasmic domain of CXCR4 and subsequent binding of arrestin-2 and 3 lead to internalization through endocytosis followed by lysosomal degradation. However, in addition to signal termination, arrestin-2 and 3 also induce several mitogen activated protein kinases and other pathways suggesting an importance of arrestins in CXCR4 mediated cell signaling (Cheng et al. 2000; Sun et al. 2002).

## 1.7. SDF-1 and Myocardial Infarctions

Heart failure arises as a consequence of coronary artery disease and it is most severe after myocardial infarction. In the western world coronary artery disease is the leading cause of deaths. This condition leads to limited oxygen supply (ischemia), irreversible muscle damage and cardiomyocyte death (Fox et al. 2001; Dickstein et al. 2008). The use of stem and progenitor cells as part of the therapeutic approach aims to repair and replace damaged vascular and cardiac tissue thereby inducing true myocardial regeneration. However, certain studies were reported with inefficient stem cell homing and engraftment to ischemic hearts after intravenous infusion. Therefore, it was suggested that better understanding of the stem cell homing factors, mechanisms and time course of expression could lead to optimize the stem cell therapeutic approaches in myocardial regeneration (Barbash et al. 2003).

Although many chemotactic factors seem to be involved in the process of myocardial infarction, SDF-1 was identified as a major stem cell homing factor. Binding of SDF-1 to CXCR4 on stem and progenitor cells seems to play an essential role in the homing as well as mobilization of stem cells to infarcted region. Many experimental studies could further prove the involvement of SDF-1 $\alpha$  in myocardial repair after infarction. The SDF-1-mediated mobilization of BM-derived stem cells to the ischemic heart was shown to result in angiogenesis and improved myocardial function (Askari et al. 2003; Abbott et al. 2004; Kucia, Dawn, et al. 2004; Elmadbouh et al. 2007). This induction of SDF-1 $\alpha$  expression in ischemic injury seems to be dependent on HIF-1 $\alpha$  (Ceradini et al. 2004). HIF-1 $\alpha$  also induces the expression of CXCR4 on progenitor cells which might help to guide these cells towards SDF-1 gradients in ischemic tissues (Tang, Zhu, et al. 2009). The elevation of SDF-1 $\alpha$  expression was also shown in serum samples and cardiac tissue of patients with myocardial infarction (Yamani et al. 2005; Leone et al. 2006). In support of this view, several investigations reported that BM-derived stem cells are released into peripheral blood after myocardial infarction in a SDF-1-dependent manner and are then chemoattracted towards a cardiac SDF-1 gradient (Kucia, Dawn, et al. 2004).

Due to the chemoattractant properties of SDF-1, these findings led to the hypothesis that it is involved in the process of stem cell homing and might thus play an important role in ischemic organ repair. There are reports suggesting that apart from stem cell

mobilization, SDF-1 activates cell survival signaling pathways and exerts cardioprotective properties in myocardial repair (Hu et al. 2007; Saxena et al. 2008). Since then, a large number of studies focused on using SDF-1 alone or in combination with other mobilizing factors as novel therapeutic methods to enhance stem cell mobilization to sites of cardiac ischemia and augment left ventricular function.

### **1.7.1. SDF-1/CXCR4 Axis and Therapeutic Applications in Myocardial Infarctions**

Since SDF-1 was identified as a potential stem cell homing factor, a large number of preclinical studies focused on using the chemokine as a potential therapeutic target to induce cardiac regeneration after myocardial infarction. Many of these studies confirmed the significance of the SDF-1/CXCR4 axis in mobilization of BM-derived stem cells to sites of ischemic injury (Askari et al. 2003; Abbott et al. 2004; Kucia, Dawn, et al. 2004; Elmadbouh et al. 2007). Table 1 and Figure 8 summarize the different models and methods of delivery used for therapeutic applications of SDF-1 $\alpha$ .

In general, different concepts have been described in order to modify the SDF-1/CXCR4 axis. An indirect approach by using G-CSF administration in a rabbit ischemic reperfusion model was shown by Misao and colleagues (Misao et al. 2006). They reported a G-CSF-mediated increase of SDF-1 $\alpha$  levels and rapid mobilization of CXCR4<sup>+</sup> cells towards infarcted areas. The scar size was decreased and left ventricular ejection fraction and end diastolic dimensions were significantly ameliorated in the G-CSF group. The beneficial effects observed were inhibited by the CXCR4 antagonist AMD3100, implying that SDF-1 in interaction with its receptor plays a key role in G-CSF-mediated stem cell recruitment to the infarcted heart. As another approach, SDF-1 $\alpha$  can be directly delivered into the ischemic myocardium. *In vitro* and *in vivo* studies using ischemic reperfusion models and a pretreatment with SDF-1 $\alpha$  resulted in decreased infarct size and increased resistance to hypoxic damage and apoptotic cell death via activation of ERK-1/2 and AKT phosphorylation (Hu et al. 2007). Saxena *et al.* presented beneficial effects upon intramyocardial injection of SDF-1 $\alpha$  into the peri-infarct zone of infarcted mouse hearts (Saxena et al. 2008). They noticed cardioprotective properties of the chemokine through activation of antiapoptotic pathways including protein kinase B (PKB) as well as VEGF-



mediated neoangiogenesis. Moreover, adenoviral delivery of SDF-1 $\alpha$  (AdV-SDF-1) in experimental MI showed increased c-kit<sup>+</sup> cell mobilization with improved cardiac structure and function through angiogenic and antifibrotic effects (Tang, Wang, et al. 2009).

**Table 1: Summary of concepts used for therapeutic delivery of SDF-1 in experimental models of myocardial ischemia (Ghadge et al. 2010).**

Species	Delivery method	Homing cells	Effect	Reference
Rat	SDF-1-overexpressing cardiac fibroblasts + G-CSF	CD117 <sup>+</sup> , CD34 <sup>+</sup> , endothelial cells	LV function $\uparrow$ , LV mass & anterior wall thickness $\uparrow$ , End-diastolic diameter $\downarrow$	(Askari et al. 2003)
Mouse	Adenoviral-mediated SDF-1 $\alpha$ overexpression (AdV-SDF-1)	Lin <sup>-</sup> / GFP <sup>+</sup> BM cells	Stem cell homing $\uparrow$ , Expression of CXCR4, VCAM-1, ICAM-1, VEGF, MMP-9 $\uparrow$	(Abbott et al. 2004)
Rat	Nonviral SDF-1 $\alpha$ transfection in skeletal myoblasts	CD117 <sup>+</sup> , CD34 <sup>+</sup> , CD31 <sup>+</sup>	Vessel density $\uparrow$ , LVEF and LVFS $\uparrow$ , Posterior wall and septum thickness $\uparrow$ , Cell survival pathways $\uparrow$	(Elmadbouh et al. 2007)
Mouse	Left ventricular cavity infusion of SDF-1 $\alpha$		Infarct size $\downarrow$	(Hu et al. 2007)
Mouse	Local delivery of SDF-1 $\alpha$ into ischemic myocardium	GFP <sup>+</sup> , vWF <sup>+</sup>	Infarct area $\downarrow$ , LVFS & vessel density $\uparrow$	(Sasaki et al. 2007)
Rat	Intramyocardial delivery of protease-resistant S-SDF-1 (S4V)	CXCR4 <sup>+</sup> / c-Kit <sup>+</sup>	LVEF $\uparrow$ , Capillary density $\uparrow$	(Segers et al. 2007)
Rat	Syngeneic MSCs overexpressing SDF-1	GFP <sup>+</sup> , $\alpha$ -actin smooth muscle cells, connexin-45 <sup>+</sup> cells	Cardiomyocyte survival $\uparrow$ , Apoptosis & LV dimensions $\downarrow$ , LVFS $\uparrow$ , Vascular density $\uparrow$	(Zhang et al. 2007)
Mouse	Intramyocardial injection of SDF-1 $\alpha$		Scar tissue $\downarrow$ , LV function & neoangiogenesis $\uparrow$ , Cardiac protection & Akt activation $\uparrow$	(Saxena et al. 2008)
Rat	Intramyocardial delivery of SDF-1 $\alpha$ + EPCs + Cyclosporin A	CD31 <sup>+</sup> , BrdU <sup>+</sup>	LV function & coronary flow rate $\uparrow$ , Inflammation $\downarrow$ , Neovascularization $\uparrow$	(Schuh et al. 2008)
Rat	Adenoviral-mediated SDF-1 $\alpha$ overexpression (AdV-SDF-1)	c-Kit <sup>+</sup>	Angiogenesis and anti-fibrosis $\uparrow$ , Expression of TGF $\beta$ 1, TIMP-1, TIMP-2 $\downarrow$ , LV function $\uparrow$	(Tang, Wang, et al. 2009)
Mouse	Genetic and pharmacological inhibition of SDF-1 degradation + G-CSF	CD45/CD34/ CXCR4 <sup>+</sup> , c-Kit <sup>+</sup> , Sca-1 <sup>+</sup>	Cardiac remodelling $\downarrow$ , Neovascularization $\uparrow$ , LV function and survival rate $\uparrow$	(Zaruba et al. 2009)
Mouse	Intramyocardial delivery of lentiviral-engineered MSCs overexpressing SDF-1 $\alpha$	GFP <sup>+</sup> BM cells, CXCR4 <sup>+</sup> , c-Kit <sup>+</sup> , CD31 <sup>+</sup>	Transplant survival $\uparrow$ , LV function & vascular density $\uparrow$ , LV remodeling & apoptosis $\downarrow$	(Zhao et al. 2009)



A study by Abbott *et al.* demonstrated that intracoronary infusion of BM-derived stem cells 48 hours after coronary artery ligation induced the recruitment of stem cells to the heart, but pronounced effects were only observed upon the forced expression of SDF-1 $\alpha$  by adenoviral gene delivery (Abbott *et al.* 2004). Accordingly, the administration of AMD3100 blocked the effect of SDF-1-mediated stem cell mobilization after MI. These findings led to a number of studies that combined direct cell injection with forced SDF-1 $\alpha$  expression. The transplantation of syngeneic skeletal myoblasts overexpressing human SDF-1 $\alpha$  in a rat model of myocardial infarction led to increased progenitor cell homing, induction of the cell survival signals Akt and Bcl2 as well as augmented angiomyogenesis (Elmadbouh *et al.* 2007).

Later on, another study using intravenous infusion of mesenchymal stem cells overexpressing SDF-1 into the infarct zone showed significant effects on cardiac function and increased vascular density (Zhang *et al.* 2007). However, these beneficial effects were proposed to be due to preservation of cardiac function rather than cardiac regeneration. Furthermore, MSCs overexpressing insulin-like growth factor (IGF-1) demonstrated paracrine activation of SDF-1 $\alpha$  signaling and massive stem cell mobilization into infarcted hearts and displayed extensive angiogenesis with better cardiac function (Haider *et al.* 2008). The mobilized cells exhibited an antiapoptotic nature and increased cell survival through activation of PI3K and Akt phosphorylation suggesting cardioprotective effects of SDF-1. Askari and coworkers even combined the transplantation of SDF-1-expressing autologous cardiac fibroblasts into the peri-infarct zone with G-CSF administration and showed significant homing of c-kit<sup>+</sup>, CD34<sup>+</sup> and endothelial cells to injured myocardium upon this treatment (Askari *et al.* 2003). However, despite of stem cell mobilization and improved cardiac function, they did not observe signs for cardiac regeneration. Hence, cardiac remodeling might be explained by secondary effects induced by the mobilized cells. Finally, a recent study applied a heterotopic transplanted rat heart model to show enhanced bone marrow progenitor cell homing to both acute ischemic recipients and progressive ischemic transplanted hearts (Zhao *et al.* 2009). MSCs overexpressing SDF-1 $\alpha$  injected into the myocardium of both hearts resulted in a significant mobilization of progenitor cells into damaged areas and an extended survival of transplanted hearts.

Altogether, most of the studies suggest that SDF-1-mediated therapeutic approaches are beneficial after myocardial infarction, most likely due to the induction of cell

surviving signaling pathways as well as the promotion of neovascularization. However, evidences for true myocardial regeneration are missing. A limitation in the use of SDF-1 is the rapid diffusion of the protein and its degradation upon tissue injury by proteolytic enzymes such as matrix metalloproteinase-2/9 (MMP-2/9) and CD26/DPPIV (Petit et al. 2002). This proteolytic degradation might limit the therapeutic effect of SDF-1 in myocardial infarction. To overcome such effects, Segers *et al.* designed a bioengineered fusion protein called S-SDF-1 (S4V) that is resistant to MMP-2 and CD26/DPPIV but retains its chemotactic potential (Segers et al. 2007). The intramyocardial delivery of this fusion protein into infarcted hearts resulted in an induction of stem cell recruitment and improved cardiac function.

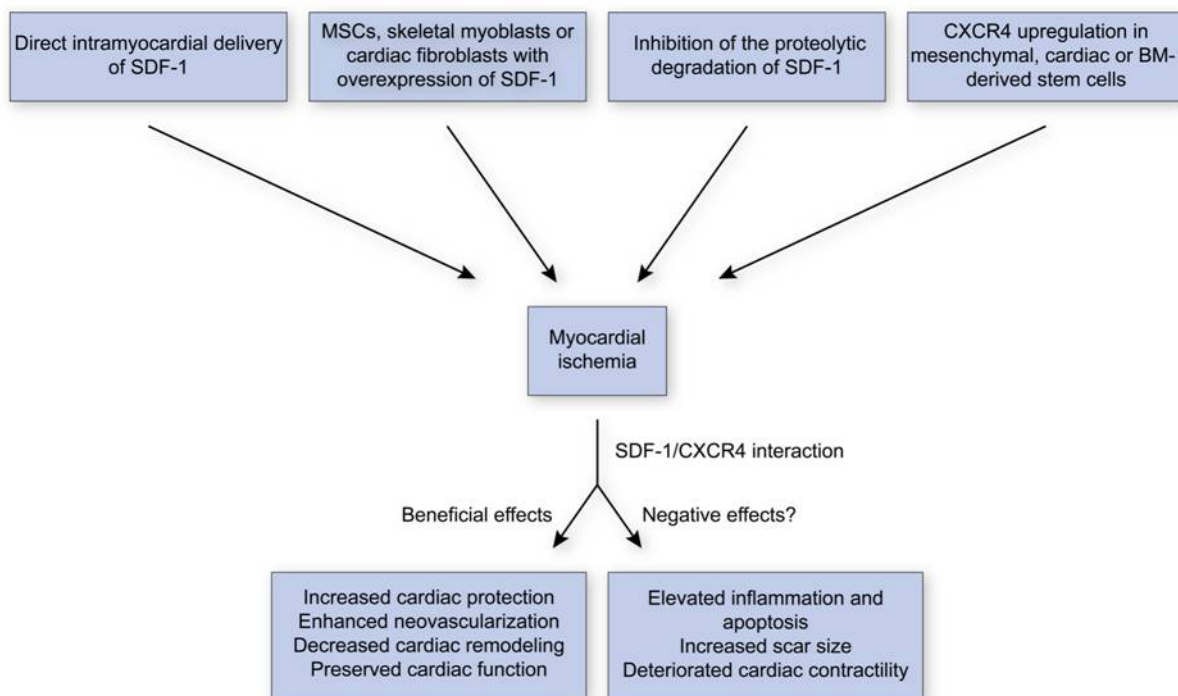


**Fig.8: Schematic representation of the therapeutic approaches using SDF-1 and CXCR4 in experimental models of myocardial infarction (Ghadge et al. 2010).**

Recent experimental evidence by Zaruba *et al.* further demonstrated that the novel therapeutic concept of genetic and pharmacological inhibition of DPPIV in combination with G-CSF administration induced stem cell mobilization after MI in mice (Zaruba et al. 2009). The inhibition of DPPIV activity led to the stabilization of active myocardial SDF-1 protein, which further intensified the myocardial homing of CXCR4<sup>+</sup> progenitor cells induced by G-CSF towards infarcted areas and preserved cardiac function through increased angiogenesis and decreased cardiac remodeling.

---

These results indicate that stabilizing the local SDF-1 protein in injured tissue represents a novel therapeutic strategy to promote myocardial repair.

On the other hand, a number of studies focussed on modulating CXCR4 expression on a variety of stem cells. The retroviral-mediated overexpression of CXCR4 in mesenchymal stem cells delivered intravenously into a rat ischemic reperfusion model resulted in enhanced migration of CXCR4-MSCs into the infarct zone (Cheng et al. 2008). This was accompanied by decreased LV remodeling and enhanced LV function in the CXCR4-MSC treated animals, suggesting that modifying CXCR4 receptor expression might be as beneficial for post-infarction myocardial repair as the manipulation of SDF-1. Accordingly, the use of a murine hypoxic preconditioning model demonstrated hypoxia-induced CXCR4 expression in the cardiac progenitor cell population CLK (cardiosphere-derived, Lin<sup>-</sup>c-kit<sup>+</sup> progenitor cells) upon myocardial infarction (Tang, Zhu, et al. 2009). This resulted in enhanced recruitment of intravenously infused cells to the infarcted area, decreased scar size and better cardiac function. Both the treatment of cells with normoxic conditions and the administration of a CXCR4 inhibitor abolished these positive effects, further indicating the crucial role of CXCR4 expression on cardiac and BM progenitor cells. A recent study demonstrated that the *in vitro* cultivation of BM-derived stem cells leads to an upregulated expression of CXCR4 compared to freshly isolated cells (Shiba et al. 2009). Implantation of these cultivated CXCR4<sup>+</sup> cells restored blood flow and enhanced ischemic tissue neovascularization, suggesting its therapeutic implication in cardiac repair.

Besides that, several priming agents such as C3a, des-Arg C3a, hyaluronic acid or sVCAM-1 might potentially be involved in SDF-1-dependent homing of HPCs and pharmacological modulation may have therapeutic implications in myocardial regeneration (Kucia, Jankowski, et al. 2004). Additionally, many stimulatory factors such as M-CSF, SCF, erythropoietin and statins, alone or in combination with other factors have been shown to regulate the SDF-1/CXCR4 axis and to induce CXCR4<sup>+</sup> stem cell mobilization into the circulation accompanied by advantageous effects in ischemic cardiac diseases (Vasa et al. 2001; Cottler-Fox et al. 2003; Vandervelde et al. 2005; Misao et al. 2006; Morimoto et al. 2007; Brunner et al. 2009).

In summary, a number of studies supported the benefit of SDF-1 and its receptor CXCR4 in the process of myocardial regeneration. The positive effects are most likely due to the SDF-1-mediated attraction of CXCR4<sup>+</sup> stem and progenitor cells

---

from the BM to the site of injury where they are able to integrate, proliferate and possibly differentiate in order to generate new myocardial tissue or at least have positive paracrine effects on cardiomyocyte survival and cardiac function. Moreover, SDF-1 seems to be important for ischemic tissue neovascularization and angiogenesis by recruiting endothelial progenitor cells (Yamaguchi et al. 2003).

### 1.7.2. Negative Implications of SDF-1 Therapy in MI

The majority of findings describe SDF-1 as a potent chemoattractant for stem and progenitor cells leading to the mobilization of cells to sites of injury, thereby playing an essential role in organ repair and ischemic tissue neovascularization. However, there are several recent studies demonstrating negative effects of the SDF-1/CXCR4 axis in the pathophysiology of MI (Fig. 8). First hints emerged from an *in vitro* study from Pyo *et al.* that reported negative inotropic effects of SDF-1 on adult cardiomyocytes through inhibiting calcium transients and thereby decreasing cardiac contractility (Pyo et al. 2006). The overexpression of CXCR4 by adenoviral infection of cardiomyocytes in response to SDF-1 stimulation enhanced the negative modulation of cardiac contractility, and the administration of a CXCR4 inhibitor abolished the depressed contractile response. The observed negative inotropic responses might be due to a direct effect of SDF-1 on cardiomyocyte function, indicating that the local delivery of the chemokine may result in decreased cardiac function. In a porcine model of MI, animals were subjected to catheter-based transendocardial injection of SDF-1 $\alpha$  into the peri-infarct myocardium (Koch et al. 2006). The outcome revealed an increase in vessel density and a reduction in collagen levels, but no beneficial effects of SDF-1 on myocardial perfusion and scar size. Surprisingly, left ventricular function even deteriorated in the SDF-1 $\alpha$ -treated group compared to untreated controls. The lack of positive effects of SDF-1 in this *in vivo* model might be explained by the delayed delivery of SDF-1 post-infarction. Nevertheless, results of the study raised safety concerns about therapeutic applications of SDF-1. In addition, Chen *et al.* recently confirmed the negative impact of the SDF-1/CXCR4 axis upon MI by demonstrating detrimental effects of adenovirus-mediated CXCR4 expression in a rat ischemic reperfusion model (Chen et al. 2010). Ad-CXCR4 overexpression led to increased scar size and impaired cardiac function associated with significant increase in inflammatory cell infiltration and augmented myocardial apoptosis towards the ischemic zone. In line with this, the

administration of AMD3100 in post-infarction rats led to a significant reduction in infarct size and ameliorated left ventricular systolic function with partially decreased non-infarcted left ventricular (NILV) hypertrophy. These findings imply that SDF-1 $\alpha$  directly promotes the hypertrophic changes of the heart. To confirm this hypothesis, SDF-1 $\alpha$  was administered to norepinephrine-induced hypertrophied neonatal rat ventricular myocytes ([Proulx et al. 2007](#)). This resulted in a significant increase in <sup>3</sup>H-leucine uptake and ANP and BNP protein synthesis, whereas AMD3100 selectively inhibited the effect on protein synthesis. Another interesting study in a transgenic Mst1 mouse model of dilated cardiomyopathy displayed that BM-derived fibroblast cells (fibrocytes) were recruited to nonischemic failing hearts where they contributed to cardiac remodeling by fibrosis induction ([Chu et al. 2010](#)). These fibrocytes were shown to express CXCR4 and are thereby attracted to the failing heart via myocardial SDF-1 gradients, implying that SDF-1 may promote the pathogenesis of myocardial remodeling in chronic heart failure. These unexpected findings dispute the therapeutic application of SDF-1 $\alpha$  to promote stem cell trafficking towards ischemic damaged heart.

The controversial results regarding the outcome of SDF-1-mediated therapy might be explained by the use of diverse experimental models, variable time points and delivery methods with multiple cell types in acute and chronic cardiac ischemia. Nevertheless, the data show that profound investigation is needed in order to carefully evaluate the therapeutic potential of SDF-1 in stem cell-mediated cardiac repair before commencing clinical studies.

## 2. Objective of the Study

SDF-1 is a major stem cell homing and mobilizing factor. The transient upregulation of SDF-1 $\alpha$  in damaged organs is involved in the process of organ repair through retention of bone marrow derived endogenous progenitor or stem cells (hematopoietic, endothelial). SDF1 $\alpha$  is expressed constitutively in normal adult heart, and is known to be upregulated after myocardial infarction. The potential role of the SDF-1/CXCR4 axis in postnatal cardiac development and function is not well understood. Besides that, the pathophysiological role of SDF-1 during post infarcted cardiac repair is needed to be elucidated.

To answer these questions, the present study aimed to produce a conditional cardiac knockout mouse model for SDF-1. This model allowed characterizing the physiological role of SDF-1 in heart development and cardiac function. To further understand the role of SDF-1 in cardiac hypertrophy and pathogenesis of cardiac fibrosis, the animals were infused with angiotensin-II. This study assesses the possible role of SDF-1 in the development of cardiac hypertrophy and tissue fibrosis in the process of disease progression. In addition to that, literature evidence suggests that SDF-1 has a crucial role in myocardial ischemia and angiogenesis and potential therapeutic implications in myocardial repair. To elucidate the role of SDF-1 in MI and cardiac remodeling, we analyzed the model by performing myocardial infarction. Overall this project aims to understand the pathophysiological mechanisms of SDF-1 involved in cardiac hypertrophy and myocardial infarction. This study also aimed to understand the specific role of SDF-1 in regulating inflammation, tissue fibrosis and progenitor cell trafficking during process of ischemic tissue repair.

### 3. Materials and Methods

#### 3.1. Materials

##### 3.1.1. Chemicals and Reagents

Table 2: Chemicals

Chemicals	Produced , Location
$\alpha$ - <sup>32</sup> P] CTP	PerkinElmer, Meriden, CT, USA
Acetic Acid	Roth, Karlsruhe
Acrylamid-/Bisacrylamid 19:1	Roth, Karlsruhe
Acrylamid-/Bisacrylamid 37, 5:1	Roth, Karlsruhe
Agarose	Invitrogen, Groningen
Ammoniumpersulfate (APS)	Sigma, Steinheim
Ampicillin	Serva, Heidelberg
Angiotensin-II	Merck, Darmstadt
Arabinose	Sigma, Steinheim
Bactoagar	Difco Microbiology
Bactotryptone	Difco Microbiology
BH4	Sigma, Steinheim
Boric Acid	Sigma, Steinheim
Bradford Reagent	Sigma, Steinheim
Bromophenolblue	Sigma, Steinheim
BSA	Sigma, Steinheim
Chloroform	Sigma, Taufkirchen
Complete Protease Inhibitor Cocktail Tablets	Roche, Mannheim
Coomassie Brilliant Blue R250	Sigma, Steinheim
DAPI	Sigma, Steinheim
DEPC	Serva, Heidelberg
Dextrane Sulfate	Merck, Darmstadt
DMEM	Gibco, Paisley, Scotland, UK
DNaseI	Boehringer, Mannheim
dNTPs	Amersham Bioscience, NJ, USA
DTT	Sigma, Steinheim
EDTA	Sigma, Steinheim
EGTA	Sigma, Steinheim
Ethanol	Roth, Karlsruhe
Ethidiumbromide	Sigma, Steinheim
Fe(NH <sub>4</sub> ) <sub>2</sub> (SO <sub>4</sub> ) <sub>2</sub>	Sigma, Steinheim
FBS	Gibco, Paisley, Scotland, UK
Fluorescence Mounting Medium	Dako, Glostrup, DK
G-418	Sigma, Steinheim
G418-Sulfate (Geneticin)	Invitrogen, Groningen
Glucose	Sigma, Steinheim
Glycerol	Roth, Karlsruhe
H <sub>2</sub> O <sub>2</sub>	Sigma, Steinheim
Ham's F12K	Gibco, Paisley, Scotland, UK
Harnstoff	Sigma, Steinheim
HCl	Roth, Karlsruhe
IPTG	Fermentas, Burlington, CDN
Isoflurane	Abbott, Wiesbaden

Isopropanol	Sigma Taufkirchen
Calciumacetate	Sigma, Steinheim
Kanamycin	Sigma, Steinheim
KCl	Sigma, Steinheim
Ketavet (ketamine 100 mg/ml)	Pharmacia Erlangen, Germany
KH <sub>2</sub> PO <sub>4</sub>	Merck, Darmstadt
LB-Agar	Sigma, Taufkirchen
MEM	Gibco, Paisley, Scotland, UK
Methanol	Roth, Karlsruhe
MgCl <sub>2</sub>	Sigma, Steinheim
Milk powder	Roth, Karlsruhe
Na <sub>2</sub> HPO <sub>4</sub>	Roth, Karlsruhe
NaH <sub>2</sub> PO <sub>4</sub>	Roth, Karlsruhe
NaCl	Roth, Karlsruhe
NaOH	Roth, Karlsruhe
NP-40	Sigma, Steinheim
NTPs	Promega, Madison, WI, USA
Paraffin	Roth, Karlsruhe
Penicillin/Streptomycin	Gibco, Paisley, Scotland, UK
PFA	Roth, Karlsruhe
Phosphatase Inhibitor Cocktail I + II	Roche, Mannheim
PMSF	Sigma, Steinheim
Proteinase K	Boehringer Mannheim, Germany
Random Hexamer Primer	Boehringer Mannheim, Mannheim
RNasin	Promega, Madison, WI, USA
Roti®-Block	Roth, Karlsruhe
Roti®-Load	Roth, Karlsruhe
Saccharose	Merck, Darmstadt
SDS	Serva, Heidelberg
Sodium acetate	Sigma, Steinheim
TEMED	Sigma, Steinheim
Tris	Roth, Karlsruhe
Triton X-100	Sigma, Steinheim
TRIZOL	Invitrogen, Carlsbad, CA, USA
Trypsin/EDTA	Gibco, Paisley, Scotland, UK
Tween-20	Sigma, Steinheim
Urea	Merc, Darmstadt
X-Gal	Fermentas, Burlington, CDN
Xylol	Roth, Karlsruhe
Yeastextract	Merck, Darmstadt
β-Mercaptoethanol	Sigma, Steinheim

### 3.1.2. Enzymes, Kits and Markers

Table 3: Kits, Enzymes and Markers

Componenets	Produced, Location
DNaseI	Roche, Mannheim
Expand™ Long Template PCR System	Boehringer Mannheim, Mannheim
Hyperladder 1	Bioline, Luckenwalde
JetStar Plasmid Purification MAXI Kit 2.0	Genomed GmbH, Löhne
M-MLV Reverse Transkriptase	Promega, Madison, WI, USA
Precision Blue Protein™ Standard All Blue	BioRad Laboratories Richmond, USA



Prime-it RmT Random Primer Labeling-Kits	Stratagene, Cedar Creek, TX, USA
Proteinase K	Merck, Darmstadt
QIAquick® Gel Extraction Kit	Qiagen, Hilden
QuickSpin Columns for radiolabeled DNA	Roche, Mannheim
Quick-Load 100bp ladder	NEB, Frankfurt a. M.
Restriction Enzymes	New England Biolabs, MA, USA
RNaseA	Boehringer Mannheim, Mannheim
RNeasy MiniElute Cleanup-Kit	Qiagen, Hilden
SeeBlue®Plus2 Pre-stained Protein Standard	Invitrogen, Carlsbad, CA, USA
Shrimp Alkaline Phosphatase	Roche, Mannheim
SP6-RNA-Polymerase	Promega, Madison, WI, USA
SuperSignaling® West Dura Extended Duration	Pierce, Rockford, IL, USA
TaqDNA Polymerase	Invitrogen, Carlsbad, CA, USA
Trichrom-Masson-Kit	Sigma, Steinheim
T4-DNA-Ligase	Promega, Madison, WI, USA
T7-RNA-Polymerase	Promega, Madison, WI, USA
Universal Buffer für Taqman®	Roche, Mannheim
Wizard® SV Gel and PCR Clean-up System	Promega, Madison, WI, USA
λ DNA/EcoRI + HindIII Marker, 3	Fermentas, Burlington, CDN

### 3.1.3. Antibodies

Table 4: Antibodies

Antibodies	Dilution	Blocking	Produced, Location
Primary			
Rabbit anti-SDF-1	1:1000	4% Milk /TBST	Abcam, Cambridge, UK
SDF-1 alpha (D32F9) XP™ rabbit	1:50	Donkey serum/ 1XPBS	Cell signaling, Denver, MA, USA
Mac-2	1:50	Donkey serum/ 1XPBS	Acris Antibodies, Herford, Germany
Secondary			
Goat-anti-mouse HRP	1:2000	TBST	Pierce, Rockford, USA
Goat-anti-rabbit HRP	1:2000	TBST	Pierce, Rockford, USA
Anti-rat Cy3 conjugated	1:300	1XPBS	Jackson Immuno Research, Suffolk, USA
Anti-rabbit Cy3 conjugated	1:300	1XPBS	Jackson Immuno Research, Suffolk, USA

### 3.1.4. Cloning Vectors (Plasmids and BAC)

Plasmids were propagated and isolated in E.Coli strain XL-1 Blue.

*Table 5: Plasmids*

Vector	Produced, Location
pGEM-T-easy	Promega, Heidelberg
pBluescript II SK (+)	Stratagene, La Jolla, CA, USA
pNEOduoFRT	AG.Prof. C. Birchmeier, MDC, Berlin
pDTA	AG.Prof. C. Birchmeier, MDC, Berlin

*Table 6: BAC*

BAC	Produced, Location
RP24-195P20	BACPAC, Oakland, USA

### 3.1.5. Primers

The primers were synthesized by the company Biotex GmbH (Berlin-Buch) and delivered in a lyophilized state. The lyophilized oligonucleotides were diluted in water to 50  $\mu$ M or 50pmol/ $\mu$ l concentration and stored at -20° C for long term usage. The primers diluted to final working concentration of 5 $\mu$ M for PCR reactions.

### 3.1.6. Cell Lines

The embryonic stem cells and fibroblasts were obtained from the laboratory of Prof. Carmen Birchmeier (MDC, Berlin-Buch).

*Table 7: Cell Lines*

Cell lines	Organism	Cell type
E 14.1 ES-Cells	Mus musculus	Inner Cell Mass of Embryo
Fibroblast Cells	Mus musculus	Embryos of the mouse strain ros <sup>ex</sup> with neomycin resistance

### 3.1.7. Bacterial Strains

Table 8: Bacterial Strains

Strain	Application
DH5 alpha	Plasmid-DNA-Amplification
XLblue	Plasmid-DNA Amplification
DY380	Heat induced homologous Recombination
EL250	Arabinose induced <i>Flp</i> -Recombination
EL350	Arabinose induced <i>Cre</i> -Recombination

### 3.1.8. Mouse and Rat Strains

The gene targeted SDF-1<sup>flox</sup> mice and SDF-1 transgenic rat lines were produced in the group of Prof. M. Bader at the MDC and the SDF-1 knockout mice were maintained on a C57BL/6J inbred background. The SDF-1 transgenic rat lines were maintained on the back ground of Sprague Dawley Hanover strain ordered from the company Dimed Schönwalde.

### 3.1.9. Lab Equipment and Materials

Table 9: Lab Equipment and Materials

Lab Equipment and Materials	Produced, Location
8-Channel-Pipette M300	Biohit, Rosbach v. d. Höhe
96-Well-Photometer anthos htII	Anthos Labtech Instruments, Salzburg, AT
Aldo-Xer-Gel dryer	Schütt-Labortechnik, Göttingen
Alzet®-Osmotic Pumps	Cupertino, CA, USA
Animal Feed	Sniff, Soest
Automatic Pipette Witoped XP	Witeg Labortechnik GmbH, Wertheim
Bacterial Shaker Certomat®H	B.Braun, Melsungen
Balance 440-43N	Kern & Sohn GmbH, Baldingen-Frommern
Binocular MZFLIII	Leica, Wetzlar
Incubator	Heraeus Instuments GmbH, Düsseldorf
Cell Culture Incubator Heracell	Heraeus Instuments GmbH, Düsseldorf
Cell Culture dishes	TPP®, Trasadingen, SUI
Centrifuge Megafuge 1.0R	Heraeus Instuments GmbH, Düsseldorf
Centrifuge Sigma 3K12	Sigma, Osterode am Harz
Centrifuge Sorvall®PC5C Plus	Kendro, Hanau
Cryo 1°C Freezing Container	Nalgene®Nunc, Rochester, NY, USA
Cryotubes Cryo.S	Greiner bio-one, Frickenhausen
Cryostat Microm HM560	Cryo-Star Microm, USA

---

Dialysis Membranes	Millipore, Billerica, MA, USA
One-way Pipettes Cellstar®1, 2, 5, 10, 25 ml	Greiner bio-one, Frickenhausen
Electroporator 2510	Eppendorf, Hamburg
Falcon-Tubes TPP®	Trasadingen, Schweiz
Fluorescent Microscope Axioplan 2 imaging	Carl Zeiss Jena GmbH, Jena
GenePulse® cuvettes	BioRad Laboratories, Richmond, USA
Horizontal Agarose Gel Electrophoresis Chamber	Biometra, Göttingen
Hybridizationoven 3032	GFL, Hannover
iCycler iQ5	BioRad Laboratories Richmond, USA
LabTec Chamber Slides	Nunc, NY, USA
Laminair®HB2448	Heraeus Instruments GmbH, Düsseldorf
Liquid Scintillation Analyzer Tri-Carb 1900 TR	PerkinElmer, Meriden, CT, USA
Magnetfish MR3001	Heidolph, Schwabach
Microtome SM2500	Leica Microsystems GmbH, Wetzlar
Microwave 8020	Privileg, Fürth
Millar-Catheter	Millar, A Gulf Freeway Houston, TX, USA
Millipore-Filter	Millipore
Microscope CKX31	Olympus Deutschland GmbH, Hamburg
Nitrocellulose membranen	Amersham Bioscience, Little Chalfon, UK
Nylonmembranen	Amersham Bioscience, Little Chalfon, UK
Pasteurpipettes	Roth, Karlsruhe
PCR-Tubes	Biozym Scientific GmbH, Oldendorf
pH-Meter pH Level 1	WTW, Weilheim
Phosphoimager Fujix BAS2000	Fuji, Tokyo, J
Phosphoimagerplatte BAS-III	Fuji, Tokyo, J
Photometer GeneQuant pro	Amersham Bioscience, Little Chalfon, UK
Pipettes	Gilson, Langenfeld
Polymax 1040	Heidolph Instruments, Schwabach
Potter-Homogenizator	Roth, Karlsruhe
Power Supply PowerPac™HC	BioRad Laboratories Richmond, USA
PVDF-Membrane	Amersham Bioscience, Little Chalfon, UK
Quartz cuvettes Suprasil®	Hellma, Müllheim
Refrigerated Condensation Trap RT100	Savant Instruments, Farmingdale, NY, USA
Roller Mixer SRT1	Snijders, Tilburg, NL
Save-Lock Tubes	Eppendorf, Hamburg
SDS-PAGE-Gel Electrophoresis chamber	BioRad Laboratories Richmond, USA
SpeedVac SVC100	Savant Instruments, Farmingdale, NY, USA
Tank blotter	BioRad Laboratories Richmond, USA
Table Centrifuge 5415D	Eppendorf, Hamburg
Table Centrifuge Biofuge pico	Heraeus Instruments GmbH, Düsseldorf
Table Centrifuge Labofuge 400e	Heraeus Instruments GmbH, Düsseldorf
Test-Tube Rotator	Snijders, Tilburg, NL
Thermal cycler PTC-200	BioRad Laboratories Richmond, USA
Thermomixer 5436	Eppendorf, Hamburg
Tissue-Tek O.C.T Compound	Sakura, Zoeterwoude, Niederlande
Transilluminator Multimage™Light Cabinet	Alpha Innotech Corporation, CA, USA
Ultrasound Sonicator Sonoplus	Bandelin electronic, Berlin
Ultra-Turrax T25 basic IKA®	Labortechnik, Staufen
Vacuum pump Vacusafe comfort	IBS Integra Bioscience, Chur, SUI
Vertical Gel Electrophoresis Chamber	Biometra, Göttingen
Visual Sonics Vevo770 (Echo Unit)	Toronto, Ontario, Kanada
Vortexer Genic 2	Bender & Hobein AG, Zürich, SUI
Water bath	GFL, Burgwedel
Whatman Paper	Whatman®, International, Maidstone, UK
X-ray Films	Fotochemische Werke GmbH, Berlin

---

## 3.2. Methods

### 3.2.1. Nucleic Acids

#### 3.2.1.1. Isolation of Plasmid and BAC DNA – Rapid Alkaline Lysis Method

The Isolation protocol of plasmid DNA from bacterial cell culture is a modification of the methods of Birnboim and Doly (1979) and Ish-Horowicz and Burke (1981). Four ml (4ml) of LB medium with appropriate antibiotic were inoculated with a single bacterial colony and incubated at 37° C with shaking overnight. 2 ml of this culture was centrifuged at 13 000 g for 1 min. The pellet was resuspended in 300 µL of solution E1. Cells were lysed by adding 300 µL of E2 solution. 300 µL of E3 solution was added to the tube to neutralize following lysis, and immediately mixed by inverting. Cell debris and chromosomal DNA were pelleted by centrifugation at 13000 g, RT for 5 minutes. The supernatant was transferred into a new tube and 0.6 ml of isopropanol was added to precipitate the DNA. After centrifugation (13 000 g, RT, 10 min) and washing with 70% ethanol, air-dried pellet was resuspended in 50 µL TE buffer or ddH<sub>2</sub>O. 2-5 µL of DNA was taken for the control digestion. For long term storage, DNA was kept at -20° C.

E1 solution  
(GTE-buffer)

50mM Tris-HCl pH 8.0  
10 mM EDTA pH 8.0  
100µg/ml RNaseA

E2 solution  
(Lysis buffer)

200 mM NaOH  
1 % SDS

E3 solution

3 M Potassium Acetate pH 5.5

#### 3.2.1.2. Maxi Preparation

For larger scale, plasmid DNA was isolated from 200 ml of overnight bacterial cell culture using JetStar Plasmid Purification MAXI Kit 2.0 according to the manufacturer's instruction. The DNA was usually dissolved in 100-400 µL of TE buffer and kept at -20° C.

### 3.2.1.3. Isolation of Genomic DNA From Tail Biopsies For PCR

To isolate genomic DNA from tail, 2-5 mm mouse tail tip was cut off and put into 1.5 ml microcentrifuge tube. 100 µl of tail lysis buffer was added. The sample was incubated at 55°C overnight with shaking (800 rpm). On the second day, the tube was incubated at 95°C for 20 minutes to inactivate the proteinase K. Afterwards 750 µl TE/RNase were added to samples and 2 µl of the template were used for the PCR.

### 3.2.1.4. Isolation of Genomic DNA From Tail and Tissues For Southern Blot

1-2 cm of tail or fine grinded tissue powder (50-100 mg) was incubated in 500 µl of lysis buffer containing proteinase K (10 mg/ml) at 55°C overnight with shaking. In the morning the samples were centrifuged (10 000 rpm, 1 min) the aqueous phase was transferred into a new tube. Added equal volume of phenol, chloroform: Isoamylalcohol solution (25, 24:1), mixed gently and thoroughly. Centrifuged sample (10 000 rpm, 4°C, 10 min) and transferred the aqueous solution into a new tube and repeated the phenol chloroform extraction. DNA was precipitated by adding 2 volumes of cold ethanol-salt mix (1:10 EtOH, 3M NaAc pH 5.2) to aqueous phase and centrifuged (10 000 rpm, 4°C, 15 min). The pellet was washed twice with 70% ethanol, dried and resolved in 100-200 µl of TE-buffer or ddH<sub>2</sub>O. The concentration of extracted DNA was estimated. DNA was kept at -20°C.

Lysis buffer	Tris-HCl pH 8.0 100 mM Proteinase K 1 mg/ml EDTA 5 mM NaCl 200 mM SDS 0.2 %
TE buffer	Tris-HCl pH 8.0 10 mM EDTA 1 mM 20 µg/ml RNase A

### 3.2.1.5. Isolation of Total RNA From Mouse Tissues

To isolate total RNA, tissues were minced and homogenized in liquid nitrogen to fine powder. The TRIZOL reagent was added to powder (100mg tissue powder / 1 ml Trizol) and carefully resuspended. The isolation protocol was performed according to the manufacturers instructions. The RNA was precipitated by adding 0.5 ml of isopropanol. Finally, the pellet was washed with 70% ethanol, dissolved in 80-100  $\mu$ l of DEPC H<sub>2</sub>O. RNA was kept at -20°C.

The RNA isolation with TRIZOL has the advantage of low DNA contamination. The RNA preparations were incubated with DNase I (0.1 u /  $\mu$ L) for 30 min at 37° C prior to their use in the production of cDNA. This was followed by the DNase inactivation at 75 ° C for 10min.

**DEPC-water**      DEPC - 0.1%    stirred overnight at 37 °C, autoclaved

### 3.2.1.6. Measurement of the Nucleic Acid Concentration

The quantification of nucleic acids was determined on the spectrophotometer by measuring absorption of the samples at wavelengths 260 nm and 280nm in precision Quartz cells.

**DNA:**  $OD_{260} = 1 = 50 \mu\text{g/ml ds DNA}$ ,

**RNA:**  $OD_{260} = 1 = 40 \mu\text{g/ml RNA}$ ,

The concentration was calculated according to the formula:  $C = (A_{260} - A_{320}) \times f \times c$

C= concentration of sample ( $\mu\text{g}/\mu\text{l}$ )

$A_{260}$  = absorption at 260 nm

$A_{320}$  = absorption at 320 nm

f = dilution factor

C=0.05  $\mu\text{g}/\mu\text{l}$  for double stranded DNA

C=0.04  $\mu\text{g}/\mu\text{l}$  for RNA

C=0.03  $\mu\text{g}/\mu\text{l}$  for single stranded DNA

And the quality of nucleic acids (i.e. contamination with salt and protein) was checked at the ratio 260/280.

**DNA:**  $OD_{260/280} = 1.8$

**RNA:**  $OD_{260/280} = 2.0$

### 3.2.1.7. Separation of DNA on Agarose Gel Electrophoresis

1-2% (w/v) of agarose gels were used to separate the DNA molecules depended on their molecular size (0.1kb -10kb). The DNA samples were mixed with 0.1 volumes of 10x DNA loading buffer and loaded in agarose gel lanes and placed in electrophoresis chamber. The gel electrophoresis chamber filled with 1x TAE buffer and run at 1-8 V / cm gel electrophoresis. To visualize the DNA, agarose gels contained approximately 0.5 g / ml ethidium bromide and were irradiated under UV light transilluminator (300 nm). The sizes and concentrations of individual DNA bands were estimated by comparison with molecular weight markers.

<b>1x TAE-Buffer</b>	Tris-Acetate, pH 7.8	40 mM
	EDTA	1 mM
<b>10x DNA loading Buffer</b>	Saccharose	40 %
	Bromophenolblue	0.02 %
	in TE-Buffer	

### 3.2.1.8. DNA Extraction From Agarose Gel

After visualization of separated DNA fragments on agarose gels through UV transilluminator, the desired bands of size were excised from gel with a scalpel. The DNA extraction procedure is followed by using QIAquick® Gel Extraction Kit according to manufacturer instructions. An aliquot of extracted DNA further verified in agarose gel electrophoresis.

### 3.2.1.9. Restriction Digestion of DNA

The restriction enzyme digestion was performed by incubating double-stranded DNA molecules with an appropriate amount of restriction enzyme in their respective buffer



as recommended by the supplier at optimal reaction temperature. A reaction mixture contains 0.2-1 µg of DNA, 1µl of enzyme (approximately 10U), 1µl of 10 x buffer and ddH<sub>2</sub>O. The mixtures were incubated for 1-2 h at the temperature specified by the manufacturer. For larger scale of DNA enzymatic digestion, the reaction carried out with increased amount of enzyme and overnight incubation. Double enzymatic digestions were incubated at optimal buffer activity over 75-100% or by sequential digestion with low salt followed by high salt buffers.

### 3.2.1.10. Ligation of DNA Fragments

Highly efficient ligation of linear DNA fragments into an appropriate vector was performed by using T4 DNA ligase enzyme in a ratio about 1:3 (Vector: insert). A 10µl ligation reaction mixture contains:

*Table 10: Reaction components for Ligation*

Vector DNA	30 ng
Insert DNA	50-100 ng
Ligation buffer (10x)	1 µl
T4 DNA ligase (5 U/µl)	1 µl
In a total volume of 10 µl, filled up with dH <sub>2</sub> O	

The ligation reaction was incubated overnight at 16 °C or room temperature and afterwards transformed in E.coli bacteria.

### 3.2.1.11. DNA Sequencing

DNA sequencing of all plasmids and cloned PCR products were performed by the company Invitex (Berlin-Buch). All the primers for sequencing were provided by Bio-Tez company (Berlin-Buch).

### 3.2.1.12. Reverse Transcription (RT)

The preparation of cDNA from DNaseI pretreated total RNA was performed as follows: 2-5 µg of total RNA was mixed with 5 µl of random hexamer primers (20 µM) in a volume of 15 µl DEPC H<sub>2</sub>O. To avoid formation of RNA secondary structures the mixture was heated to 65°C for 5 min, and then quickly

chilled on ice. After a brief centrifugation, the following master mix was added to the reaction mixture:

*Table 11: Reaction components for Reverse Transcription*

5x First strand buffer	6 $\mu$ l
0.1 M DTT	3 $\mu$ l
5 mM dNTPs	3 $\mu$ l
RNasin (10 U/ $\mu$ l)	1 $\mu$ l
M-MLV (200 U/ $\mu$ l)	2 $\mu$ l

All the components in the reaction mixture were mixed gently and centrifuged shortly and incubated at 37°C for 1 hour. Afterwards the reaction was inactivated by heating the samples at 80°C for 10min. 2-3 $\mu$ l of the cDNA solution was used for realtime PCR quantification.

### 3.2.1.13. Polymerase Chain Reaction (PCR) for Cloning and Genotyping

The PCR conditions were optimised and performed according to general rules.

*Table 12: Reaction components for PCR*

Genomic DNA	2 $\mu$ l
PCR buffer (10x)	5 $\mu$ l
upper Primer (5 $\mu$ M)	2 $\mu$ l
lower Primer (5 $\mu$ M)	2 $\mu$ l
dNTPs (5mM)	2 $\mu$ l
MgCl <sub>2</sub> (50mM)	2 $\mu$ l
Taq Polymerase (1U)	0,3 $\mu$ l
ddH <sub>2</sub> O	34,7 $\mu$ l

For genotyping of transgenic rats and conditional SDF-1 knockout mice and for sub-cloning of DNA fragments, PCRs were performed in a 50 $\mu$ l reaction mixture containing Taq DNA polymerase. Most of the PCR reactions had similar cycling conditions with changes in annealing temperature (AT) and elongation time (ET) depending on the oligonucleotides and product size.

The reaction mixture was pipetted into PCR tubes and subjected to the following program in the Peltier thermal Cycler PTC-200 (Biozym):

Table 13: Program conditions for PCR

Step	Time	Temperature	Cycles
Initial Denaturation	5 min	95°C	1 x
Denaturation	30 sec	95°C	} 35 x
Annealing	45 sec	56 - 65°C	
Elongation	30 sec	72°C	
FinalElongation	5 min	72°C	1 x

2-5 µl of PCR reaction was mixed with DNA loading dye and analysed on 1-2% agarose gels electrophoresis. The following primers were used for genotyping and sub cloning:

Table 14: Primers for construct of transgenic MLC-2-SDF-1 rat by BAC Gap repair method

Construct	Name	Primer sequence 5'-3'
pBlueScript-SK+	SDFMLC-H5_up	CCATCGATACCTCGGTGTCCTCTTGCTGTCCA
	SDFMLC-H5_lo	GGAATTCCTCCGCGCCGAACCCACTCT
pBlueScript-SK+	SDFMLC-H3_up	GGAATTCCTGAAGATGGAGAAAAACAGG
	SDFMLC-H3_lo	ATTCTTGCGGCCGCGGGGAGAAAGGAGGAT- -GATTGAT

Table 15: Primers for the SDF1 targeting vector construct for the production of conditional "knockout" mouse.

Construct	Name	Primer sequence 5'-3'
pDTA	SDFHomo5up	GAATGCGGCCGCTGCCTGTTTCCGCTCATATG
	SDFHomo5lo	CCACTAGTTGTAGACTATCCAGAAATCA
pDTA	SDFHomo3up	GGACTAGTACCTGGCAATATTTGTCTGT
	SDFHomo3lo	GGGCCCGGGAGTAGCCCTGGGCTTGAAAG
pNEOduoFRT	SDFloxp5a_up	ACGCGTCGACGAGTGAGACCCAGTCATTTT
	SDFloxp5a_lo	GCGAAGCTTTGGATTCCCAGCCAAAGTCT
	SDFloxp5b_up	CGGGATCCAGTTATTCTAACTGTAGATT
	SDFloxp5b_lo	GGACCGCGGGAGGCTGGGTCGTAGAGCTT
pNEOduoFRT	SDFloxp3a_up	ACGCGTCGACGGAGGACCCGCAGGATTGTT
	SDFloxp3a_lo	GCGAAGCTTCCAAGCCATGCACTTCGAGC
	SDFloxp3b_up	GAATGCGGCCGCGAATTCCTATAGGTTCA- -GTGGTGAGG
	SDFloxp3b_lo	GGACCGCGGATAGCTTGGGTAAGTCTGA

*Table 16: Primers for genotyping transgenic SDF-1 rat*

Name	Primer sequence 5'-3'
TgSDF F gen	AGCACAGAGCATCGTTCCCA
TgSDF R gen	ACCGAGTTCTTTCTCCGCGA

*Table 17: Primers for genotyping conditional knockout SDF-1 mice*

Name	Primer sequence 5'-3'
SdfFloxF4	ATCTCTGGGAGACCTGTTTGG
SdfFloxR4	GGACTGCTAGGCTTAGGGCAA
SdfFloxR5	CAGCGCGAGTTCAAGAGCT
SdfFloxR7	CGCTATGACGGCAATAAAAAG

*Table 18: Reaction components for PCR genotyping SDF-1 knockout mice*

Genomic DNA	2 µl
PCR buffer (10x)	5 µl
Primer F4 (5µM)	2µl
Primer R4 (5µM)	1µl
Primer R5 (5µM)	1µl
Primer R7 (5µM)	1µl
dNTPs (5mM)	2µl
MgCl <sub>2</sub> (50mM)	2µl
<i>Taq</i> Polymerase (1U)	0,3µl
ddH <sub>2</sub> O	34,7µl

*Table 19: Primers for southern hybridization probes*

Name	Primer sequence 5'-3'
SDF-1 5probe up	ATGAGGACTTCCTTTTCAATTTTAC
SDF-1 5probe lo	ATTTTTTATGAGATTGAACGTATGT
SDF-1 3probe up	TCCTGTGGCAGCCGGCTACAGTCTC
SDF-1 3probe lo	TGCAGGTCCTTCCGGAAGGCGTTTA

*Table 20: Primers for genotyping Cre*

Name	Primer sequence 5'-3'
SDF-1 cre F	GACCGTACACCAAATTTGCC
SDF-1 cre R	TAGAGCCTGTTTTGCACGTT
MLC2vCre F2	ATTTTTAAACCCAGGGGAGA
MLC2vCre R2	TAGTTTTTACTGCCAGACCGC

### 3.2.1.14. Southern Blot

Southern blot is a method widely used to detect the molecular weight and specific DNA sequences in the genomic DNA samples.

#### 3.2.1.14.1. Gel Electrophoresis and Blotting

10µg of genomic DNA was digested overnight in a restriction digestion mixture with appropriate enzymes in a volume of 30-40µl. The digested DNA was loaded on 1% agarose gel electrophoresis as described before. The gel was photographed before blotting. The gel was rinsed in sterile water and submerged into a clean plastic box containing denaturing buffer. The box was shaken slowly on a platform shaker for 30-45min at room temperature. The DNA was transferred onto nylon membrane with transfer buffer (10x SSC) by the capillary transfer method (Dunn and Sambrook 1980). After overnight transfer in transfer buffer, the membrane was air dried and DNA was fixed by exposing to UV light for 2 min in UV stratalinker 2400 (Stratagene).

<b>Denaturation Buffer</b>	NaCl	1.5M
	NaOH	0.5M
	Distilled H <sub>2</sub> O	Add to final volume of 1lit
<b>Transfer Buffer (10x SSC, pH 7-8)</b>	NaCl	3.0M
	Na-citrate	0.3M
	Distilled H <sub>2</sub> O	Add to final volume of 1 lit

#### 3.2.1.14.2. Probe Labeling

The probe labeling was carried out by the Prime-It RmT Random Primer Labeling Kit (Stratagene, USA). Purified PCR products were labeled by random 9-mer priming to multiple sites of DNA and further incorporation of radioactive nucleotides into newly synthesized DNA carried by magenta DNA polymerization reaction. About 25-50 ng of DNA in 42 µl H<sub>2</sub>O were denatured at 95°C for 5 min and chilled on ice. Then 5 µl of radioactive [ $\alpha$ -<sup>32</sup>P] dCTP (10 µCi/µl) labeled nucleotide, 3 µl of magenta DNA polymerase (4 U/µl) were added to the denatured samples and the labeling reaction was incubated for 20 min at 37°C. The probe was purified with Microspin<sup>TM</sup> G50 Column (Pharmacia) before hybridization.

### 3.2.1.14.3. Hybridization

Membranes were prehybridized at 65°C for 2 h using 20 ml of prehybridization buffer, and then buffer was replaced with 10 ml hybridization buffer and the membrane was incubated for 2 hours before adding the denatured probe. Hybridization was performed at 65°C overnight. Membranes were washed twice at 65°C for 20 min first with 150 ml of washing solution I, followed with 250 ml of washing solution II and III. Membranes were dried briefly on Whatman paper, sealed in plastic foil (Saran wrap) and exposed to Phosphoimager plate BAS-III overnight. The plates were developed using Phosphoimager Fujix BAS2000.

<b>Prehybridization Buffer</b>	Tris pH 8.0	50mM
	EDTA pH 8.0	10mM
	SSC	5x
	Denhardtts	5x
	SDS	0.5%
	SS DNA	100mg/ml
	dH <sub>2</sub> O	add to final volume 25 ml
<b>Hybridization Buffer</b>	Tris pH 8.0	50mM
	EDTA pH 8.0	10mM
	SSC	5x
	Denhardtts	5x
	SDS	0.5%
	SS DNA	100mg/ml
	Dextran Sulfate	10%
dH <sub>2</sub> O	add to final volume 25 ml	
<b>Washing Solution I</b>	SSC	2x
	SDS	0.5%
	dH <sub>2</sub> O	add to final volume 150 ml
	kept at RT	
<b>Washing Solution II</b>	SSC	0.5x
	SDS	0.5%
	dH <sub>2</sub> O	add to final volume 250 ml
	kept at 65°C	
<b>Washing Solution III</b>	SSC	0.1x
	SDS	0.5%
	dH <sub>2</sub> O	add to final volume 250 ml
	kept at 65°C	

### 3.2.1.15. Real-Time-PCR Quantification (TaqMan®-PCR)

Real-time PCR is an efficient and highly sensitive method for relative quantification of gene expression. Taqman PCR is one among the different forms of realtime PCR methods based on the principle of sequence-specific DNA probes consisting of oligonucleotides that are labelled with a fluorescent reporter and a quencher (TAMRA/FAM) which permits detection of hybridized probe with its complementary DNA target. The degradation of the fluorescent probe by 5' to 3' exonuclease activity relieves the quenching effect and allows the fluorescence emission measured via FRET. The fluorescence detected in the real-time PCR is directly proportional to the fluorophore released and the amount of cDNA template present in the PCR.

*Table 21: Reaction components for real-time Taqman-PCR*

cDNA	2.5 µl
Forward Primer (5 µM)	2.0 µl
Reverse Primer (5 µM)	2.0 µl
Sonde (TAMRA/ FAM) (10 µM)	1.0 µl
Universal PCR Master Mix	12.5 µl
ddH <sub>2</sub> O	5.0 µl

*Table 22: Program conditions for real-time Taqman-PCR*

Step	Time	Temperature	cycles
Initial Denaturation	10 min	95°C	1 x
Denaturation	15 sec	95°C	40x
Annealing & Elongation	60sec	60°C	
		4°C	For ever

*Table 23: primers for real-time Taqman-PCR*

Name	Primer sequence 5'-3'
GAPDH-F	AACGACCCCTTCATTGACCTC
GAPDH-R	CTTCCCATTCTCAGCCTTGACT
GAPDH-T	ACCCACGGCAAGTTCAACGGCAA
VEGF-70F	CATCTTCAAGCCGTCCTGTGT
VEGF.txt-136R	CTCCAGGGCTTCATCGTTACA
VEGF.txt-93T	CGCTGATGCGCTGTGCAGGCT
SDF1 F	GAGCCAACGTCAAGCATCTG
SDF1 R	CAGCCGTGCAACAATCTGA
SDF1 P	AAATCCTCAACACTCCAAACTGTGCC

---

ANP F	GAGAAGATGCCGGTAGAAGA
ANP R	AAGCACTGCCGTCTCTCAGA
ANP P	ATGCCCCCGCAGGCCCGG
BNP F	CTGCTGGAGCTGATAAGAGA
BNP R	TGCCCAAAGCAGCTTGAGAT
BNP P	CTCAAGGCAGCACCCCTCCGGG
GATA-4	CCCTGGAAGACACCCCAAT
GATA-4 R	TGGACATGGCCCCACAAT
GATA-4 P	TCGATATGTTTGATGACTTCTCAGAAGGCAGAG
Nkx2-5 F	TGACCCAGCCAAAGACCCT
Nkx2-5 R	CCATCCGTCTCGGCTTTGT
Nkx2-5 P	AAAGAGCTGTGCGCGCTGCAGA
TGF $\beta$ 1 F	AAACGGAAGCGCATCGAA
TGF $\beta$ 1 R	GGGACTGGCGAGCCTTAGTT
TGF $\beta$ 1 P	CCATCCGTGGCCAGATCCTGTCC
Collagen-1 $\alpha$ F	CTTCACCTACAGCACCCCTTGTG
Collagen-1 $\alpha$ R	GATGACTGTCTTGCCCCAAGTT
Collagen-1 $\alpha$ P	ACGGCTGCACGAGTCACACCG
Fibronectin F	GTTCGGGAGGAGGTTGTTACC
Fibronectin R	GAGTCATCTGTAGGCTGGTTTAGG
Fibronectin P	CCTTGGTCCACAGAGT

---

### 3.2.2. Western Blot

#### 3.2.2.1. Protein Isolation from Tissues

50-100 $\mu$ g of frozen tissues samples were minced in liquid nitrogen to fine powder and mixed in 1 ml of protein extraction RIPA buffer (with 1 mM PMSF and Complete Protease Inhibitor cocktail). Afterwards, the mixture was transferred to Eppendorf tubes and incubation on ice for 30 min, and centrifuged at 13,000 g, 20 min, 4 ° C. The protein concentration of the supernatant was determined photometrically by the Bradford protein assay method. Aliquots were with 50  $\mu$ g of total protein created, stored at -80 ° C or used directly in SDS-PAGE analysis.

<b>RIPA Buffer</b>	NaCl	150 mM
	Tris-HCL pH 7.5	50 mM
	NP-40	1 %
	DOC (Natriumdeoxycholot)	0,5 %
	SDS	0,1 %
	PMSF	1 mM
	Complete Protease Inhibitor Cocktail	1 Tablette / 10 ml



### 3.2.2.2. Measurement of Protein Concentration

The total protein concentration was estimated by Bradford method in 96 well plates. Isolated total protein samples were diluted (1:5-1:10) in RIPA or lysis buffer before the measurement depends on the standard concentrations range and 5  $\mu$ L of each diluted sample was mixed with 250  $\mu$ L of the Bradford reagent. In parallel, a standard curve with known BSA concentrations (0.1 – 2.5  $\mu$ g BSA/ $\mu$ L) in the lysis buffer was used. The samples were incubated at RT for 10 min. The 96 well plates with all the samples and standards were measured for the protein concentration using a photometer at 595 nm. The protein concentration was graphically calculated based on the BSA standard curve.

### 3.2.2.3. SDS-Polyacrylamide Gel Electrophoresis (SDS-PAGE)

SDS-PAGE used to perform immunological detection of proteins based on size fraction by gel electrophoresis. For the separation using SDS-PAGE, protein samples (50 $\mu$ g) were denatured with Roti ®-Load SDS loading buffer for 5 min at 95 ° C and cooled on ice. 8-15% resolving gel and 5% stacking gel were prepared using Bio-rad Mini-Protean®3 Electrophoretic Cell. After removing the comb, the protein samples were loaded on the gel, and the gel was run at the 80 V for 15 minutes and then at 150 V for about 1 h in SDS-PAGE running buffer.

<b>Resolving gel (8-15 %)</b>	Acrylamid-/Bisacrylamid 37:5:1	8 - 15 %
	Tris-HCL pH 8.8	375 mM
	SDS	0.1 %
	TEMED	0.25 %
	APS	0.1 %
<b>Stacking gel (5%)</b>	Acrylamid-/Bisacrylamid 37:5:1	5 %
	Tris-HCL pH 6.8	125 mM
	SDS	0.1%
	TEMED	0.25 %
	APS	0.1 %
<b>1x Running Buffer</b>	Tris	25 mM
	Glycin	200 mM
	SDS	0.1 %

### 3.2.2.4. Blotting of Proteins

For blotting, proteins were separated in the SDS-PAGE gels and electrotransferred to PVDF membranes for 1-2 hrs at 250mA (depends on protein size) under constant current in the precooled transfer buffer using Bio-rad Mini Trans-Blot Electrophoretic transfer Cell. After protein transfer the membrane was blocked in blocking solution (1x TBS, 5% Non-Fat milk) at room temperature for 1h. The blocked membrane was washed with TBST at room temperature three times for 10 min. the primary antibody diluted (depends on antibody) in 1x TBST, 5% Non-Fat milk and placed with blocked protein membrane in a rolling shaker at 4° C over night. On the following day the membrane was washed with 1x TBST at room temperature 3-4 times for 10 min.

The diluted HRP-labeled secondary antibody in 5% milk/TBS-T (1:2000) was applied at RT for 1h. Once again membranes were washed in 1x TBST at room temperature 3-4 times for 10 min. After final wash an enzymatic reaction was performed with the membranes using SuperSignaling® West Dura Extended Duration Substrate (Pierce) or ECL Western Blotting Analysis System (GE Healthcare) according to the manufacturer's instructions. After 5 min incubation the membranes were exposed in a dark room with X-ray film for 5 sec to maximum 1hr and the film was developed. An optimum exposure was determined according to the quality of the developed film.

<b>Transfer Buffer</b>	Tris	25 mM
	Glycin	200 mM
	Methanol	20 %
<b>TBS</b>	Tris	50 mM
	NaCl	150 mM
	pH 7.5	
<b>TBST</b>	Tween20 in TBS 0,1 %	

### 3.2.3. Bacterial Cell Culture

#### 3.2.3.1. Preparation of Electro Competent Cells

A single colony of E.coli strain DH5αLB was inoculated in 5 ml of LB medium and the culture was grown overnight in a shaker at 37° C. On the following day 1ml of

overnight culture was inoculated into 250ml of LB medium and the culture was grown to an  $O.D_{600}$  of 0.6. The culture was kept on ice for 10min, and transferred to prechilled tubes and centrifuged at 2600 g at 2° C for 15 min. To wash, the pellet was resuspended in 250 ml sterile ice cold 10% glycerol and centrifuged. The above washing steps were repeated for three times. The pellet was again resuspended in 10 ml and finally in 1 ml of sterile ice-cold 10% glycerol. 40  $\mu$ L of cells were aliquoted and frozen immediately in liquid nitrogen and stored at -80° C.

### 3.2.3.2. DNA Transformation in Competent Bacterial Cells

The electroporation method was used to transfer BAC or ligated plasmid DNA into competent bacterial cell. The aliquoted electro competent cells were thawed on ice and mixed with 1 $\mu$ L of ligation reaction or 10  $\mu$ g of freshly prepared BAC DNA.

The cells/DNA mix was transferred to a prechilled Pulse® electroporation (column size 0.1 cm) cuvette, and subjected to a 5 msec pulse in an electroporator for a pulse exposure of 1350 mV. LB medium was quickly transferred to the cuvette, and the mixture was gently pipeted up and down. The LB medium culture was incubated with shaking at 37° C for 1 hr. After incubation, 100  $\mu$ L cell culture was spread on LB medium plates with appropriate antibiotics and supplements. The rest of culture was centrifuged down to concentrate the cells to 100  $\mu$ L and transferred on to another LB plate. The plates were incubated overnight at 37° C for colony selection and further cultivation.

<b>LB Plates</b>	Bactoagar	10-15 %
	X-Gal	100 $\mu$ g/ml
	IPTG	80 $\mu$ g/ml
	Ampicillin	100 $\mu$ g/ml
	or Kanamycin	15 $\mu$ g/ml
	or Chloramphenicol	15 $\mu$ g/ml
	or Tetracycline	3 $\mu$ g/ml
<b>LB Medium</b>	Yeast extract	5 g
	Bactotrypton	10 g
	NaCl	10 g
	Ampicillin	100 $\mu$ g/ml
	ad.1000 ml H <sub>2</sub> O	
		or Kanamycin
	or Chloramphenicol	15 $\mu$ g/ml
	or Tetracycline	3 $\mu$ g/ml.

### 3.2.3.3. Homologous Recombination in Bacteria (Gap Repair)

Gap repair method is a new form of recombineering method for generating conditional knock out mutations in mice through targeting into ES cells. This is a phage based E.coli recombination system which allows to subclone larger DNA fragments from BAC into high copy number plasmid in a shorter time without need of any restriction enzymes and ligation process. The advantage of this method is greater flexibility of inserting the loxP sites and selectable marker cassette to any specific locations. Homologous recombination in E.coli is mediated by heat inducible (42°C) red proteins *exo*, *bet*, *gam* encoded by bacteriophage red genes from a defective prophage integrated into the E. coli chromosome.

To generate the SDF-1 conditional knockout vector we used E.coli strains DY380, EL250 and EL350. At first the homologous arms of 500bp length for the SDF-1 gene were PCR amplified from specific BAC DNA and cloned into pDTA vector and linearized. Later DY380 bacterial cells were cultivated by inoculating the glycerol stock into 5ml LB medium and cultured overnight at 32°C. Next day 1 ml of overnight culture was inoculated into 100 ml LB medium and cultured to an OD<sub>600</sub> of 0.5-0.6.

To perform heat induced homologous recombination in DY380 cells, the culture was kept at 42°C in a shaker for 15 min and then cooled on ice for 10min. After that the bacterial culture was pelleted down by centrifugation at 2500g for 10 min followed by three washing steps in sterile and prechilled 10% glycerol solution. Each washing step centrifugation was performed with increased speed at 3000g, 6500g and 7700g. After final washing, the pellet was dissolved well in a small volume of 10% glycerol and aliquoted into 40µl. The fresh aliquots were immediately used for electroporation or frozen in liquid nitrogen. The cells were electroporated with 1µl (50-100ng) of linear plasmid DNA along with BAC DNA. The cells were plated on LB medium with the appropriate antibiotic for positive colony selection of homologous recombination.

Similarly to target the first loxP site into plasmid DNA, the neo cassette vector was subcloned and homologues recombination was performed for the 3' side of exon1 of SDF-1 gene. To induce cre recombinase, EL350 cells were grown to an OD<sub>600</sub> of 0.4 and the culture was induced with L(+)- arabinose (a final concentration 0.1%) for 1 hour at 32°C. The EL350 cells were electroporated with pDTASDF-1 with 3' floxed neo vector and the positive clones for pDTASDF-1 with only one loxP sequence on

the 3' end of exon1 of SDF-1 were selected and similarly the second floxed neo cassette with only one loxP sequence was targeted into the targeting vector on the 5' side of exon1. Positive clones were selected and this construct was used as final targeting vector into embryonic stem cells. To verify the loxP and frt sequences in the final construct, the targeted plasmid vector was electroporated into both EL350, EL250 and selected for positive clones as described before.

### **3.2.4. Cell Culture**

The embryonic stem cells and feeder cells were kindly provided by the group Carmen Birchmeier at MDC and cultured according to Dieter Riethmacher and Alistair Garrat (C. Birchmeier).

#### **3.2.4.1. Preparation of Feeder Cells**

Frozen feeder cell vials from passage P2 or P3, were thawed rapidly in a 37°C water bath, seeded on 1X15cm culture dish and cells were allowed to grow to confluency. Then feeder cells were splitted by trypsin-EDTA treatment and resuspended in feeder medium and plated on 3X15 dishes to grow, and aliquoted into frozen cryovials stored at -70°C . A frozen aliquots was thawed and seeded on gelatine (0.1%) coated 15cm dish and the cells were treated with mitomycin C (1mg/ml) per 15cm dish and incubated for 2 hours at 37°C. After incubation cells were washed with PBS and fresh medium was added, the cells were trypsinized and seeded into new dishes, which are then ready to use for ES cell culture.

#### **3.2.4.2. ES Cell Culture and Electroporation**

A frozen ES cell vial was thawed rapidly in 37°C water bath and the cell suspension was transferred into 15ml Falcon tube with ES cell medium. The cells were centrifuged down and resuspended well in fresh ES cell medium to ensure proper singularization of cells. Cells were seeded on 6cm dish for 1-2 days and followed by trypsinization and plating on 10cm dish after 1-2 days of growth they are ready to be electroporated. To electroporate ES cells, the gene targeted vector was linearized and purified by phenol chloroform method and the concentration was determined. ES

cells in a final concentration of  $1.2 \times 10^7$  /800  $\mu$ l in PBS were mixed with 20 $\mu$ g of linearized vector and transferred to a electroporation cuvette and subjected to a 2 msec pulse in an electroporator for a pulse exposure capacity of 1200  $\mu$ F. After electroporation, cells were transferred to ES cell medium containing LIF and seeded on gelatine coated 3X10cm dishes with mitomycin treated feeder cells. On next day, cells were treated with G418 (400 $\mu$ g/ml) in ES cell medium and allowed to grow until colonies became visible with a spherical shape. The G418 resistant colonies were picked up into 96 well feeder plates and the cells were further splitted into two 96 well feeder plates. One plate of cells was kept frozen in freezing medium at -70°C for blastocyst injection and the second one was used for southern analysis to select positive clones. To perform southern analysis, the 96 well ES cell plates were treated with lysis buffer overnight at 55°C to 60°C and the DNA was precipitated with cold ethanol-salt mix. The DNA pellet was washed with 70% ethanol and dried. Restriction cocktail was added to the plates for digestion and southern analysis was performed as described before.

<b>Feeder Medium</b>	DMEM w/glutamax	500ml
	FCS	60ml
	Non essential amino acids (100x)	5.7ml
	Penicillin/Streptomycin (100x)	5.7ml
	Mercapto-ethanol (50mM)	1.2ml
<b>ES Cell Medium</b>	DMEM w/glutamax	500ml
	FCS	90ml
	Non essential amino acids (100x)	6.0ml
	Penicillin/Streptomycin (100x)	6.0ml
	Mercapto-ethanol (50mM)	1.2ml
	LIF	180 $\mu$ l
<b>G418</b>	Dissolve 100mg Geneticin in 1ml of ddH <sub>2</sub> O	
<b>Mitomycin</b>	Dissolve 2mg Mitomycin in 100 $\mu$ l of DMSO+1.9ml PBS	
<b>Freezing Medium</b>	ES Cell Medium	28.35ml
	FCS (25%)	15 ml
	DMSO (10%)	6.65ml

<b>Lysis Buffer</b>	Tris, pH7.5	10mM
	EDTA	10mM
	NaCl	10mM
	Sarcosyl	0.5%
	Filter and store at RT	
<b>EtOH-NaCl Mix</b>	Proteinase K	200µg/ml
	5M NaCl (or 3M NaAc pH5.2)	1.5µl
	EtOH	100 µl
<b>Restriction Cocktail</b>	Restriction enzyme buffer	1x
	Restriction enzyme	10-15 units
	BSA	100µg/ml
	RNAse	50µg/ml
	In 50 µl	

### 3.2.5. Animal Experiments & Breeding

#### 3.2.5.1. Animals

The SDF-1 knockout mice and transgenic rats were generated, bred and maintained in the animal facility of the Max-Delbrück Center for Molecular Medicine. All experimental protocols and organ collection were performed in accordance with the guidelines for the humane use of laboratory animals by MDC and were approved by Berlin State Office of Public Health and Safety and Security (LAGetSi). Experimental animals were maintained in a sterile environment of individually ventilated cages (Tecniplast) under standardized conditions (at a temperature of  $21\pm 2^{\circ}\text{C}$ , with a humidity of  $65\pm 5\%$ ) with an artificial 12 h light/dark cycle, with free access to standard chow (0.25% sodium; SSNIFF) and drinking water ad libitum. The pups were weaned at an age of 4-5 weeks and for the experiments all animals at the age of 12 weeks-20 weeks were used.

#### 3.2.5.2. Generation of SDF-1 Transgenic Rat

For production of transgenic rats, the SD Hanover rat strains was used. The female rats were induced to superovulate by intraperitoneal injection of gonadotrophin PMSG (Intervet), 48hr later followed by the injection of hCG (human chorionic

gonadotropin) and mated with males to collect the fertilized eggs on the following day. One cell embryos were cultured into M2 medium containing 0.1% (w/v) hyaluronidase to remove cumulus cells. The linearized DNA fragment (3ng/μl) was dissolved in microinjection buffer and microinjected into the male pronucleus of fertilised one-cell SD rat oocytes and eggs were transferred into the oviducts of pseudopregnant females. The pups born following microinjection were analyzed by PCR genotyping from the tails for transgene positive offspring.

<b>Microinjection Buffer</b>	Tris-HCl pH 7.4 EDTA	8 mM 0.15 mM
------------------------------	-------------------------	-----------------

### 3.2.5.3. Generation of SDF-1 Chimeras

To isolate blastocyst donors, 3-5 weeks old female C57Bl/6 mice were induced to superovulate by intraperitoneal injection of gonadotrophin PMSG (Intervet) and 48hr later followed by the injection of hCG and mated with males and checked for vaginal plugs on next morning. In parallel, for uterus transfer of blastocysts, pseudopregnancy was induced in female mice which were mated with vasectomized male (outbred - NMRI or F1 hybrid - C57Bl/6XDBA) and checked for vaginal plugs. The donor mice were sacrificed after 3.5 days and blastocysts were isolated in M2 medium and later incubated in M16 medium in a CO<sub>2</sub> incubator until microinjection. ES cells were injected into host blastocysts and embryos were transferred into day 2.5 foster mother. After 17 days new born pups were recognised by coat colour. The chimeric mice were inbred with C57Bl/6 for several generations and maintained on a C57Bl/6 background. The genotypes were analysed with southern hybridization and optimized PCR for routine analysis.

### 3.2.5.4. Echocardiography

The transthoracic echocardiographic examinations in mice were performed at the MDC with the help of technical assistant Martin Taube. Before conducting the echo measurements, mice were anesthetized by isoflurane inhalation; the chest hair was removed with a topical depilatory agent and applied with ultrasound transmission gel to both the transducer and the contact area on the mouse. The measurements were



made with a Visual Sonics Vevo 770 and a 45-MHz ultrasound linear probe especially suitable for the investigation of small animals.

Two-dimensional images were recorded in parasternal long and short-axis projections with guided M-mode recordings at the midventricular level in both views. LV wall thickness, interventricular septum (IVS) and posterior wall (PW) thickness, and internal dimensions at diastole and systole (LVIDd and LVIDs, respectively) were measured. LV fractional shortening  $[(LVIDd - LVIDs)/LVIDd] \times 100$  (%), LV Ejection fraction  $[(\text{end-diastolic}^3 - \text{end-systolic}^3) / \text{end-diastolic}^3] \times 100$  (%), and LV mass  $[1.05 (\text{IVS thickness} + LVIDd + \text{PW thickness})^3 - LVIDd^3]$  were calculated from the M-mode measurements.

### 3.2.5.5. Angiotensin-II Infusion in Mice

To perform angiotensin-II (Ang-II) infusion, 3-4 months old mice were used for experiments. For subcutaneous infusion of Ang-II (dose 1.4 mg/ kg/ 24h) in mice, Alzet osmotic pumps with pumping time of 14 days (pump model 1002, volume capacity 100 $\mu$ l) and 28 days (pump model 2004, volume capacity 200  $\mu$ l) were ordered and used according to the instructions. All the pumps chosen for infusion had a constant flow rate of 0.25  $\mu$ l/h. An average body weight of 25g per animal was taken for calculation and the pumps were filled with the appropriate amount of Ang-II solution, which was dissolved in sterile saline. To ensure the accuracy of pumps and the absence of air bubbles, the pumps were weighed before and after filling with Ang-II solution on a precise balance. The pumps were kept in sterile saline at 37°C for 24 hours prior to implantation.

For the implantation, the animals were anesthetized with isoflurane inhalation and the pumps were introduced through a 0.5-cm-long incision under the skin of the neck and sutured.

Pump Model	Volume Capacity	Flowrate	Duration
1002	100 $\mu$ l	0.25 $\mu$ l/h	14days
2004	200 $\mu$ l	0.25 $\mu$ l/h	28days

### **3.2.5.6. Cold Organ Preparation and Collection**

Mice were isoflurane anesthetized and opened from the abdomen to chest and blood was collected from the abdominal aorta and transferred immediately into EDTA tubes (7mM final concentration). The samples were centrifuged for 10 min at 2200 rpm at 4°C in a table centrifuge and aliquots were fractionated and stored at -80° C. Simultaneously, heart and lung were dissected out into a physiological saline solution, rinsed, and the relative organ weight was determined as % of body weight. The organs were quickly frozen in liquid nitrogen shortly and stored in -80°C.

$$\text{Relative organ weight (\%)} = \text{organ weight (mg)} / \text{body weight (mg)} \times 100\%$$

### **3.2.5.7. Electrocardiogram**

The mice were isoflurane anesthetized (1.6 vol% isoflurane/air) and the body temperature was maintained at 37°C using a heating pad and adhesive electrodes were inserted subcutaneously into the right forelimb and into each hindlimb. The standard ECG intervals were over 6 lines as measured by Royer et al. (2005) described. The basal ECGs lasted 5 min and then the animals were subjected to myocardial infarctions by performing permanent left coronary artery ligation (LAC) and the records lasted another 5 minutes. The acquired data were evaluated by offline analysis.

### **3.2.5.8. Permanent LCA Ligation**

These experiments in mice were conducted with the help of technical assistant Astrid Schiche. Control and mutant mice, 10-16 weeks of age, from the same background were used. Mice were isoflurane anesthetized and body temperature was kept at 37°C as described before. They were artificially ventilated with a respirator until end of experiment. Myocardial infarction (MI) in mice produced by permanent ligations of the left coronary artery (LCA) with a 7-0 nylon surgical suture under a dissecting microscope. Successful ligation of the LCA was verified visually by the colour change of the ischemic area, and ECG was monitored continuously throughout the operation.

After MI, mice were subjected to echocardiography measurements as previously described, at the time points 1,2,4 weeks and after 4 weeks of the mice were analyzed cardiac MRI. After physiological analysis mice were sacrificed and the organs were excised as previously described.

### **3.2.5.9. Cardiac MRI**

For the MRI experiments anaesthesia was induced using isoflurane (1.0-2.0 ppm in oxygen) keeping the mice free by breathing at a rate between 50-70 per minute. Body temperature and breathing rate were monitored during the whole experiment. Images were acquired on a 9.4T MRI system with the use of a four element surface coil dedicated to mouse brain imaging (Biospect, Bruker, Ettlingen, Germany). A set of coronal and axial slices were acquired in each animal using a T2 weighted turbo spin echo MRI-sequence with the following imaging parameters: FOV 2.5x2.5cm, Matrix 384x512, TE 33ms, TR 2200 (coronal slices) and 3800 (axial slices), slice thickness 0.3 mm, resulting in an in plane resolution of 50x70  $\mu$ m.

FOV: Field of View
TE: Echo time
TR: Repetition Time

### **3.2.5.10. Histological Methods**

#### **3.2.5.10.1. Tissue Fixation, Embedding and Sectioning**

To prepare the paraffin sections, tissues were freshly isolated and fixed for 48h in 4% PFA at 4°C. Then the specimens were washed twice with PBS and dehydrated in a methanol bath continuously (each 1h in 25%, 50%, 75% and twice in 100% methanol in PBS). This was followed by 1h incubation in 100% ethanol and 1h in toluene to dehydrate the preparations completely. For paraffin embedding, the biopsies were immersed in paraffin at 60°C. Two days after the biopsy was placed in fresh paraffin. To cut, the tissue was placed in a metal mold, aligned, layered with fresh paraffin and the grid was covered. After the paraffin has hardened the tissue was cut slowly either at 4°C or on the microtome (Microm HM360) in 5 microns slices. These sections were placed in 45°C bath to get smoothed and placed on glass slides.

#### **3.2.5.10.2. Hematoxylin and Eosin (H&E) Staining**

The hematoxylin and eosin (H&E) staining was based on the recommendations of the manufacturer's instructions. This staining method colours nuclei of cells in blue and the counterstaining with alcoholic solutions of eosin Y, colours other structures in red, pink or orange. Before staining, the paraffin sections were deparaffinized in 3x3' xylene baths, followed by descending ethanol series (3x3' 100%, 1x3' 95%, 1x3' 80%, 1x5' dH<sub>2</sub>O rehydrated) following the manufacturer's protocol.

#### **3.2.5.10.3. Masson-Goldner Trichrome Staining**

The masson trichrome staining was based on the recommendations of the manufacturer. It is a three dye staining protocol which shows muscle fibers and keratin in red, collagen and bone in blue or green, cytoplasm in pink or light red and nuclei in brown or black. This staining method was applied to visualize the fibrotic tissue in the heart. Before staining, the paraffin sections were deparaffinized in 3x5' xylene baths, followed by descending ethanol series (each 3x5' in 100%, 2x5' 96%, 1x5' 70%) following manufacturer's protocol.

#### **3.2.5.10.4. Sirius Red Staining**

Sirius red staining is the best known method to detect collagen. This staining method colours collagen in red on a pale yellow background and nuclei will be in black or brown (if stained). The sections were deparaffinized and rehydrated as described before and followed the manufacturer's protocol.

#### **3.2.5.10.5. Cryosections**

To produce cryosections, the freshly prepared heart tissue was rinsed in PBS and aligned on a piece of card board. The tissue was shortly frozen in 2-methyl butane which was previously cooled on dry ice. The sections were stored at -80 ° C. Before cutting, the tissue was directly aligned on the stamp of the cryostat and embedded with TissueTec. The frozen sections were performed with a cryostat (HM560 Microm Cryo-Star; Microm customized), and the average thickness was 12 or 20 microns.

The sections were mounted on adhesive slides, dried at 37 ° C and airtight packaging stored at -80 ° C.

#### **3.2.5.10.6. Immunofluorescence Staining on Cryosections**

To perform immunofluorescence staining on frozen sections, the section containing slides were first thawed, dried at room temperature, and fixed in acetone for 10 min at -20°C. The section was equilibrated for 30 min at RT or left in 1x PBS pH 7.4 for 10 min to swell. Subsequently, the slides were incubated for 15-30 min with PBS-T (1xPBS and Tween 20). Then they were kept in a moist chamber for 30 min and blocked with 5% normal donkey serum in PBS-T. It follows overnight incubation with the primary antibody in 1xPBS at 4° C in a moist chamber. On the following day the slides were washed 3X15' with TBS. Subsequently, the objects were incubated for 2 hours with a fluorescence-coupled secondary antibody and washed again 3x15' with TBS. Before the section was viewed by a fluorescence microscope, it was embedded in a DAPI (4',6-diamidino-2-phenylindole) containing medium to stain the nuclei.

## 4. Results

### 4.1. Generation of the SDF-1 $\alpha$ Transgenic Rat

#### 4.1.1. Cloning of DNA Construct for the Overexpression of SDF-1 $\alpha$ in Rat Heart

To generate a transgenic rat line with cardiomyocyte specific overexpression of SDF-1 $\alpha$ , short genomic DNA PCR fragments were subcloned into the multiple cloning site of pBluescript SK+ vector followed by BAC recombineering method. To this construct myosin light chain-2 (MLC-2) promoter was cloned upstream of the SDF-1 $\alpha$  sequence to achieve tissue specific expression (Fig.9A). The final pBluescript SK+ (MLC2SDF-1 $\alpha$ ) construct was released by digesting with restriction enzymes KpnI and NotI and separated on agarose gel electrophoresis (Fig.9B). The desired construct was purified with gel extraction method and dissolved in microinjection buffer. The resulting 9kb DNA construct was microinjected into male pronucleus of zygotes, which were then reimplanted into pseudopregnant rats.

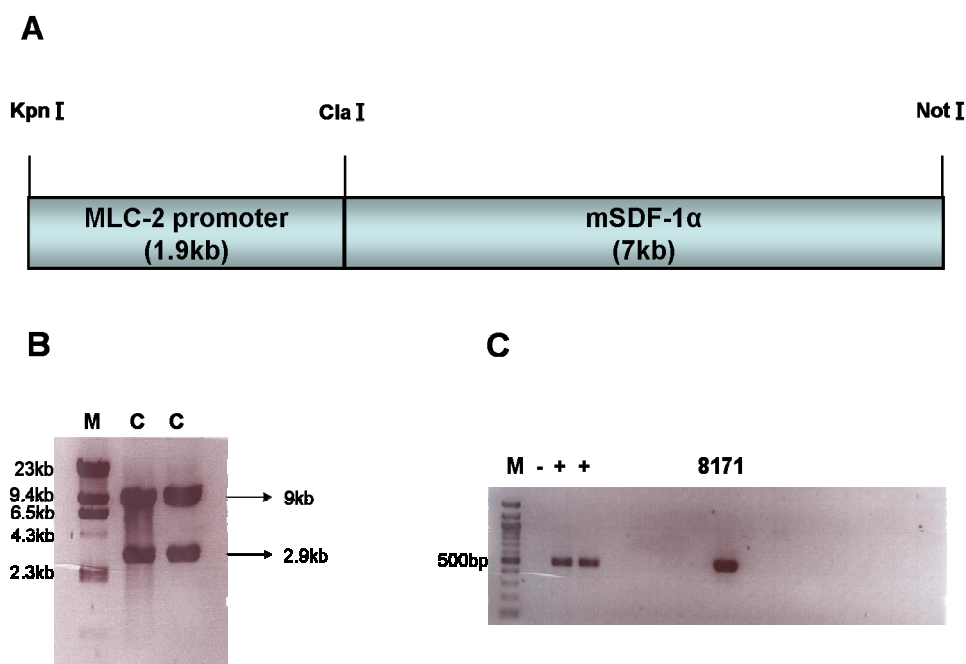


**Fig.9: Construct to produce the transgenic rat with cardiomyocyte specific overexpression of SDF-1 $\alpha$ .** (A) Schematic representation of cloning the MLC-2 promoter and mouse SDF-1 $\alpha$  gene into pBluescript SK+ vector. (B) The cloned vector was restriction digested with KpnI and NotI for pronuclear injection. M, Marker; C, transgenic construct. (C) Detection of positive founder Line 8171 by PCR genotyping. M, marker; +, positive control and -, negative control.

The micro-injection has been performed in the laboratory of Prof. Dr. Michael Bader, at Max Delbrück Center for Molecular Medicine. PCR genotyping analyses were done and a positive founder (8171) was obtained (Fig 9C). The founder was further mated with wild type rats to get heterozygous animals for experiments.

#### 4.2. Expression Analysis of SDF-1 $\alpha$ in the Transgenic Rat Heart

The transgenic overexpression of SDF-1 $\alpha$  in rat heart was analyzed with detection of protein by western blot analysis. However the transgenic line 8171 showed no overexpression of SDF-1 $\alpha$  as compared with basal expression of SDF-1 $\alpha$  in control rats (Fig 10). Due to lack of proper overexpressing model we were not able to perform further functional studies with this line.

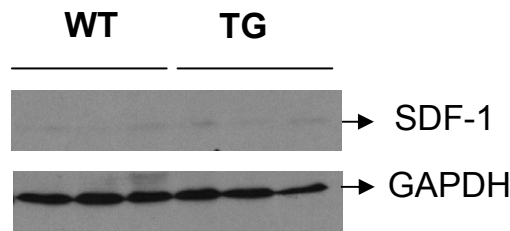


**Fig.10: Detection of cardiomyocyte specific SDF-1 $\alpha$  overexpression in the transgenic rat.** Western blot analysis of SDF-1 $\alpha$  and GAPDH protein in the cardiac homogenate of wild type and transgenic rats.

#### 4.3. Generation of the Conditional SDF-1 Knockout (KO) Vector

##### 4.3.1. Construction of the Cre-LoxP Vector

Gene targeting in embryonic stem cells has become a powerful method to produce KO mice and elucidate the gene function. However, ubiquitous deletion in mice might lead to embryonic lethality and is of limited use for postnatal studies. To avoid these problems, Cre-LoxP system has been developed to produce conditional KO mice. This system allows producing mice with tissue and timely specific deletion of gene. To produce Cre-LoxP vector for SDF-1 gene we followed the protocol of BAC recombineering or GAP repair method as described before by Copeland *et al.*

## Results

The schematic representation of Cre-LoxP vector construction was shown in Fig.11A. The genomic DNA fragment containing SDF-1 exon1 was subcloned from BAC (RP24-195P20) into linearized plasmid DTA (pDTA) vector using GAP repair method.

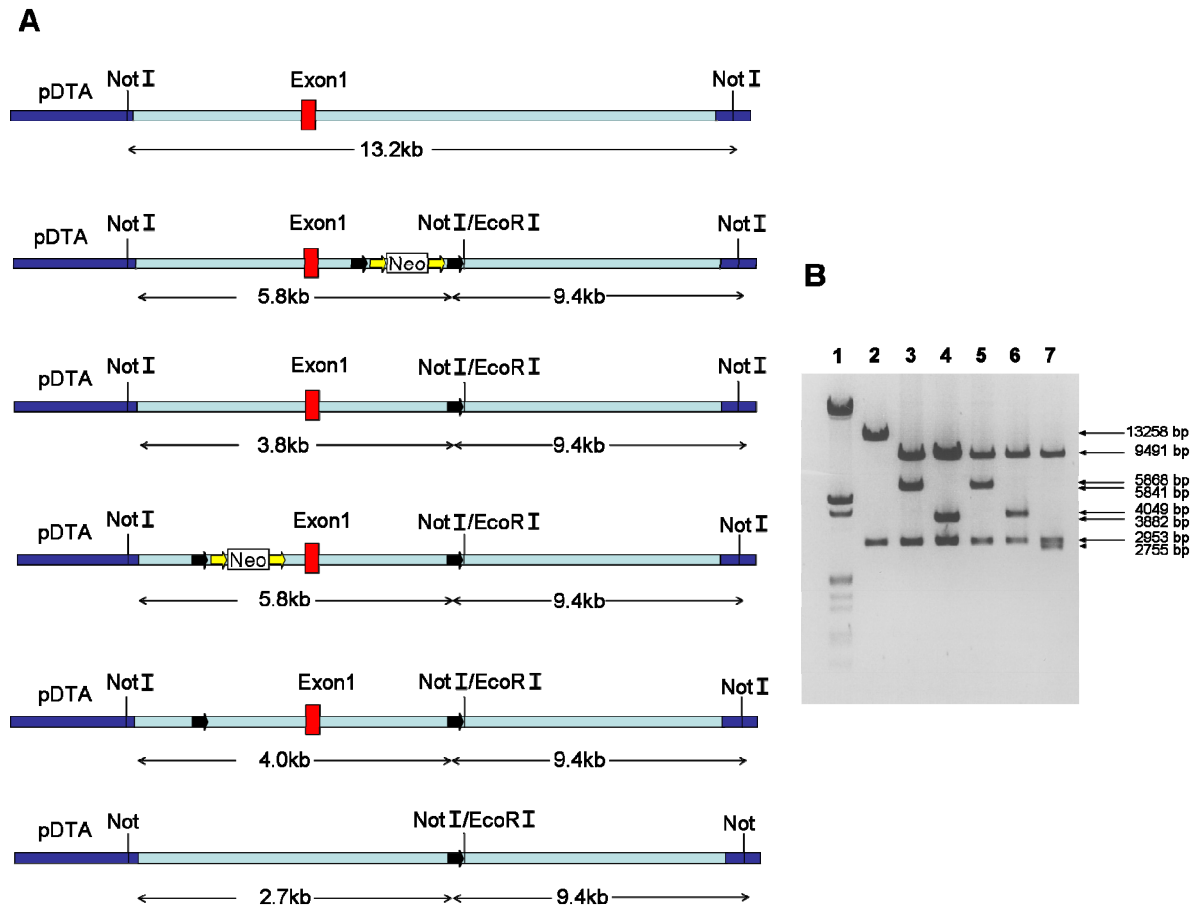


**Fig.11: Construction of the Cre-LoxP vector to produce the conditional SDF-1 KO mice.**

(A) Schematic representation of sequential steps to introduce the genomic DNA and loxP sequence into pDTA vector using homologous recombination method (Black arrows – loxP sequences, Yellow arrow – *frt* sequences). (B) Restriction digestion pattern of all plasmids with NotI enzyme during gene targeting vector construction. Lane 1, Marker; Lane 2, BAC DNA retrieved pDTA; Lane 3, first targeting vector with floxed Neo cassette; Lane 4, excised Neo cassette vector; Lane 5, second targeting vector with floxed Neo cassette; Lane 6, flpe recombinant based excised Neo cassette; Lane 7, cre recombinant based excised exon-1 pDTA-SDF-1 construct.

To confirm the retrieving of BAC DNA into the pDTA vector, the vector DNA was restriction digested with NotI (Fig.11B, 2). The 13.2 kb fragment represents the exon1 and flanked intronic sequences of SDF-1 gene and 3kb fragment present in all lanes is the pDTA backbone sequence. After BAC DNA sequence retrieved into pDTA, the vector was targeted with first loxP site. This site was introduced downstream of the SDF-1 exon1 sequence. This was achieved by homologous



recombination of a floxed neomycin cassette (Neo) into pDTA vector followed by removing Neo gene by cre recombinase which leaves a single loxP sequence. Digesting the floxed Neo cassette containing vector with NotI enzyme releases 9.4kb and 5.8kb fragments (Fig.11B, 3) and excision of Neo cassette gives the 9.4kb and 3.8kb fragments (Fig.11B, 4). Similarly, the final construct to target ES cells was accomplished by targeting the second loxP sequence upstream of the SDF-1 exon-1 but not removing the Neo cassette this time. The restriction digestion with NotI again shows similar pattern like before in Lane 3 (Fig.11B, 5). However, before targeting the final construct into ES cells, the constructs were tested for the excision of exon-1 by cre recombinase and of the Neo cassette by flp recombinase and then digested with NotI. The Neo excised construct shows fragments sizes 9.4kb and 4.0kb similar to L4 (Fig.11B, 6) and exon-1 excised constructs shows 9.4kb and 2.7kb fragments (Fig.11B, 7) indicating correct cloning of the construct.

#### 4.4. Gene Targeting in ES Cells

The final construct for the conditional KO vector was released with PmeI and electroporated into ES cells to achieve homologous recombination between targeting construct and wildtype SDF-1 gene locus (Fig.12A).

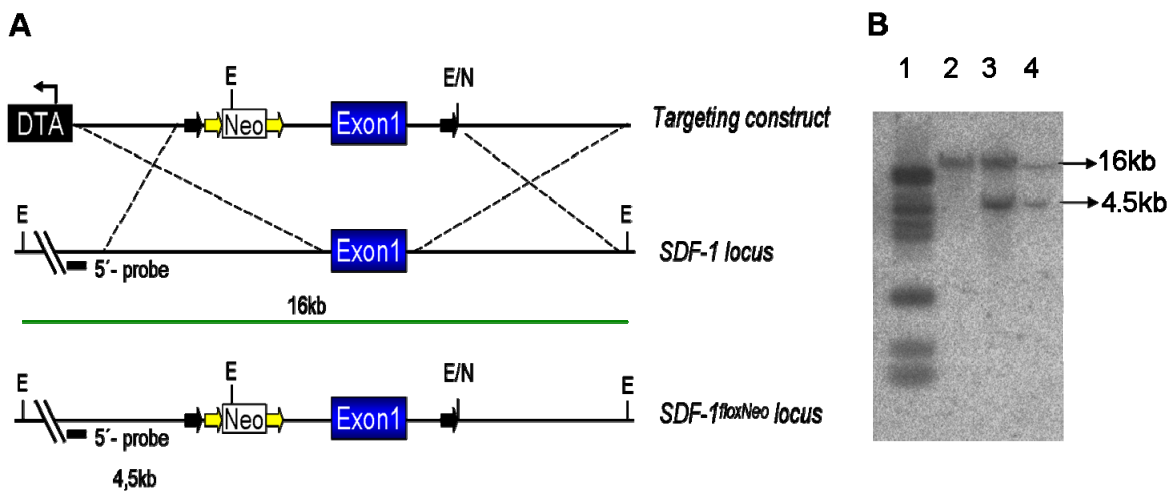


**Fig.12: Strategy to introduce SDF-1 targeted mutation into ES cells.** (A) Diagrammatic representation of homologous recombination of targeting construct and wildtype SDF-1 locus in ES cells. DTA cassette for negative selection, Black arrows – loxP sequences, Yellow arrows – *frt* sequences and neomycin cassette as Neo. The exon1 for SDF-1 shown in blue rectangles is flanked by loxP sites. The restriction sites *EcoRI* and *NotI* marked as E and N and expected *EcoRI* digested fragment are 16kb (wild type) and 4.5kb (floxed). (B) Restriction digestion and southern blotting of ES cell clones. Lane 1, Marker; Lane 2, control ES cell DNA (wild type); Lane 3&4, targeted ES cell DNA (with one floxed allele).

The antibiotic resistant clones were selected by ganciclovir and G418 treatment. The positive clones for successful homologous recombination were tested with southern hybridization. Due to the presence of an EcoRI site in the floxed Neo cassette the genomic DNA from positive clones will generate 16kb (wild type) and a 4,6 kb (floxed allele) fragment after digested with EcoRI, where as the control DNA has only a 16kb fragment from the wild type SDF-1 locus (Fig.12B).

#### 4.5. Generation of the Complete SDF-1 KO Mice

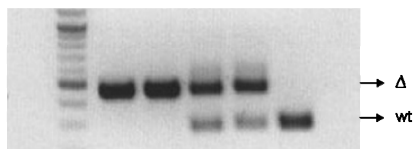
A earlier study by Nagasawa *et al.* showed that complete SDF-1 KO mice exhibit embryonic lethality with multiple developmental defects. In order to verify the phenotype of complete SDF-1 KO mice with our floxed SDF-1 model, we generated a SDF-1 KO model by breeding the SDF-1<sup>flox</sup> mice with CMV cre transgenic mice. As expected, the ubiquitous deletion of SDF-1 results in perinatal death of embryos (E17-E18.5).

**A**



-/-      -/-      +/-      +/-      +/+  
1      2      3      4      5

**B**



M 1 2 3 4 5

**C**

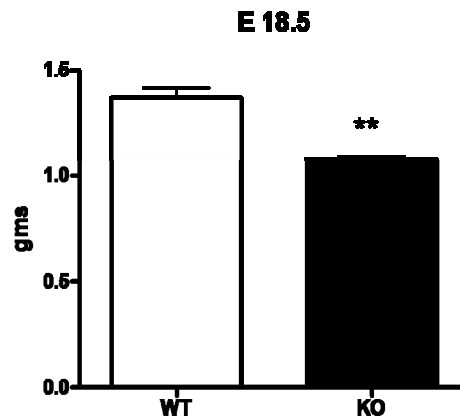


**Fig.13: Complete KO of SDF-1 and embryonic analysis.** (A) Homozygous mutants (KO) from embryonic day 18.5 (1,2) displayed smaller size compared with heterozygous and wild type (WT) mice (3,4,5). (B) Genotypings by PCR with tail DNA of embryos (C) SDF-1 mutants have reduced body weight at embryonic day 18.5. WT n=6, KO n=4. \*\*p<0.01

The homozygote mutants appeared to be smaller in size and have reduced body weight (75-80%) in comparison to controls and heterozygotes (Fig.13A&C). The PCR genotyping results correlated with body weights of embryos. The homozygote mutants have product size of 480bp ( $\Delta$ , deleted allele), controls have 280bp (wt, wild type allele) and heterozygotes show both products (Fig.13B). RT-PCR analysis from two different organs such as liver and lung showed the complete lack of SDF-1 expression in homozygote mutant embryos, whereas basal expression was observed in both heterozygotes and wild type mice (Fig.14A). Examination of  $\beta$ -actin as housekeeping gene for endogenous reference was observed in all groups. In addition to that, histological analysis (H&E staining) of the embryonic hearts from SDF-1 mutants also revealed ventricular septal closure defects (Fig.14B). Our data reproduced previous data of Nagasawa *et al.* confirming that our knockout strategy leads to the complete ablation of SDF-1 expression after cre mediated excision and suggested that SDF-1 is crucial for embryonic development.

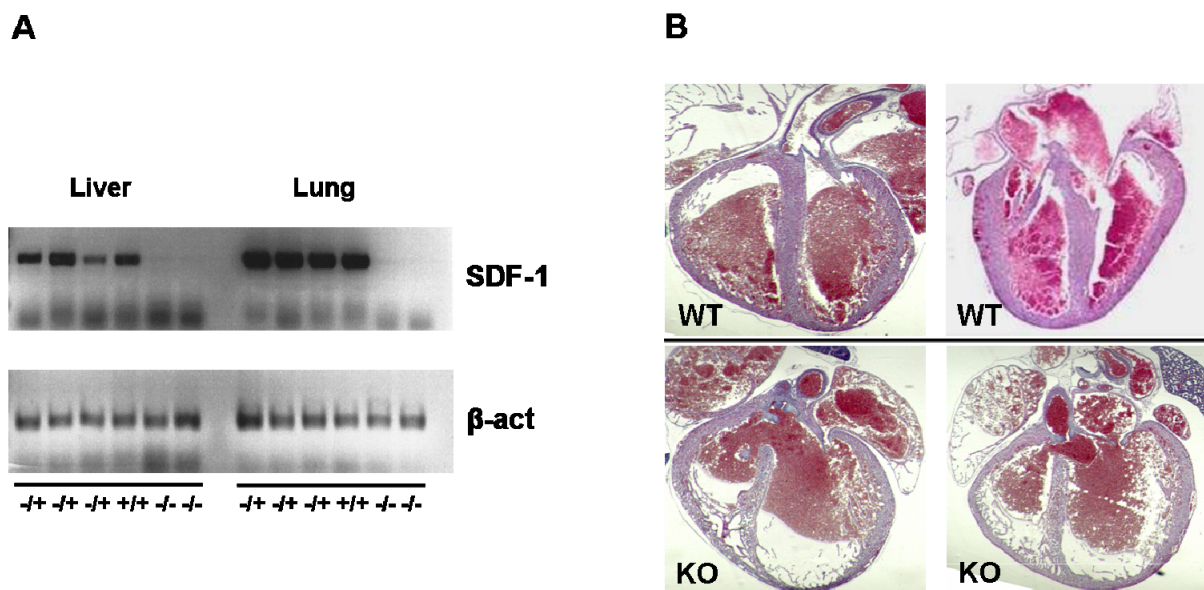


**Fig.14: RT-PCR and histological analysis of KO embryos** (A) Reverse Transcription (RT)-PCR analysis of mRNA from E18.5 organs (liver and lung) for SDF-1 and  $\beta$ -actin (+/+; wild type, +/-; heterozygote, -/-; homozygote). (B) Histological analysis by H&E staining of E18.5 heart sections of SDF-1 mutants showing ventricular septal defects.

#### 4.6. Generation of the Cardiomyocyte Specific SDF-1 KO (cKO) Mice

In order to understand the function of SDF-1 in postnatal heart we produced cardiac tissue specific KO mice of SDF-1. To generate this model the floxed SDF-1 mice

were bred with ventricular cardiomyocyte specific MLCv<sup>cre</sup> transgenic mice (Chen *et al.* 1998). However to obtain this model we adopted the methodology as described before by Özcelik *et al.* 2002. The SDF-1<sup>flox/flox</sup> mice were crossed with mice heterozygous for a null mutation of SDF-1 that also carries the MLCv<sup>cre</sup> allele (MLCv<sup>cre/+</sup>; SDF-1<sup>+/-</sup>). The offspring were born at mendelians ratio and viable. To distinguish the genotypes, mice were tested by routine PCR analysis. The PCR was optimized to distinguish between wild type allele (wt), floxed allele (flox) and deleted allele ( $\Delta$ ) (Fig.15A). In heterozygote mice (SDF-1<sup>+/flox</sup>; MLCv<sup>cre/+</sup>) specific deletion was observed in cardiac tissues sample whereas deletion was not observed in other tissues such as tail DNA samples. However, due to the null allele in homozygote (SDF-1<sup>-/flox</sup>; MLCv<sup>cre/+</sup>), it is not possible to distinguish the deletion allele between cardiac and tail DNA samples. Further southern hybridization was performed to detect the recombination efficiency of DNA samples from cardiac samples between three different genotypes (SDF-1<sup>+/flox</sup>, SDF-1<sup>+/flox</sup>; MLCv<sup>cre/+</sup>, SDF-1<sup>-/flox</sup>; MLCv<sup>cre/+</sup>) (Fig.15B). The recombination efficiency was more then 60% in homozygous mutant tissue and lack of 100% was due to mosaicism of cre expression and other cell types present in heart preparations.

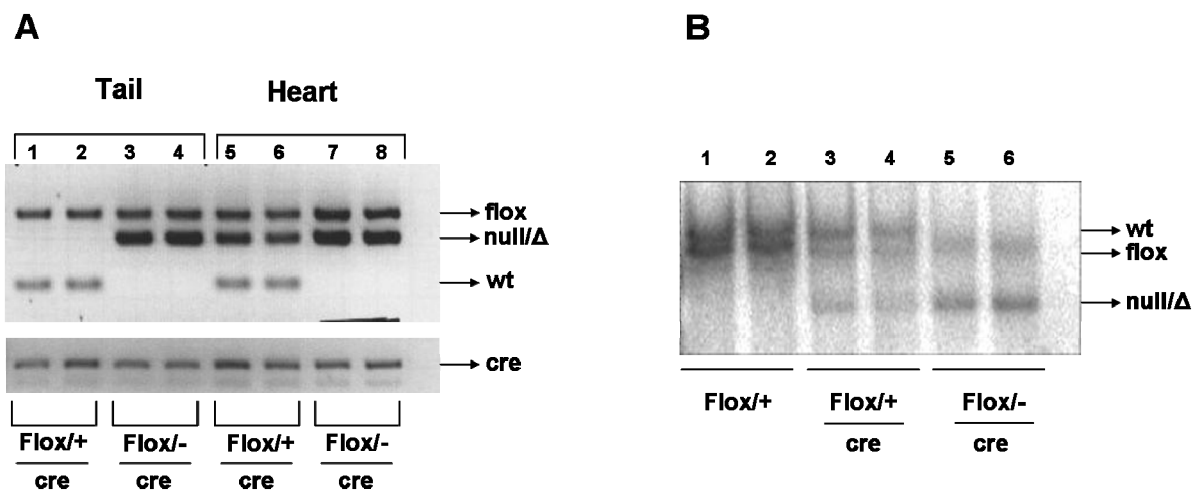


**Fig.15: Cardiomyocyte specific mutant model for SDF-1.** (A) PCR genotyping of genomic DNA from tail (lanes 1-4) and heart (lanes 5-8), of MLC2v<sup>cre/+</sup>; SDF-1<sup>flox/+</sup> (control mice, lanes 1,2,5,6) or MLC2v<sup>cre/+</sup>; SDF-1<sup>flox/-</sup> (conditional SDF-1 mutant mice, lanes 3,4,7,8). (B) Southern hybridization of cardiac DNA samples of mice digested with enzyme EcoRV and NotI. The genotypes used for analysis were SDF-1<sup>flox/+</sup> (lanes 1,2), MLC2v<sup>cre/+</sup>; SDF-1<sup>flox/+</sup> (lanes 3,4), MLC2v<sup>cre/+</sup>; SDF-1<sup>flox/-</sup> (lanes 5,6). The fragment sizes were 10.8 kb (wt), 8.5 kb (flox), 6.5 kb (null/ $\Delta$ ).

#### 4.7. Expression Analysis of Cardiac SDF-1 Levels in cKO Mice

The Expression of cardiac SDF in cKO mice was analyzed by real-time taqman method. The specific primers and probes for detection of SDF-1 were designed and the quantification was normalizing with the internal reference control gene GAPDH. The cardiomyocyte KO mutant hearts showed significant reduction of SDF-1 expression in comparison to control hearts (Fig.16A). Simultaneously SDF-1 protein quantification performed by western blot method (Fig.16B), and relative quantification against GAPDH also displayed decrease in SDF-1 protein expression in ventricular tissue (Fig.16C).

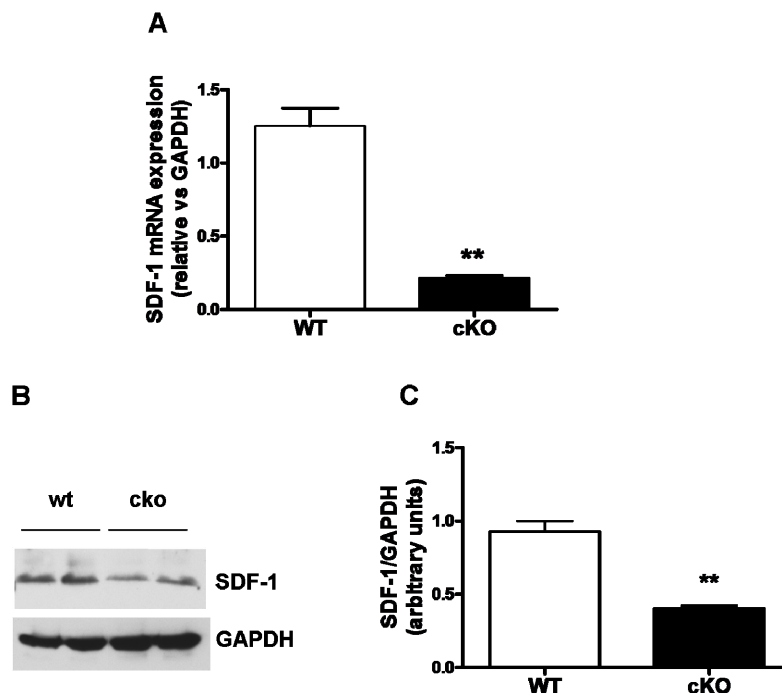


**Fig.16: Expression analysis of myocardial SDF-1.** (A) Real-time PCR quantification of mRNA in heart tissues of wild type (WT) and cardiac KO mice (cKO). WT n=3, cKO n=3. (B) Western blot detection of SDF-1 protein and endogenous reference protein GAPDH. (C) Relative quantification of SDF-1 protein normalizing with GAPDH protein. \*\*p<0.01

#### 4.8. Characterization of Basal Cardiovascular Physiology of the SDF-1 cKO Mice

The cardiomyocyte specific KO mice showed no mortality during postnatal life and appeared normal without any malformation. The cKO mice were used for further physiological studies.

#### 4.8.1. Echocardiography Characterization of Cardiac Function

Echocardiography (ECHO) is a standard ultrasound method used to diagnose cardiovascular disorders. Besides electrocardiogram (ECG), echocardiography is a one of the major noninvasive methods to record the two dimensional image of the heart. This method allows measuring the geometry of the left ventricle such as LV wall thickness and internal diastolic and systolic diameters. In addition to that, from the diameters the accurate assessment of cardiac functional parameters including ejection fraction (EF) and fractional shortening (FS) is possible. EF is considered as a main predictor for prognosis of cardiac function. In general, the healthy individual should have an ejection fraction between 50%-65%. Patients with poor prognosis of cardiac function have significantly reduced EF.

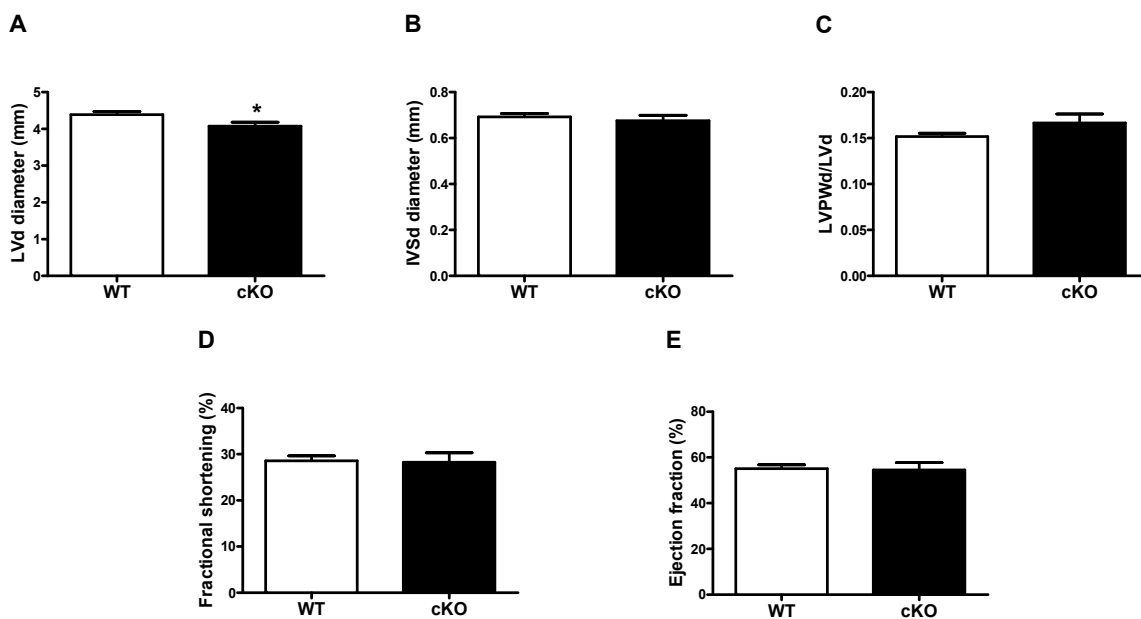


**Fig.17: Echocardiographic analysis of 3 months old cardiomyocyte specific SDF-1 KO (cKO) and wild type (WT) mice.** Diastolic diameter of left ventricle (A) and intraventricular septal thickness (B) and the ratio of left ventricular diastolic posterior wall thickness and diastolic diameter (LVPWd/LVd) (C) are shown. Systolic functional parameters, fractional shortening (D) and ejection fraction (E) were determined. All the parameters showed no significant changes between WT and cKO groups except the moderately reduced diastole diameter in cKO mice. The data represents means  $\pm$  standard error of mean. WT  $n=16$ , cKO  $n=10$ . \* $p<0.05$

To characterize the cardiac function under basal conditions we used the cKO SDF-1 mice for echocardiographic analysis at the age of 3 months. The cKO mice showed moderately smaller diastolic diameters (Fig.17A); nevertheless, these mice showed no significant difference in their left ventricular performance and no signs of any abnormal geometry of cardiac chambers compared to control groups. From the analysis of EF and FS, no altered systolic and diastolic function was observed in cKO in compared to controls (Fig.17D&E). The intraventricular septal thickness (IVS), a measurement for cardiac hypertrophy that also not showed any difference in these groups (Fig.17B) and similarly the ratio of left ventricular posterior wall thickness in diastole (LVPWd) and the diastolic diameter (LVd) of the left ventricle was the same in both groups (Fig.17C). These mice were again analyzed with echo measurements at the age of 12 months. In this group we also couldn't observe any significant difference in cardiac functional parameters (Fig.18A&B).

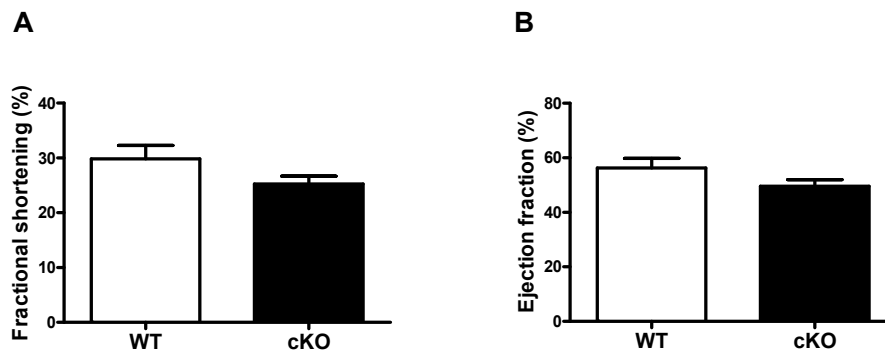
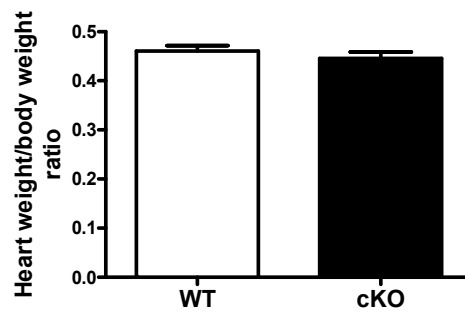


**Fig.18: Echocardiographic analysis of 12 months old cardiomyocyte specific SDF-1 KO (cKO) and wild type (WT) mice.** Systolic functional parameters, fractional shortening (A) and ejection fraction (B) were determined. All the parameters showed no significant changes between WT and cKO groups. The data represents means  $\pm$  standard error of mean. WT  $n=9$ , cKO  $n=6$ .

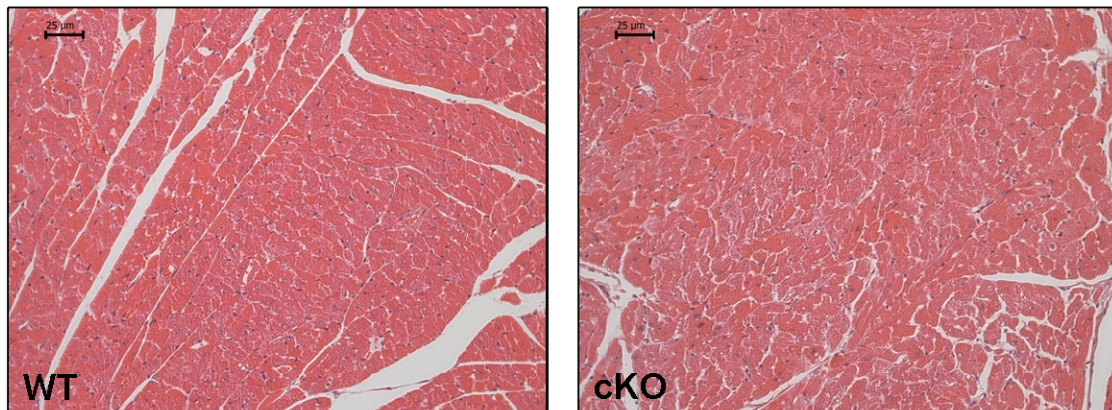
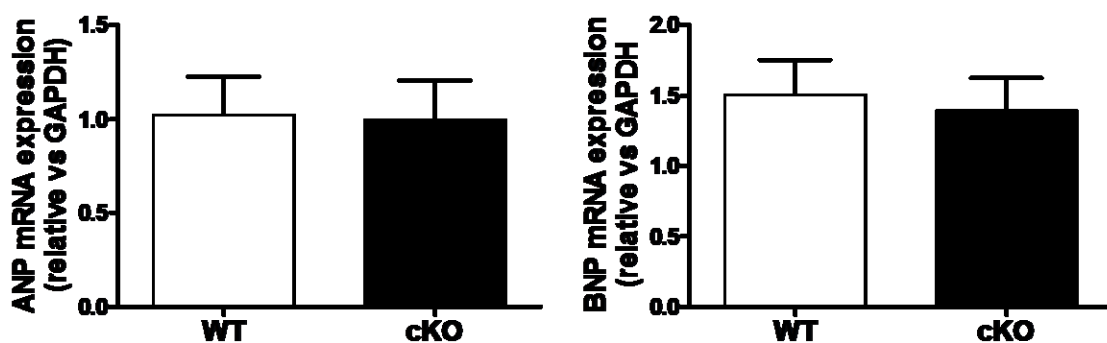
#### 4.8.2. Cardiac Morphology and Histology of SDF-1 cKO Mice

After the echocardiography analysis had revealed no significant differences between wild type and the mutant animals, we performed cardiac morphology and histological studies to confirm this phenotype. Initially, we measured the heart weight to body weight ratio as indicator for cardiac hypertrophy (Fig 19). As expected, we couldn't detect any abnormality in the ratio between mutants and controls.





**Fig.19: Heart weight to body weight ratio of SDF-1 mutants and WT mice.** The heart weight to body weight ratio of 3 months old mice showed no significant differences. The data represents means  $\pm$  standard error of mean. WT n=11, cKO n=9.

**A****B**

**Fig.20: Histology and quantification of cardiac hypertrophy markers in 12 months old mice.** (A) Hematoxylin-eosin (H&E) staining of heart sections of wild type (WT) and SDF-1 mutant mice (cKO). (B) Quantification of mRNA expression of cardiac hypertrophy markers ANP and BNP relative to the expression of the housekeeping gene GAPDH using TaqMan-PCR<sup>®</sup>. The relative quantification between the two groups shows no significant difference. The data represents means  $\pm$  standard error of mean. WT n=6, cKO n=6.



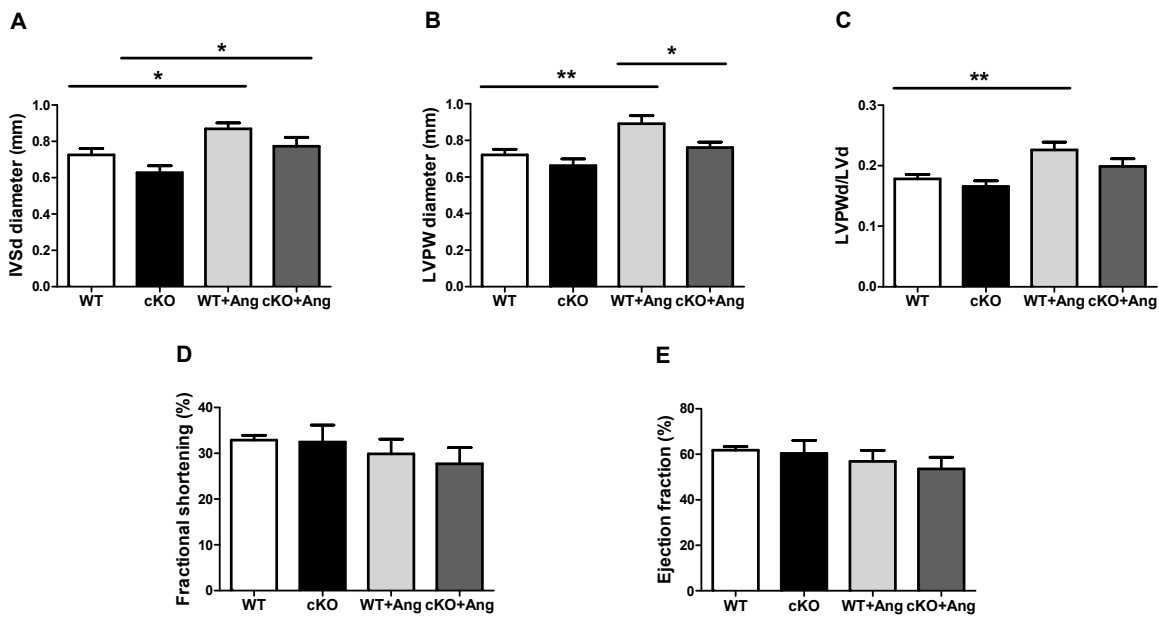
Furthermore, histological staining was performed with the hematoxylin-eosin (H&E) method to detect any aberrant muscle structure (Fig 20A). These staining also showed no signs of hypertrophy and normal morphology in mutant hearts. Finally, we quantified the expression of the cardiac hypertrophy markers, atrial natriuretic peptide (ANP) and Brain natriuretic peptide (BNP) (Fig.20B) in cardiac tissues by using TaqMan<sup>®</sup> quantitative – PCR method. The ANP and BNP mRNA levels were not altered between the wild type and mutant groups.

#### **4.9. Cardiac Function and Morphology of SDF-1 cKO Mice in Ang-II Induced Cardiac Hypertrophy**

To investigate the pathological role of SDF-1 in the myocardium during cardiac hypertrophy, cardiac hypertrophy was induced in SDF-1 mutants and control mice with angiotensin-II (Ang-II) using osmotic mini pumps for two weeks. The hypertrophy induced mice were analyzed by echocardiography and histological studies.

##### **4.9.1. Echocardiography Characterization of Cardiac Function in Cardiac Hypertrophy**

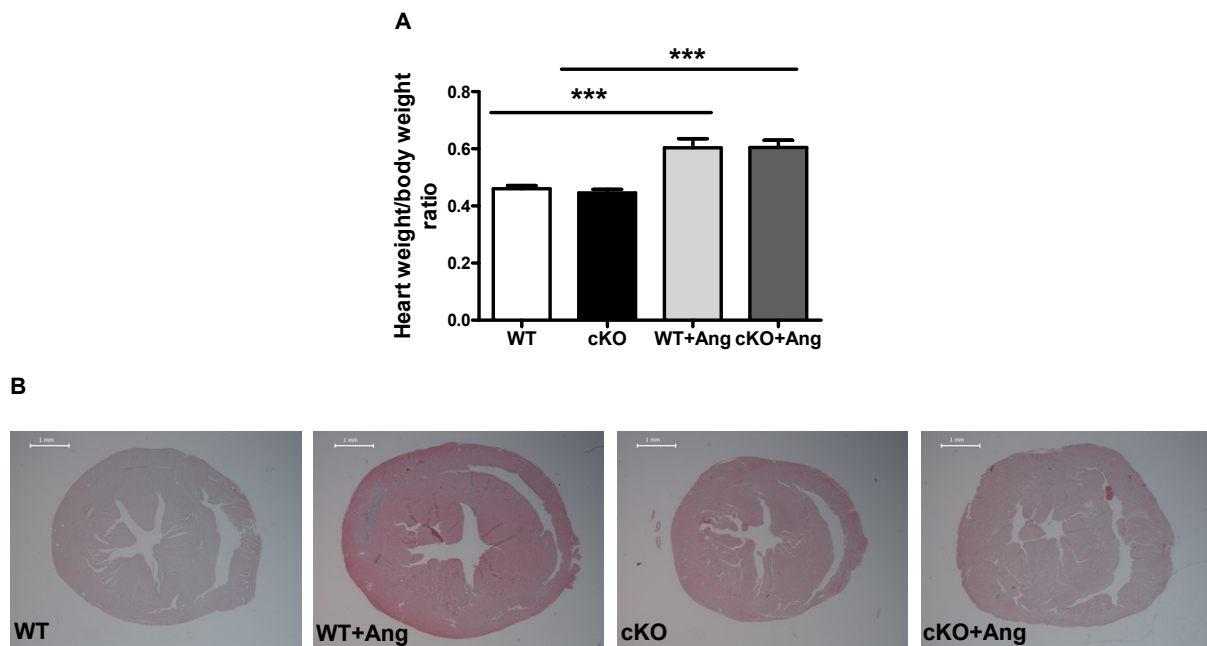
Echocardiographic assessment of cardiac function of 3 months old SDF-1 cardiomyocyte specific mutants and wild type controls after Ang-II induction showed increased geometry of left ventricular chamber diameters in both groups with increased interventricular septum and posterior wall thickness (Fig.21A&B). However the mutants exhibited a moderate resistance to cardiac hypertrophy including the reduced posterior wall thickness and the ratio of posterior wall thickness and left ventricular diastolic diameter compared to controls (Fig.21B&C). The geometry of chambers, the left ventricular diastolic and systolic diameters and cardiac contractility parameters such as ejection fraction (Fig.21F) and fractional shortening (Fig.21E) were not significantly changed in both groups after Ang-II induction.



**Fig.21: Echocardiography analysis of 3 months old cardiomyocyte specific SDF-1 KO (cKO) mice and wild type (WT) in Ang-II induced cardiac hypertrophy.** Intraventricular septal thickness (A) and posterior wall thickness (B) and the ratio of left ventricular diastolic posterior wall thickness and diastolic diameter (LVPWd/LVd) (C) are shown. The systolic functional parameters, fractional shortening (D) and ejection fraction (E) were determined. The data represents means  $\pm$  standard error of mean. WT n=7, cKO n=6, WT+Ang n=6, cKO+Ang n=6. \* $p$ <0.05, \*\* $p$ <0.01

#### 4.9.2. Cardiac Morphology and Histology in Cardiac Hypertrophy

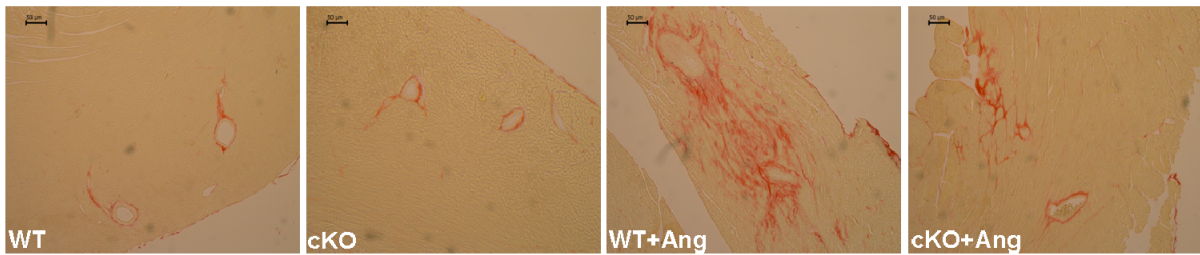
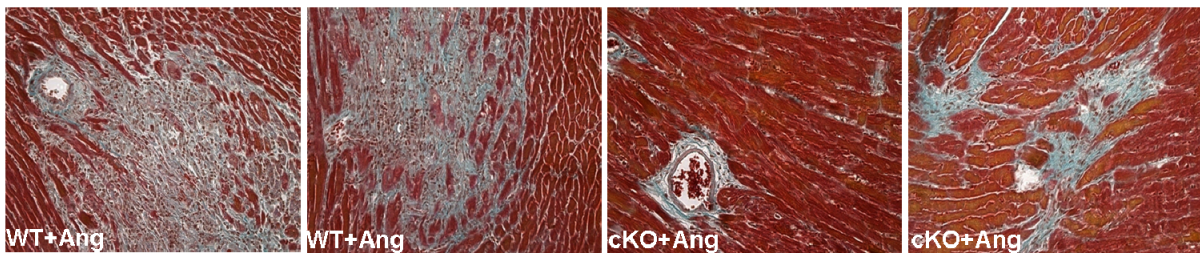
Based on the echocardiography analysis, increase in left ventricular hypertrophy after stimulation with Ang-II was further quantified by measuring heart weight body weight ratio. Both untreated mutant and control groups were compared with Ang-II treated groups (Fig.22A). After Ang-II treatment both groups have a significant increase in the heart weight to body weight ratio, however, there was no significant difference between wild type Ang-II and cKO Ang-II groups. The histological staining was performed with H&E method to detect aberrant muscle structure (Fig.22B). This staining also showed induction of cardiac hypertrophy in mutant hearts and control hearts compared to untreated groups. However, the hypertrophy between the treated groups was not significantly different.



**Fig.22: Relative heart weight to body weight ratio and morphology of SDF-1 cKO mutants and wild type mice during Ang-II induced cardiac hypertrophy.** (A) The heart weight to body weight ratio of 3 months old mice showed statistically significant differences after stimulation with Ang-II. (B) Hematoxylin-eosin (H&E) staining of transverse heart sections of wild type (WT) and SDF-1 mutant mice (cKO) and Ang-II stimulation groups. The data represents means  $\pm$  standard error of mean. WT n=11, cKO n=9, WT+Ang n=6, cKO+Ang n=6. \*\*\* $p$ <0.001

#### 4.9.3. Histological Analysis of Cardiac Fibrosis in Cardiac Hypertrophy

Angiotensin-II is known as a key factor involved in the pathogenesis of cardiovascular diseases, through the regulation of inflammation and fibrosis. Due to the profibrotic effect it induces both interstitial and perivascular cardiac fibrosis. Here, we analyzed the histochemistry of cardiac fibrosis levels in our experimental model by different histological staining methods such as Masson's trichrome (Fig.23B) and Sirius red (Fig.23A). These methods allow the detection of collagen fibers in heart sections. Basal cardiac fibrosis in controls and mutants is undetectable and very low staining was seen in small vessels. As expected intense perivascular and interstitial fibrosis was observed in controls after the Ang-II stimulation, however the cardiac SDF-1 mutants showed significantly less cardiac fibrosis.

**A****B**

**Fig 23: Representative Sirius red and Masson's trichrome staining of SDF-1 (cKO) mutants and wild type (WT) mice in Ang-II induced cardiac hypertrophy.** (A) Sirius red staining of collagen fibers (red) in left ventricular transverse sections of heart from all four experimental groups (WT, cKO, WT+Ang, cKO+Ang). (B) Masson's trichrome staining of collagen content (blue) in left ventricular transverse sections of heart from Ang-II stimulated groups (WT+Ang, cKO+Ang).

#### 4.9.4. Gene Expression Analysis in Cardiac Hypertrophy

The cardiac functional and histological data obtained during Ang-II induced hypertrophy suggested that cKO SDF-1 mutants are moderately resistant against cardiac hypertrophy and fibrosis. In order to further confirm this cardiac protection in mutants, we performed gene expression analysis and quantification of markers for cardiac hypertrophy and fibrosis.

##### 4.9.4.1. SDF-1 Expression in Cardiac Hypertrophy

SDF-1 is known to be upregulated transiently in the process of inflammation and organ injury. Here we quantified the SDF-1 levels in cardiac tissue of untreated and Ang-II stimulated groups (Fig.24). Consistent with our previous real-time quantification data, SDF-1 levels were lower in cKO mice compared to controls. A

tendency of upregulation was seen after Ang-II stimulation in wild type and mutants but it did not reach significant in both groups.

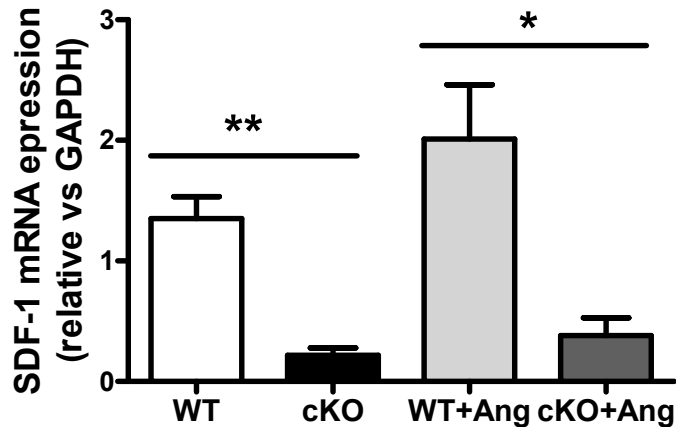


**Fig 24: Relative quantification of SDF-1 mRNA in cKO mutants and wild type mice after Ang-II induced cardiac hypertrophy.** Quantification of mRNA expression of SDF-1 relative to the expression of the housekeeping gene GAPDH using TaqMan-PCR®. The data represents means  $\pm$  standard error of mean. WT n=3, cKO n=3, WT+Ang n=3, cKO+Ang n=3. \*\* $p < 0.01$ , \* $p < 0.05$

#### 4.9.4.2. Expression of ANP and BNP as Markers of Cardiac Hypertrophy

The pathological cardiac hypertrophy by pressure overload or volume over load is a compensatory cellular response. Cardiac hypertrophy is characterized by induction of fetal gene reexpression to compensate the cardiac response. The induction of natriuretic peptides such as ANP, and BNP is the most common characteristic occurring during this response. The ANP and BNP mRNA levels were quantified in cardiac tissues by using TaqMan® quantitative – PCR method as described before. The ANP (Fig 25A) mRNA expression was not significantly altered in all groups and BNP (Fig 25B) mRNA was only upregulated in SDF-1 cKO mice.

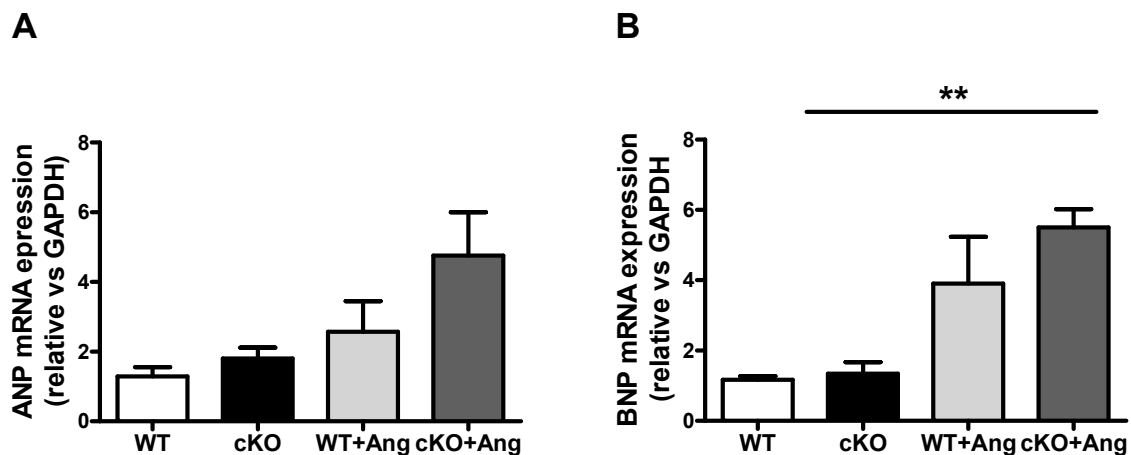


**Fig 25: Relative quantification of cardiac hypertrophy markers in SDF-1 cKO mutants and wild type mice during Ang-II induced cardiac hypertrophy.** Quantification of mRNA expression of cardiac hypertrophy markers ANP (A) and BNP(B) relative to expression of the housekeeping gene GAPDH using TaqMan-PCR®. The data represents the means  $\pm$  standard error of mean. WT n=3, cKO n=3, WT+Ang n=3, cKO+Ang n=3. \*\*p<0.01

#### 4.9.4.3. Expression of Fibrosis Markers in Cardiac Hypertrophy

Histological analysis had revealed differences in fibrosis levels in Ang-II stimulated groups. To confirm this evidence fibrosis marker such as collagen-1 $\alpha$  and fibronectin levels were quantified. Collagen-1 $\alpha$  mRNA was significantly upregulated in wild type Ang-II induced group compared to basal wild type group, where as cKO mutants showed no significant alteration in collagen-1 $\alpha$  expression after stimulation compared to untreated mutants (Fig.26A). Similarly TGF- $\beta$  also known to play a vital role in tissue fibrosis showed a tendency to be upregulated only in controls after Ang-II induction (Fig.26C). Fibronectin is another marker for fibrosis, which was upregulated in both groups after stimulation; however the effect in controls was statistically significant and in cKO mutants it was not (Fig 26B).

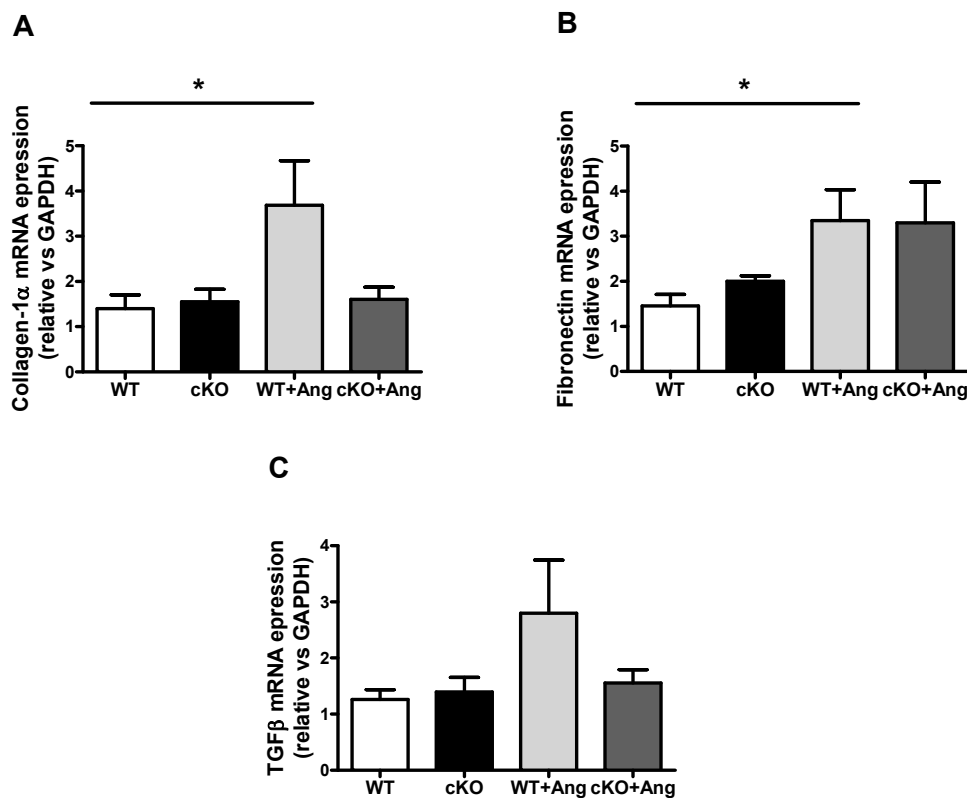


**Fig.26: Relative quantification of fibrosis markers in SDF-1 cKO mutants and wild type mice during Ang-II induced cardiac hypertrophy.** Quantification of mRNA expression of fibrosis markers Collagen-1 $\alpha$  (A), Fibronectin (B) and TGF- $\beta$  (C) relative to the expression of housekeeping gene GAPDH using TaqMan-PCR<sup>®</sup>. The data represents the means  $\pm$  standard error of mean. WT n=3, cKO n=3, WT+Ang n=3, cKO+Ang n=3. \* $p$ <0.05

#### 4.10. Characterization of Cardiac Function and Morphology of SDF-1 cKO Mice in Myocardial Infarction (MI)

It has been described in many studies, that SDF-1 upregulation in myocardial infarction has a crucial role in stem cell recruitment and myocardial repair. However due to the lack of a clear genetic model, the substantial role of SDF-1 in myocardial infarction needed to be studied. To investigate the pathological role of SDF-1 in myocardial ischemia, the cardiac SDF-1 mutants and control mice were subjected for myocardial infarction by permanent ligations of the left coronary artery (LCA). The infarcted mice were analyzed with echocardiography, cardiac MRI, histological studies and gene expression studies.

#### 4.10.1. Echocardiography Characterization of Cardiac Function in MI

Echocardiographic assessment of cardiac function was performed in 3 months old SDF-1 cardiomyocyte specific mutants and wild type controls before creating myocardial infarction as a basal measurement (0d). The echo measurements were repeatedly taken after creating infarctions at regular intervals including 7days (7d), 14 days (14d) and 28days (28d).

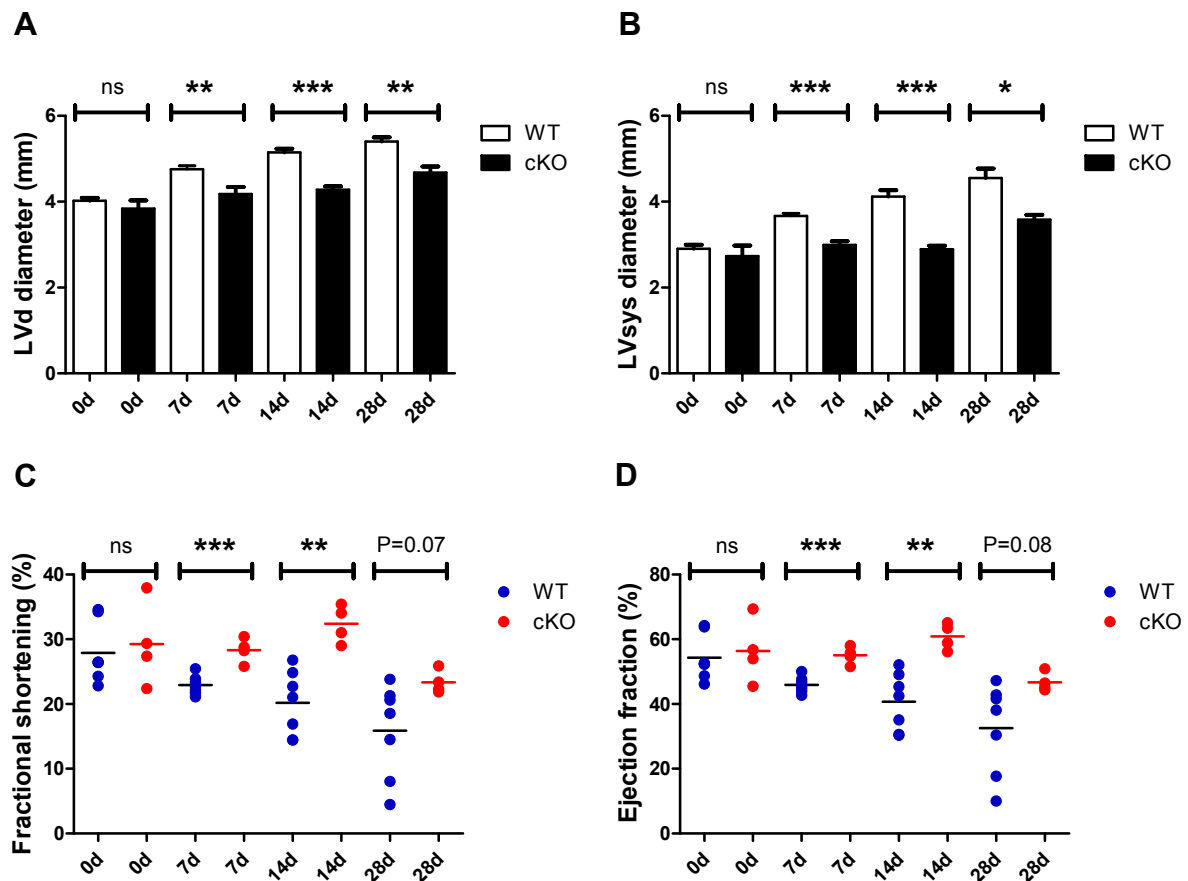


**Fig.27: Echocardiography analysis of 3 months old cardiomyocyte specific SDF-1 KO (cKO) mice and wild type (WT) during myocardial infarction.** Left ventricular diastolic diameter (A), and systolic diameter (B) are shown. Systolic functional parameters, fractional shortening (C) and ejection fraction (D) were determined. All the parameters were statistically significant between wild type (WT) and mutant mice (cKO). The data represents the means  $\pm$  standard error of mean. WT n=7, cKO n=4. \*\*\* $p < 0.001$ , \*\* $p < 0.01$ , \* $p < 0.05$ , ns- not significant



After myocardial infarction increase in left ventricular chamber diameters such as left ventricular diastolic and systolic diameters were observed in both groups (Fig.27A&B). However, the mutants exhibited a very significant resistance to left ventricular chamber dilation and increased cardiac protection after myocardial infarctions compared to controls. This altered geometry was very significantly distinguishable between the SDF-1 mutants and control mice after MI on day 7 and further extended up to day 28. In correlation to the altered geometry of the left ventricular diastolic and systolic diameters, the cardiac contractility parameters such as ejection fraction (Fig.27D) and fractional shortening (Fig.27C) were significantly improved in SDF-1 mutants, whereas controls exhibit intense cardiac remodeling with impaired cardiac function.

#### **4.10.2. Cardiac MRI Characterization of Cardiac Function in MI**

Cardiovascular magnetic resonance imaging or cardiac MRI is a non invasive medical imaging technology that allows diagnosing the cardiac function and structure in patients with cardiovascular disorders. Unlike other methods which use ionized radiation, cardiac MRI uses a powerful magnetic field, radio waves and a computer to generate the detailed structure of the heart. Cardiac MRI allows to assess the anatomy of the heart such as size and thickness of the chambers and scar size in myocardial infarctions and LV function. In our study we performed the cardiac MRI in mice with myocardial infarction. After final echo measurements on day 28 of myocardial infarction, both control mice and mutants were subjected to cardiac MRI to assess cardiac structure and function (Fig.28). Coherently to the echo data the mutants showed an improved cardiac function compared to controls. The cardiac contractility parameters such as LV ejection fraction (Fig.28A) and stroke volumes (Fig.28B) were depressed in controls, whereas mutants were significantly protected. Despite of these significant changes the infarct area was not significantly altered (Fig.28C). In controls, the LV images of cardiac MRI from 2 chamber view (short axis) and 4 chamber view (long axis) (Fig.29A&B) displayed with enlarged LV chambers with thin scar; whereas mutants have moderately remodeled chambers with a thick scar.

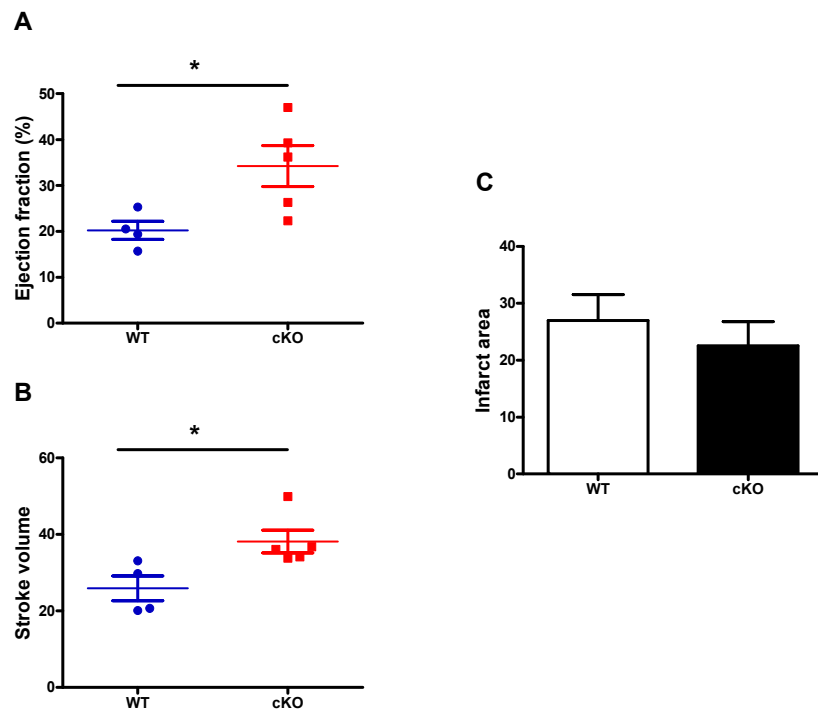


**Fig.28: Cardiac MRI characterization of cardiomyocyte specific SDF-1 KO (cKO) and wild type (WT) mice after 28d of myocardial infarction.** Left ventricular ejection fraction (A), and stroke volume (B) are shown. The infarct area (C) was determined. The cardiac functional parameters were statistically significant between wild type (WT) and mutants mice (cKO). The data represents the means  $\pm$  standard error of mean. WT n=4, cKO n=5. \* $p < 0.05$

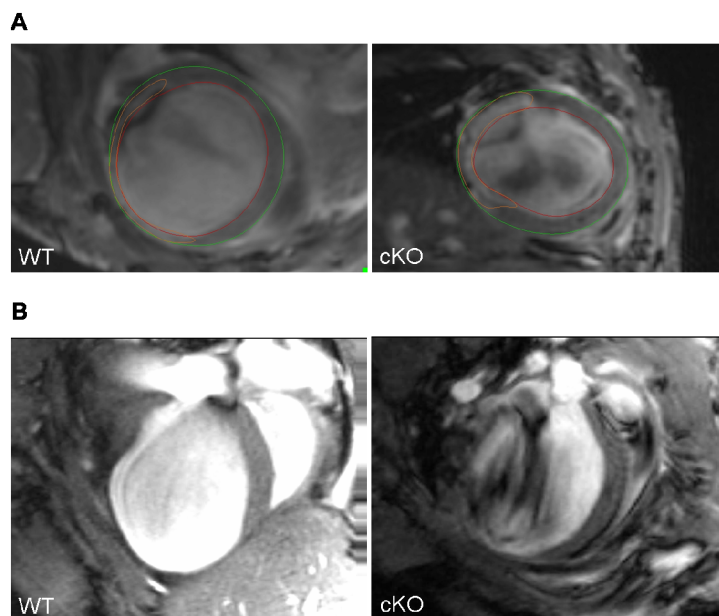


**Fig.29: Cardiac MRI imaging of cardiomyocyte specific SDF-1 KO (cKO) and wild type (WT) mice after 28d of myocardial infarction.** (A) Two chamber view of short axis plane with labeled contours. The green represents outer line, red for inner line of the LV chamber and orange for infarct area. (B) The four chamber view of horizontal long axis plane.

### 4.10.3. Histological Analysis in MI

To characterize the cardiac morphology in experimental myocardial infarcted hearts after final echo (28d) and cardiac MRI analysis, the hearts were excised and cut in transverse plane in the middle of the infarct area of the left ventricular chamber. Both mutant and control infarcted heart sections were analysed immediately under light microscopy for cardiac morphology (Fig.30A). As expected mutant hearts have smaller infarcts compared to control animals. In order to detect the scar tissues specifically, paraffin sections were stained by Sirius red (Fig.30B). In these stained sections also the scar size was quantified in percent of left ventricular cross sectional area (Fig.30C).

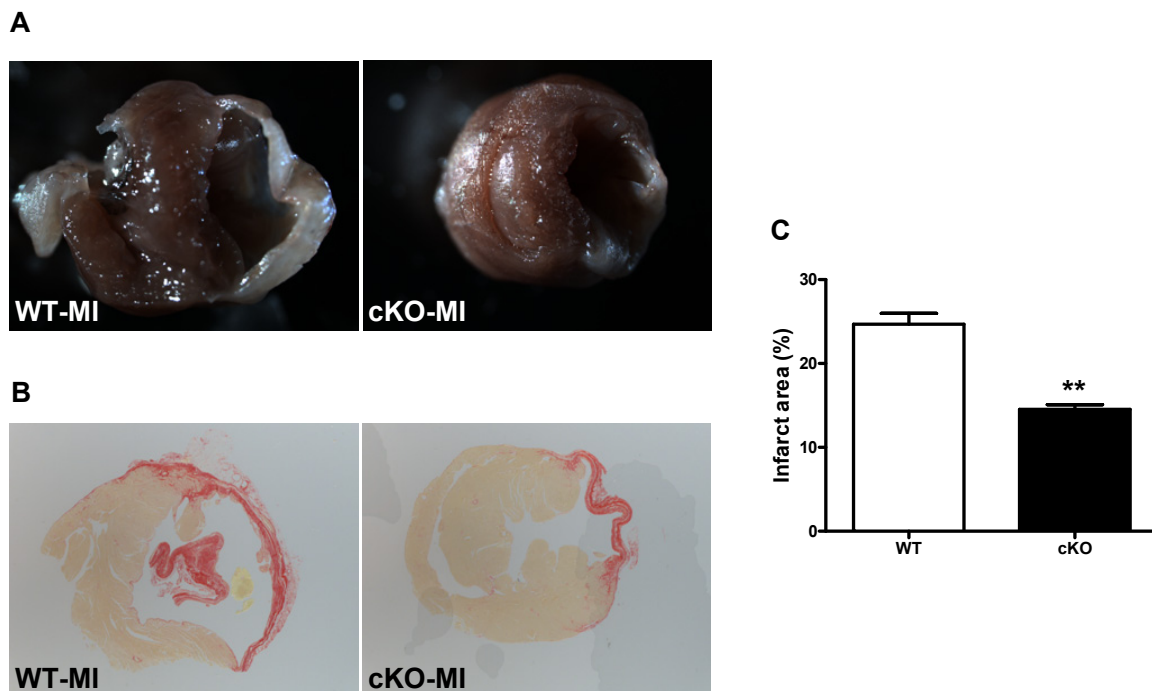


**Fig.30: Representative heart morphology and Sirius red staining of SDF-1 cKO mutants and wild type mice after myocardial infarction.** (A) Transverse plane heart sections from wild type (WT) and mutant (cKO) mice. (B) Sirius red staining of collagen fibers (red) in transverse sections of heart from the experimental groups. The heart sections from controls showed dilated left ventricular chambers with increased scar size. (C) Infarct area determined by relative quantification to the left ventricular cross sectional area. The data represents the means  $\pm$  standard error of mean. WT n=4, cKO n=3, 4 sections per each mouse. \*\*p<0.01

#### 4.10.4. Gene Expression Analysis in MI

Myocardial infarction is accompanied by cardiac remodeling which induces various structural changes such as cardiac hypertrophy and tissue fibrosis. Cardiac remodeling is an adaptive cellular response to cardiac dysfunction and myocardial death. The induction of expression of cardiac hypertrophy (ANP, BNP) and fibrosis relevant proteins is a most common characteristic occurring during this response.

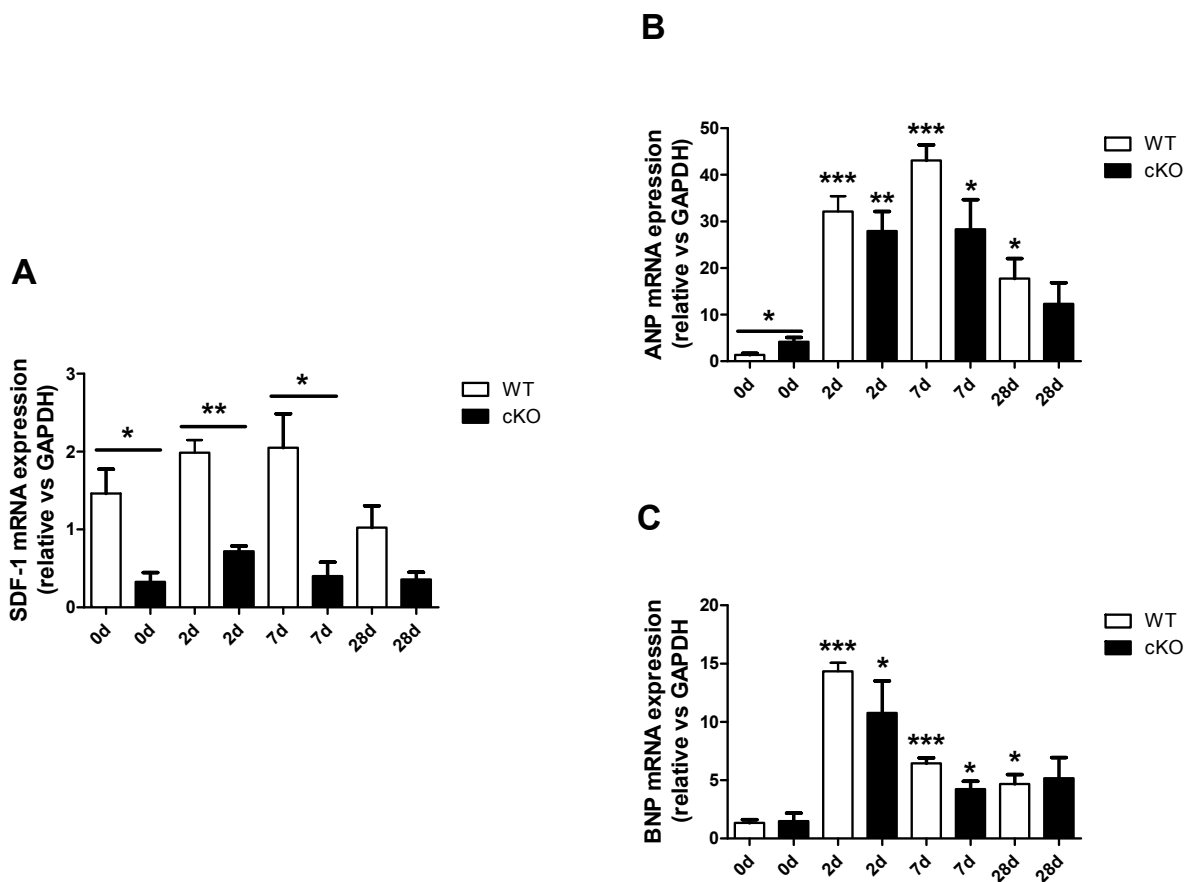


**Fig 31: Expression analysis of SDF-1 and cardiac hypertrophy markers in SDF-1 (cKO) mutants and wild type mice during myocardial infarction.** Quantification of mRNA expression of SDF-1 (A), cardiac hypertrophy markers ANP (B) and BNP (C) relative to the expression of housekeeping gene GAPDH using TaqMan-PCR<sup>®</sup>. The expressions were compared at different time points 0d, 2d, 7d, 28d. The data represents the means  $\pm$  standard error of mean. WT  $n=3$ , cKO  $n=3$  per each group. \*\*\* $p<0.001$ , \*\* $p<0.01$ , \* $p<0.05$ .

To verify the evidence of cardiac protection in cardiac SDF-1 mutants, we performed gene expression analysis and quantification of markers for cardiac hypertrophy and

fibrosis. Earlier studies had described that SDF-1 is induced transiently after myocardial infarction up to 1 week. Here we quantified the SDF-1 levels in cardiac tissue of sham and infarcted groups at different time points (0d, 2d, 7d, 28d) (Fig.31). Like in our previous real-time quantification data (Fig.24), SDF-1 mRNA levels were lower in cKO mice compared to wild type mice (Fig.31A). Although there was no statistical significant induction of SDF-1 after MI, a tendency of upregulation was seen after infarction in wild type and mutants up to 7d and whereas expression declined at 28d. The ANP and BNP mRNA levels were quantified in cardiac tissues using TaqMan® quantitative – PCR method as described before. The ANP (Fig.31B) and BNP (Fig.31C) mRNA levels were significantly upregulated in both wild type and mutant groups after myocardial infarction. Although there was no significant difference between infarcted groups, mice with myocardial infarction showed more ANP and BNP expression compared to basal expression.

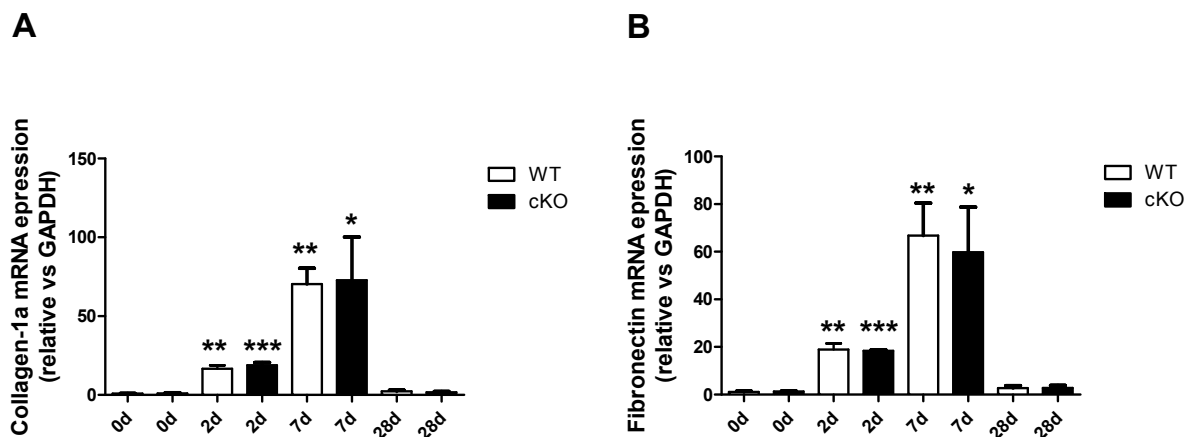


**Fig.32: Expression analysis of cardiac fibrosis markers in SDF-1 cKO mutants and wild type mice during myocardial infarction.** Quantification of mRNA expression of Collagen-1 $\alpha$  (A), Fibronectin (B) relative to the expression of housekeeping gene GAPDH using TaqMan-PCR®. The expression studies were compared at different time points 0d, 2d, 7d, 28d. The data represents the means  $\pm$  standard error of mean. WT n=3, cKO n=3 per each group. \*\*\* $p$ <0.001, \*\* $p$ <0.01, \* $p$ <0.05.

To quantify the cardiac fibrosis levels in infarcted groups, collagen-1 $\alpha$  (Fig.32A) and fibronectin m-RNA levels were quantified (Fig.32B). Collagen-1 $\alpha$  and fibronectin mRNA levels were significantly upregulated in both wild type and mutant infarcted groups in compared to basal groups. Despite of significant changes in cardiac function and scar size between wild type infarcted and mutant infarcted groups we did not observe differences at mRNA level for fibrosis markers between the groups.

#### 4.10.5. Analysis of Inflammatory Cell Infiltration in MI

MI is associated with inflammatory cell filtration followed by the removal of the dead tissue and extracellular remodeling. Monocyte/macrophage infiltration influences the pathogenesis of cardiac remodeling and tissues fibrosis. SDF-1 is widely known as a potent chemoattractant of monocytes and lymphocytes and also involved in various other pathophysiological diseases such as pulmonary fibrosis and atherosclerosis. Here we used Mac-2 as monocyte/macrophage cell infiltration marker and performed immunofluorescence to detect any differential cell infiltration after MI (Fig.34).

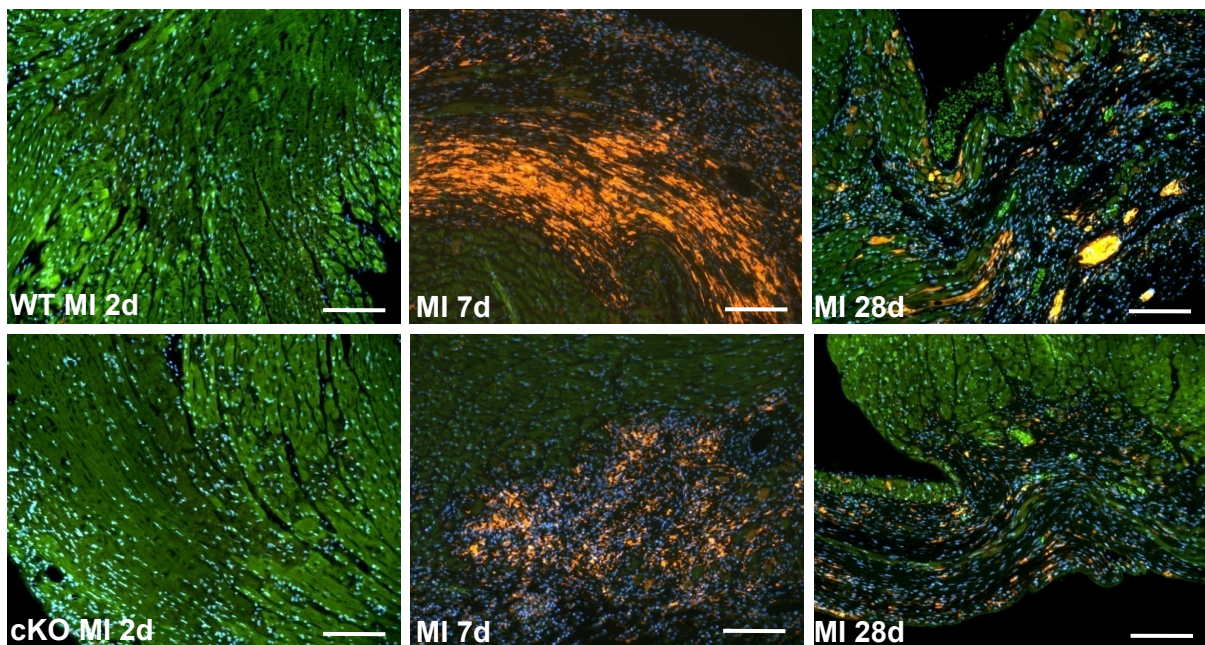


**Fig 34: *Mac-2* immunofluorescence (Cy3-FITC-DAPI) staining identifies the infiltration of monocytes/macrophages during myocardial infarction. The amount of macrophage infiltration peaked on 7d and moderately remained until 28d of MI in both WT and cKO mice. The mutants displayed reduced levels of *Mac-2* cell infiltration compared to controls.**

The monocyte/macrophage cell infiltration was elevated after 7d of MI and remained moderately increased after 28d MI. The mutants exhibited a significant reduction in monocyte/macrophage infiltration in MI hearts, compared to controls in particular in the infarcted region of the LV tissue. This suggests that SDF-1 might play a pivotal role in inflammation and cardiac tissue remodelling after MI.

## 5. Discussion

The stem cell homing signals are implicated in bone marrow stem and progenitor cell mobilization to the ischemic cardiac environment and have a pivotal role in myocardial repair (Penn et al. 2004; Vandervelde et al. 2005). SDF-1 $\alpha$ /CXCL12 is considered as the most important stem cell homing factor and acts as a central regulator of the stem cell mobilization process (Smart et al. 2008). A large number of literature data hypothesize that the SDF-1/CXCR4 pathway is important for stem or progenitor cell trafficking to the infarcted cardiac environment followed by advantageous effects on neovascularization, cardiomyocyte survival and cardiac function (Askari et al. 2003; Abbott et al. 2004; Elmadbouh et al. 2007; Saxena et al. 2008). However recent evidences possibly suggest a negative impact of SDF-1 in cardiac repair (Proulx et al. 2007; Chen et al. 2010; Chu et al. 2010).

### 5.1. Role of SDF-1 in Embryonic Development

In order to characterize the role of SDF-1 in myocardial repair, we produced a conditional SDF-1 mutant mouse model particularly for the heart. In this model we analysed the pathophysiological role of SDF-1 and the impact of the SDF-1/CXCR-4 pathway on cardiac function.

To verify the phenotype of SDF-1 mutant mice with our floxed SDF-1 mouse model, we bred these mice to ubiquitously cre expressing transgenic mice (CMV-cre) and generated a SDF-1 knockout mouse model. The SDF-1 mutant mice also displayed developmental defects and embryonic lethality indicating that our floxed allele becomes dysfunctional after excision. The SDF-1 mutant embryos at the age of E17-E18 appeared smaller in size with reduced body weight in comparison to heterozygote and wild type mice. This was further confirmed by the lack of SDF-1 expression in various organs. These data were in line with previously published data indicating that ubiquitous deletion of SDF-1 leads to perinatal death of embryos with multiple organ defects (Nagasawa, Hirota, et al. 1996). In addition to that, histological analysis of the SDF-1 KO mice hearts also showed ventricular septal closure defects confirming the importance of SDF-1 in cardiogenesis and vasculogenesis.



## 5.2. Cardiac SDF-1 in Cardiac Function

In-situ hybridization analysis revealed that the endocardium specific expression of SDF-1 begins after E12.5 suggesting that cardiac SDF-1 has a crucial role in the formation of the ventricular septum in embryonic development ([Nagasawa, Hirota, et al. 1996](#)). However, the precise role of SDF-1 in postnatal cardiac development and function is not elucidated.

In order to determine the physiological role of SDF-1 in postnatal heart, we generated a cardiac specific SDF-1 KO mouse model by using a *Mlc2v-cre* (expression begins after E9.5) knock in mouse. Despite of the cardiac defects in complete KO model, the cardiac mutant mice were viable and did not display any signs of cardiac abnormalities. Initially, we examined the mice at the age of 3 months under basal conditions with echocardiography. This non-invasive method allows determining the left ventricular cardiac dimensions and contractility. The assessment of ejection fraction and fractional shortening data showed that the mutants have normal systolic and diastolic cardiac function. An in-vitro study by Pyo et al., identified a negative inotropic effect of SDF-1 on adult rat cardiomyocytes and described a direct effect of SDF-1 on modulating cardiac contractility ([Pyo et al. 2006](#)). However, in our cardiac mutant model we didn't observe any alteration in cardiac contractility under physiological conditions. Similarly, the left ventricular diameters such as intraventricular septal thickness, left ventricular diastolic diameters and ratio of the posterior wall thickness and diastolic diameter of the left ventricle showed no significant differences in mutants suggesting no signs of cardiac hypertrophy and geometry abnormality. The mice were repeated for echo analysis at the age of 12 months. Again no significant differences in cardiac function were observed. This could be partially explained by the assumption that SDF-1 might have prominent effects under inflammation and injury rather than at basal conditions. In addition to that, SDF-1 is also expressed in multiple cell types within the heart such as endothelial cells and cardiac fibroblasts ([Saxena et al. 2008](#)). A compensatory paracrine effect might lead to the lack of phenotype of cardiac SDF-1 mutant mice under basal conditions. However a recent study by Agarwal et al. describes that cardiomyocyte specific deletion of CXCR4 has also no significant role in cardiac



development and has no adverse effect on physiology substantiating our findings (Agarwal et al. 2010).

To further describe the phenotype, the cardiac mutant mice were analyzed for cardiac morphology. The relative heart weight and body weight ratio as a measure for cardiac hypertrophy revealed no signs of cardiac hypertrophy in mutants. Additionally our histological analysis confirmed the normal cardiac morphology in mutants. The relative quantification of cardiac hypertrophy markers such as ANP and BNP also showed no significant deviation between the groups suggesting that the cardiac mutant mice under physiological conditions were normal.

### **5.3. SDF-1 and its Pathological Role in Cardiac Hypertrophy**

SDF-1 belongs to the family of chemokines, which play important roles in directing leukocyte movement during homeostasis and organ development. However SDF-1 also has a crucial role in organ injury and inflammation (Lapidot et al. 2002). In addition to that, there is limited evidence about SDF-1 role in regulating cardiac hypertrophy. A study from Proulx et al. revealed that the regulation of hypertrophy by SDF-1 might be a secondary effect to the ischemic tissue damage (Proulx et al. 2007). The administration of the CXCR4 antagonist AMD3100 in post-infarction rats led to a significant reduction in infarct size and ameliorated left ventricular systolic function with partially decreased non-infarcted left ventricular (NILV) hypertrophy. These findings suggest that SDF-1 $\alpha$  may directly promote the hypertrophic changes of the heart. In vitro analysis from SDF-1 treatment of hypertrophied neonatal rat ventricular myocytes revealed significant induction of hypertrophy by ANP and BNP mRNA and protein synthesis. This was the first evidence describing the direct effect of SDF-1 on modulating cardiac hypertrophy. Due to lack of clear evidence of SDF-1 and its role in cardiac hypertrophy, we investigated the pathological role of SDF-1 in cardiac hypertrophy and inflammation using the cardiac SDF-1 KO and wild type mice. The animals were infused with angiotensin-II as a model for cardiac hypertrophy. Echocardiography analysis showed hypertrophic alterations of left ventricular diameters such as intraventricular septum thickness and posterior wall diameter in both groups. However, mutants exhibited reduced posterior wall thickness and a smaller ratio of posterior wall thickness and left ventricular end diastolic diameter in comparison to controls. Despite of these alterations there was

no significant difference in the left ventricular diastolic and systolic diameters and the cardiac contractility parameters. The relative heart weight to body weight ratio was also not significantly different between mutants and controls. This implies that mutants might have a moderate resistance to the induction of cardiac hypertrophy.

Furthermore, the mRNA expression analysis of ANP and BNP as markers for cardiac hypertrophy was studied. After Ang-II treatment a prominent induction of BNP mRNA levels were observed in mutants and similarly there was a tendency of higher ANP mRNA expression. These results indicate cardioprotective effects in mutants and suggest that SDF-1 may be involved in the induction of cardiac hypertrophy as a primary compensatory response. In addition to that, a recent study described that angiotensin mediated the secretion of SDF-1 from cultured cardiomyocytes suggesting that SDF-1 might be involved in the pathogenesis of cardiac fibrosis in the progression to heart failure ([Chu et al. 2010](#)).

After hypertrophy induction in coherence with our previous data, gene expression analysis of SDF-1 showed a strong downregulation in mutants in comparison to controls. After Ang-II treatment there was a tendency of increase in SDF-1 expression; however it was not significant. This might be due to the delayed measurement of SDF-1 expression in our experimental group.

Cardiac hypertrophy is accompanied by fibrosis tissue deposition. Here we quantified cardiac fibrosis markers such as collagen-1 $\alpha$ , fibronectin, and TGF- $\beta$  in untreated and Ang-II treated groups. Control mice showed a strong induction of collagen-1 $\alpha$  and TGF- $\beta$  levels in support of the data from Chu et al. The SDF1- cardiac mutants displayed significant resistance to cardiac fibrosis after Ang-II treatment, suggesting that SDF-1 has an important role in induction of cardiac fibrosis. Histological analysis confirmed that the fibrosis tissue deposition was higher in controls in comparison to cardiac SDF-1 mutants. Perivascular fibrosis and inflammatory cell infiltration was markedly enhanced in controls, whereas the mutants displayed a significant reduction in cell infiltration. Although SDF-1 is known to play a key role in bone marrow stem cell mobilization, certain studies also suggest that bone marrow derived circulating fibrocyte recruitment might lead to transition to cardiac fibrosis in heart failure. Besides that, previous studies also demonstrated that cardiac fibroblasts express the receptor CXCR4 ([Hu et al. 2007](#)). A number of studies also reported that the SDF-1/CXCR4 axis is particularly important for the trafficking and extravasation of circulating fibrocytes, which eventually contribute to the pathogenesis of fibrosis

---

(Phillips et al. 2004; Dobaczewski et al. 2009). Altogether the cardiac SDF-1 KO mouse model provided concrete evidence that SDF-1 mediates cardiac fibrosis in pathological cardiac hypertrophy.

#### **5.4. SDF-1 and its Pathological Role in Myocardial Infarction**

A large numbers of studies suggest that the interaction between SDF-1 and CXCR4 has a significant role in regulating the homing and proliferation of stem cells in the BM under homeostatic conditions. Accordingly, the disruption of the BM SDF-1/CXCR4 signaling under stress-induced conditions is necessary to induce the mobilization of stem cells into the circulation. In parallel, the local elevation of SDF-1 levels in the inflamed or injured organ is capable of recruiting the mobilized cells to the site of injury where they can support tissue repair and regeneration (Fig.35). While many studies suggested the significance of the SDF-1/CXCR4 axis in mobilization of BM-derived stem cells to sites of ischemic injury leading to cardiac protection as well as promotion of tissue neovascularization (Askari et al. 2003; Abbott et al. 2004; Kucia, Dawn, et al. 2004; Elmadbouh et al. 2007), evidence for true myocardial regeneration is missing. Furthermore recent studies also demonstrated a negative impact of SDF-1 in the pathophysiology of MI (Proulx et al. 2007; Chen et al. 2010; Chu et al. 2010). Due to these controversial data, we used our conditional cardiac knockout model to evaluate the role of SDF-1 in myocardial infarction. In the present study we found interesting features of SDF-1 in experimental myocardial infarction. The mutant mice exhibited better survival rates after MI, although the difference was not statistically significant. This was further accompanied by better cardiac functional parameters such as ejection fraction and fractional shortening. The mutants also exhibited significantly reduced left ventricular diastolic and systolic diameters, suggesting that SDF1- cardiac mutants are protected after myocardial infarction. These data were further confirmed by cardiac MRI. The MRI data also shows stronger dilated chambers in controls, while mutants exhibited better left ventricular cardiac remodeling and improved cardiac function.

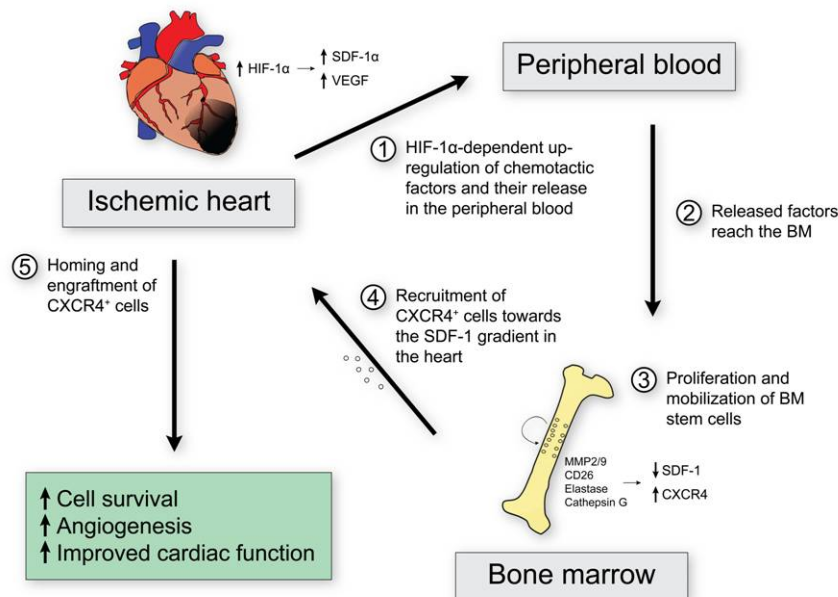


**Fig.35: SDF-1/CXCR4 interaction and its potential role in myocardial ischemia.**

1.) Myocardial infarction initiates the upregulation of the hypoxic signal HIF-1 $\alpha$ , which then induces stem cell mobilization signals such as SDF-1 $\alpha$  and VEGF and their release in the peripheral blood. 2.) These signals reach the bone marrow (BM). 3.) This leads to alterations in the BM microenvironment (e.g. induction of MMP2/9, CD26, elastase and cathepsin G) resulting in proliferation and increased CXCR4 receptor expression of stem and progenitor cells as well as SDF-1 degradation. 4.) The changes in the BM SDF-1 gradient lead to the translocation of stem and progenitor cells into the PB and their homing towards the local SDF-1 gradient initiated in the myocardium. 5.) BM stem and progenitor cells selectively home to the ischemic myocardium where they are involved in myocardial repair through cardioprotective functions and induction of angiogenesis (Ghadge et al. 2010).

Further histological studies could show that the controls have thinned left ventricular muscle with enlarged chamber and increased scar area compared to mutants. This also implies that SDF-1 augments negative effects on cardiomyocytes after myocardial infarction. Large number of studies described that autocrine release of SDF-1 in cardiomyocytes following myocardial infarction has beneficial effects on cardiomyocyte survival through activation of antiapoptotic pathways such as Akt and ERK-1/2 and has paracrine effects on progenitor cell mobilization and ischemic tissue neovascularization (Elmadbouh et al. 2007; Hu et al. 2007; Saxena et al. 2008). However, our data suggest opposite effects on cardiomyocyte function. They are concordant with other studies also describing the negative impact of SDF-1 on cardiac function.

Pyo et al. demonstrated that SDF-1 can directly depress the contractility of the myocardium (Pyo et al. 2006). In this study they describe that SDF-1 binding to

---

CXCR4 receptors on cardiomyocytes has a direct effect by blunting the inotropic response to  $\text{Ca}^{2+}$  stimulation. These effects were abrogated by the CXCR4 antagonist AMD3100. A recent study by Chen et al. examined the effect of CXCR4 by gene transfer during MI (Chen et al. 2010). The overexpression of CXCR4 in ischemic heart leads to increased recruitment of inflammatory cells and augmented cardiomyocyte apoptosis in the infarcted heart. These data suggest that the SDF-1/CXCR4 axis enhances ischemic reperfusion injury possibly due to the enhanced recruitment of inflammatory cells, the activation of proinflammatory signals such as tumor necrosis factor- $\alpha$ , and the activation of apoptotic pathways. Similar to this data we observed significant reduction of inflammatory cell influx into myocardial infarcted tissue in cardiac SDF-1 mutants suggesting that the lack of SDF-1 during MI could improve the left ventricular function through regulation of inflammation and cardiac remodeling.

To our surprise a recent study by Agarwal et al. generated a cardiac CXCR4 knockout model and described that cardiomyocyte specific deletion has no pathophysiological effects during post MI and has no significant role in cardiac remodelling (Agarwal et al. 2010). However this discrepancy can be explained by the mismatch in timings of peaks of SDF-1 and CXCR4. This study explains that SDF-1 is rapidly and transiently expressed following AMI before cardiac myocyte CXCR4 is upregulated. Our study is in contrast to many other studies, which suggest that SDF-1 mediates stem cell mobilization and beneficial effects on cardiac function. Nevertheless our data suggested that the lack or a decrease of SDF-1 $\alpha$  expression in the ischemic damaged heart can reduce inflammation and improve ventricular function, which seems to be independent of mobilization of bone marrow-derived stem and progenitor cells.

Chu et al. recently described that bone marrow derived cells (fibrocytes) contributed to cardiac fibrosis in a nonischemic failing heart model (Chu et al. 2010). This study exhibited that SDF-1 is upregulated in the failing heart inducing the mobilization of bone marrow derived fibrocytes and the transition to cardiac fibrosis. In other pathophysiological disorder such as pulmonary fibrosis, the profibrotic role of SDF-1 has been characterized (Phillips et al. 2004). This was the first study to show that circulating fibrocytes possess CXCR4 receptors and trafficked to SDF-1 gradients in lungs contributing to the pathogenesis of pulmonary fibrosis. These studies further supported our hypothesis that SDF-1 might be involved in the recruitment of cardiac

fibroblasts during post MI which leads to enhanced myocardial ischemia and cardiac remodeling.

Another study in rat MI using the selective CXCR4 receptor antagonist, AMD3100, was able to show that inhibition of SDF-1/CXCR4 interaction after MI has beneficial effects such as decreased scar size and improved cardiac contractility (Proulx et al. 2007). This was the first study to report the therapeutic implications of AMD3100 suggesting that an increase in SDF-1 $\alpha$  may contribute to scar formation and worsening of cardiac function. This hypothesis also supports our experimental model. However this study doesn't explain the exact mechanism of stem cell homing properties and its potential implications after MI. In contrast, a recent study by Dai et al. showed opposite effects of AMD3100 in MI. In this study, they described that blocking the interaction of SDF-1 $\alpha$  and CXCR4 after MI leads to depressed cardiac function, expanded scar tissue and increased apoptosis (Dai et al. 2010). Despite of this injury, c-kit<sup>+</sup> cardiac progenitor cells were increased in the risk zone in the AMD3100 treated group.

Although this and other studies may suggest SDF-1/CXCR4 interaction is important for cardiac repair and myocardial commitment or differentiation, one cannot simply ignore the negative effects of the SDF-1. The present study indicates that SDF-1 has a negative impact on cardiac function and remodeling. Collectively our data suggest that SDF-1 might play a crucial role in inflammation, pathogenesis of cardiac fibrosis and worsening of cardiac function following myocardial infarction. They also imply that cardiomyocytes may not be the major source of SDF-1 for homing of the stem cells in MI. Therapeutic targeting of SDF-1 in myocardial infarction to promote trafficking of cells should be thoroughly verified.

## **6. Summary/ Zusammenfassung**

### **6.1. Summary**

The efficacy of stem cell based therapeutic approaches has been demonstrated by stem cell mobilization to damaged regions after myocardial infarction. The stem cell mobilization process is initiated by inflamed or injured tissue that releases various signaling molecules such as cytokines, chemokines and proteolytic enzymes. Chemokines play a pivotal role in the pathophysiology of ischemic injury. The chemokine SDF-1 has a central role in regulating the mobilization of stem and progenitor cells and has potential significance in cardiac repair through induction of angiogenesis and cardioprotective functions after myocardial infarction. It has been proposed that SDF-1 $\alpha$  is a potential candidate for use as a therapeutic target in stem cell-mediated cardiac regeneration. This even led to the initiation of clinical trials in patients suffering from ischemic cardiac diseases. Despite of these beneficial effects, a number of studies also suggest a negative impact of SDF-1/CXCR4 axis on myocardial repair.

In our study we used a cardiac SDF-1 knockout model and evaluated the potential role of SDF-1 in cardiac hypertrophy and myocardial infarction. The in-vivo studies suggested that cardiac SDF-1 KO mice have no structural abnormalities and displayed normal physiological function. In cardiac hypertrophy the mutants also have no significant morphological and functional difference; however they displayed a moderately resistance to cardiac hypertrophy in comparison to wild type mice. A more detailed analysis showed that fibrosis was markedly less pronounced in mutants. These data suggest that SDF-1 have a role in the regulation of cardiac hypertrophy. Further experimental studies with myocardial infarction revealed that SDF-1 mutants show cardio protection in comparison to control mice. After MI the LV diastolic and systolic diameters were significantly enlarged in wild type mice, whereas mutants were less affected. The cardiac functional data also support the negative effect of SDF-1 on cardiomyocyte contractility after MI. The decrease in inflammatory cell infiltration in mutant hearts further substantiates the role of SDF-1 in the pathogenesis of cardiac remodelling during myocardial infarction. However, further mechanistic analyses are required to elucidate the precise role of SDF-1 in myocardial infarction. Our data suggest that intense studies are necessary in order to

cautiously analyze the therapeutic potential of SDF-1 in stem cell-mediated cardiac repair.

## **6.2. Zusammenfassung**

Die Wirksamkeit von Stammzell-basierten Therapieansätzen konnte mit der Mobilisierung der Stammzellen zu geschädigtem Herzgewebe nach Myokardinfarkt gezeigt werden. Der Prozess der Stammzellmobilisierung wird dabei durch das entzündete oder verletzte Gewebe ausgelöst, indem verschiedene Signalmoleküle wie Zytokine, Chemokine und proteolytische Enzyme freigesetzt werden. Vor allem die Chemokine nehmen eine entscheidende Rolle in der Pathophysiologie von ischämischen Verletzungen ein. Das Chemokin SDF-1 ist dabei von zentraler Bedeutung in der Regulierung der Mobilisierung von Stamm- und Vorläuferzellen und ist besonders wichtig für die Regeneration des Herzens nach Myokardinfarkt durch Anregung von Angiogenese sowie durch Verstärkung protektiver Mechanismen. Deshalb wurde SDF-1 $\alpha$  als potentieller Angriffspunkt für Stammzell-vermittelte kardiale Regeneration beschrieben. Dies führte sogar zur Initiierung klinischer Studien mit Patienten, die an Ischämie-bedingten kardialen Erkrankungen leiden. Trotz der vielfach beschriebenen positiven Effekte des Chemokins gibt es eine Reihe von Studien, die negative Auswirkungen der SDF-1/CXCR4 Achse postulieren.

In der vorliegenden Arbeit wurde ein Herz-spezifisches SDF-1 Knockout-Modell benutzt, um den Einfluss von SDF-1 auf Herzinsuffizienz sowie Myokardinfarkt zu untersuchen. Die dazu durchgeführten in vivo Studien zeigten, dass das Fehlen von SDF-1 im Herz weder zu strukturellen Auffälligkeiten noch veränderter Herzfunktion führt. Auch nach Induzierung von kardialer Hypertrophie blieb die Herzmorphologie und -funktion unverändert, allerdings zeigten die Knockout-Tiere eine leichte Resistenz gegenüber dem hypertrophen Stimulus im Vergleich zu Wildtyp-Kontrollen. Genauere Analysen ergaben, dass die Mutanten deutlich weniger Fibrose bilden. Diese Daten deuten darauf hin, dass SDF-1 eine Rolle bei der Regulierung der Herzinsuffizienz spielt. Weiterführende Experimente zeigten zudem, dass die Herzen der Knockout-Tiere nach Auslösung eines Myokardinfarkts besser geschützt sind als entsprechende Kontrollen. Während die Wildtyp-Tiere stark vergrößerte diastolische und systolische Durchmesser aufwiesen, war dieser Effekt in den Knockout-Tieren weniger stark ausgeprägt. Funktionelle Daten sowie eine verringerte Infiltration von



Entzündungszellen in den Knockout-Mäusen bestätigten den negativen Einfluss von SDF-1 auf die Herzkontraktilität nach Myokardinfarkt.

Unsere Ergebnisse zeigen, dass zukünftige mechanistische Analysen notwendig sind, um die Rolle von SDF-1 im Herz nach Auftreten eines Infarkts weiter zu entschlüsseln. Zudem sollte das therapeutische Potential von SDF-1 für Stammzell-basierte kardiale Regenerationsprozesse kritisch untersucht werden.

---

## 7. References

- Abbott, J. D., Y. Huang, D. Liu, R. Hickey, D. S. Krause and F. J. Giordano (2004). "Stromal cell-derived factor-1alpha plays a critical role in stem cell recruitment to the heart after myocardial infarction but is not sufficient to induce homing in the absence of injury." *Circulation* **110**(21): 3300-3305.
- Agarwal, U., W. Ghalayini, F. Dong, K. Weber, Y. R. Zou, S. Y. Rabbany, S. Rafii and M. S. Penn (2010). "Role of cardiac myocyte CXCR4 expression in development and left ventricular remodeling after acute myocardial infarction." *Circ Res* **107**(5): 667-676.
- Alvarez-Dolado, M., R. Pardal, J. M. Garcia-Verdugo, J. R. Fike, H. O. Lee, K. Pfeffer, C. Lois, S. J. Morrison and A. Alvarez-Buylla (2003). "Fusion of bone-marrow-derived cells with Purkinje neurons, cardiomyocytes and hepatocytes." *Nature* **425**(6961): 968-973.
- Anversa, P. and J. Kajstura (1998). "Ventricular myocytes are not terminally differentiated in the adult mammalian heart." *Circ Res* **83**(1): 1-14.
- Anversa, P., A. Leri and J. Kajstura (2006). "Cardiac regeneration." *J Am Coll Cardiol* **47**(9): 1769-1776.
- Asahara, T., T. Murohara, A. Sullivan, M. Silver, R. van der Zee, T. Li, B. Witzenbichler, G. Schatteman and J. M. Isner (1997). "Isolation of putative progenitor endothelial cells for angiogenesis." *Science* **275**(5302): 964-967.
- Askari, A. T., S. Unzek, Z. B. Popovic, C. K. Goldman, F. Forudi, M. Kiedrowski, A. Rovner, S. G. Ellis, J. D. Thomas, P. E. DiCorleto, E. J. Topol and M. S. Penn (2003). "Effect of stromal-cell-derived factor 1 on stem-cell homing and tissue regeneration in ischaemic cardiomyopathy." *Lancet* **362**(9385): 697-703.
- Balabanian, K., B. Lagane, S. Infantino, K. Y. Chow, J. Harriague, B. Moepps, F. Arenzana-Seisdedos, M. Thelen and F. Bachelier (2005). "The chemokine SDF-1/CXCL12 binds to and signals through the orphan receptor RDC1 in T lymphocytes." *J Biol Chem* **280**(42): 35760-35766.
- Baldasseroni, S., C. Opasich, M. Gorini, D. Lucci, N. Marchionni, M. Marini, C. Campana, G. Perini, A. Deorsola, G. Masotti, L. Tavazzi and A. P. Maggioni (2002). "Left bundle-branch block is associated with increased 1-year sudden and total mortality rate in 5517 outpatients with congestive heart failure: a report from the Italian network on congestive heart failure." *Am Heart J* **143**(3): 398-405.
- Balsam, L. B., A. J. Wagers, J. L. Christensen, T. Kofidis, I. L. Weissman and R. C. Robbins (2004). "Haematopoietic stem cells adopt mature haematopoietic fates in ischaemic myocardium." *Nature* **428**(6983): 668-673.
- Barbash, I. M., P. Chouraqui, J. Baron, M. S. Feinberg, S. Etzion, A. Tessone, L. Miller, E. Guetta, D. Zipori, L. H. Kedes, R. A. Kloner and J. Leor (2003). "Systemic delivery of bone marrow-derived mesenchymal stem cells to the infarcted myocardium: feasibility, cell migration, and body distribution." *Circulation* **108**(7): 863-868.
- Barry, S. P., S. M. Davidson and P. A. Townsend (2008). "Molecular regulation of cardiac hypertrophy." *Int J Biochem Cell Biol* **40**(10): 2023-2039.
- Beltrami, A. P., L. Barlucchi, D. Torella, M. Baker, F. Limana, S. Chimenti, H. Kasahara, M. Rota, E. Musso, K. Urbanek, A. Leri, J. Kajstura, B. Nadal-Ginard and P. Anversa (2003). "Adult cardiac stem cells are multipotent and support myocardial regeneration." *Cell* **114**(6): 763-776.

- Beltrami, A. P., K. Urbanek, J. Kajstura, S. M. Yan, N. Finato, R. Bussani, B. Nadal-Ginard, F. Silvestri, A. Leri, C. A. Beltrami and P. Anversa (2001). "Evidence that human cardiac myocytes divide after myocardial infarction." N Engl J Med **344**(23): 1750-1757.
- Berk, B. C., K. Fujiwara and S. Lehoux (2007). "ECM remodeling in hypertensive heart disease." J Clin Invest **117**(3): 568-575.
- Boluyt, M. O. and O. H. Bing (2000). "Matrix gene expression and decompensated heart failure: the aged SHR model." Cardiovasc Res **46**(2): 239-249.
- Brilla, C. G. and B. Maisch (1994). "Regulation of the structural remodelling of the myocardium: from hypertrophy to heart failure." Eur Heart J **15 Suppl D**: 45-52.
- Brunner, S., J. Winogradow, B. C. Huber, M. M. Zaruba, R. Fischer, R. David, G. Assmann, N. Herbach, R. Wanke, J. Mueller-Hoecker and W. M. Franz (2009). "Erythropoietin administration after myocardial infarction in mice attenuates ischemic cardiomyopathy associated with enhanced homing of bone marrow-derived progenitor cells via the CXCR-4/SDF-1 axis." FASEB J **23**(2): 351-361.
- Burger, J. A. and T. J. Kipps (2006). "CXCR4: a key receptor in the crosstalk between tumor cells and their microenvironment." Blood **107**(5): 1761-1767.
- Busillo, J. M. and J. L. Benovic (2007). "Regulation of CXCR4 signaling." Biochim Biophys Acta **1768**(4): 952-963.
- Ceradini, D. J., A. R. Kulkarni, M. J. Callaghan, O. M. Tepper, N. Bastidas, M. E. Kleinman, J. M. Capla, R. D. Galiano, J. P. Levine and G. C. Gurtner (2004). "Progenitor cell trafficking is regulated by hypoxic gradients through HIF-1 induction of SDF-1." Nat Med **10**(8): 858-864.
- Charo, I. F. and R. M. Ransohoff (2006). "The many roles of chemokines and chemokine receptors in inflammation." N Engl J Med **354**(6): 610-621.
- Chen, J., E. Chemaly, L. Liang, C. Kho, A. Lee, J. Park, P. Altman, A. D. Schechter, R. J. Hajjar and S. T. Tarzami (2010). "Effects of CXCR4 gene transfer on cardiac function after ischemia-reperfusion injury." Am J Pathol **176**(4): 1705-1715.
- Cheng, Z., L. Ou, X. Zhou, F. Li, X. Jia, Y. Zhang, X. Liu, Y. Li, C. A. Ward, L. G. Melo and D. Kong (2008). "Targeted migration of mesenchymal stem cells modified with CXCR4 gene to infarcted myocardium improves cardiac performance." Mol Ther **16**(3): 571-579.
- Cheng, Z. J., J. Zhao, Y. Sun, W. Hu, Y. L. Wu, B. Cen, G. X. Wu and G. Pei (2000). "beta-arrestin differentially regulates the chemokine receptor CXCR4-mediated signaling and receptor internalization, and this implicates multiple interaction sites between beta-arrestin and CXCR4." J Biol Chem **275**(4): 2479-2485.
- Chu, P. Y., J. Mariani, S. Finch, J. R. McMullen, J. Sadoshima, T. Marshall and D. M. Kaye (2010). "Bone marrow-derived cells contribute to fibrosis in the chronically failing heart." Am J Pathol **176**(4): 1735-1742.
- Cottler-Fox, M. H., T. Lapidot, I. Petit, O. Kollet, J. F. DiPersio, D. Link and S. Devine (2003). "Stem cell mobilization." Hematology Am Soc Hematol Educ Program: 419-437.
- Cowie, M. R., D. A. Wood, A. J. Coats, S. G. Thompson, P. A. Poole-Wilson, V. Suresh and G. C. Sutton (1999). "Incidence and aetiology of heart failure; a population-based study." Eur Heart J **20**(6): 421-428.
- Dai, S., F. Yuan, J. Mu, C. Li, N. Chen, S. Guo, J. Kingery, S. D. Prabhu, R. Bolli and G. Rokosh (2010). "Chronic AMD3100 antagonism of SDF-1alpha-CXCR4

- exacerbates cardiac dysfunction and remodeling after myocardial infarction." J Mol Cell Cardiol **49**(4): 587-597.
- De La Luz Sierra, M., F. Yang, M. Narazaki, O. Salvucci, D. Davis, R. Yarchoan, H. H. Zhang, H. Fales and G. Tosato (2004). "Differential processing of stromal-derived factor-1alpha and stromal-derived factor-1beta explains functional diversity." Blood **103**(7): 2452-2459.
- Delgado, R. M., 3rd and J. T. Willerson (1999). "Pathophysiology of heart failure: a look at the future." Tex Heart Inst J **26**(1): 28-33.
- Dickstein, K., A. Cohen-Solal, G. Filippatos, J. J. McMurray, P. Ponikowski, P. A. Poole-Wilson, A. Stromberg, D. J. van Veldhuisen, D. Atar, A. W. Hoes, A. Keren, A. Mebazaa, M. Nieminen, S. G. Priori, K. Swedberg, A. Vahanian, J. Camm, R. De Caterina, V. Dean, C. Funck-Brentano, I. Hellemans, S. D. Kristensen, K. McGregor, U. Sechtem, S. Silber, M. Tendera, P. Widimsky and J. L. Zamorano (2008). "ESC Guidelines for the diagnosis and treatment of acute and chronic heart failure 2008: the Task Force for the Diagnosis and Treatment of Acute and Chronic Heart Failure 2008 of the European Society of Cardiology. Developed in collaboration with the Heart Failure Association of the ESC (HFA) and endorsed by the European Society of Intensive Care Medicine (ESICM)." Eur Heart J **29**(19): 2388-2442.
- Dimmeler, S., J. Burchfield and A. M. Zeiher (2008). "Cell-based therapy of myocardial infarction." Arterioscler Thromb Vasc Biol **28**(2): 208-216.
- Dobaczewski, M. and N. G. Frangogiannis (2009). "Chemokines and cardiac fibrosis." Front Biosci (Schol Ed) **1**: 391-405.
- Elmadbouh, I., H. Haider, S. Jiang, N. M. Idris, G. Lu and M. Ashraf (2007). "Ex vivo delivered stromal cell-derived factor-1alpha promotes stem cell homing and induces angiomyogenesis in the infarcted myocardium." J Mol Cell Cardiol **42**(4): 792-803.
- Fazel, S., M. Cimini, L. Chen, S. Li, D. Angoulvant, P. Fedak, S. Verma, R. D. Weisel, A. Keating and R. K. Li (2006). "Cardioprotective c-kit+ cells are from the bone marrow and regulate the myocardial balance of angiogenic cytokines." J Clin Invest **116**(7): 1865-1877.
- Fernandez-Aviles, F., J. A. San Roman, J. Garcia-Frade, M. E. Fernandez, M. J. Penarrubia, L. de la Fuente, M. Gomez-Bueno, A. Cantalapiedra, J. Fernandez, O. Gutierrez, P. L. Sanchez, C. Hernandez, R. Sanz, J. Garcia-Sancho and A. Sanchez (2004). "Experimental and clinical regenerative capability of human bone marrow cells after myocardial infarction." Circ Res **95**(7): 742-748.
- Fox, K. F., M. R. Cowie, D. A. Wood, A. J. Coats, J. S. Gibbs, S. R. Underwood, R. M. Turner, P. A. Poole-Wilson, S. W. Davies and G. C. Sutton (2001). "Coronary artery disease as the cause of incident heart failure in the population." Eur Heart J **22**(3): 228-236.
- Frey, N. and E. N. Olson (2003). "Cardiac hypertrophy: the good, the bad, and the ugly." Annu Rev Physiol **65**: 45-79.
- Gao, H., W. Priebe, J. Glod and D. Banerjee (2009). "Activation of signal transducers and activators of transcription 3 and focal adhesion kinase by stromal cell-derived factor 1 is required for migration of human mesenchymal stem cells in response to tumor cell-conditioned medium." Stem Cells **27**(4): 857-865.
- Ghadge, S. K., S. Muhlstedt, C. Ozcelik and M. Bader (2010). "SDF-1alpha as a therapeutic stem cell homing factor in myocardial infarction." Pharmacol Ther.
- Gleichmann, M., C. Gillen, M. Czardybon, F. Bosse, R. Greiner-Petter, J. Auer and H. W. Muller (2000). "Cloning and characterization of SDF-1gamma, a novel

- SDF-1 chemokine transcript with developmentally regulated expression in the nervous system." *Eur J Neurosci* **12**(6): 1857-1866.
- Gnecchi, M., H. He, O. D. Liang, L. G. Melo, F. Morello, H. Mu, N. Noiseux, L. Zhang, R. E. Pratt, J. S. Ingwall and V. J. Dzau (2005). "Paracrine action accounts for marked protection of ischemic heart by Akt-modified mesenchymal stem cells." *Nat Med* **11**(4): 367-368.
- Gnecchi, M., Z. Zhang, A. Ni and V. J. Dzau (2008). "Paracrine mechanisms in adult stem cell signaling and therapy." *Circ Res* **103**(11): 1204-1219.
- Grove, J. E., E. Bruscia and D. S. Krause (2004). "Plasticity of bone marrow-derived stem cells." *Stem Cells* **22**(4): 487-500.
- Gupta, S., B. Das and S. Sen (2007). "Cardiac hypertrophy: mechanisms and therapeutic opportunities." *Antioxid Redox Signal* **9**(6): 623-652.
- Haider, H., S. Jiang, N. M. Idris and M. Ashraf (2008). "IGF-1-overexpressing mesenchymal stem cells accelerate bone marrow stem cell mobilization via paracrine activation of SDF-1alpha/CXCR4 signaling to promote myocardial repair." *Circ Res* **103**(11): 1300-1308.
- Hattori, K., B. Heissig, K. Tashiro, T. Honjo, M. Tateno, J. H. Shieh, N. R. Hackett, M. S. Quitarano, R. G. Crystal, S. Rafii and M. A. Moore (2001). "Plasma elevation of stromal cell-derived factor-1 induces mobilization of mature and immature hematopoietic progenitor and stem cells." *Blood* **97**(11): 3354-3360.
- Heissig, B., K. Hattori, S. Dias, M. Friedrich, B. Ferris, N. R. Hackett, R. G. Crystal, P. Besmer, D. Lyden, M. A. Moore, Z. Werb and S. Rafii (2002). "Recruitment of stem and progenitor cells from the bone marrow niche requires MMP-9 mediated release of kit-ligand." *Cell* **109**(5): 625-637.
- Hernandez, P. A., R. J. Gorlin, J. N. Lukens, S. Taniuchi, J. Bohinjec, F. Francois, M. E. Klotman and G. A. Diaz (2003). "Mutations in the chemokine receptor gene CXCR4 are associated with WHIM syndrome, a combined immunodeficiency disease." *Nat Genet* **34**(1): 70-74.
- Hierlihy, A. M., P. Seale, C. G. Lobe, M. A. Rudnicki and L. A. Megeney (2002). "The post-natal heart contains a myocardial stem cell population." *FEBS Lett* **530**(1-3): 239-243.
- Horwitz, E. M. (2003). "Stem cell plasticity: the growing potential of cellular therapy." *Arch Med Res* **34**(6): 600-606.
- Hu, X., S. Dai, W. J. Wu, W. Tan, X. Zhu, J. Mu, Y. Guo, R. Bolli and G. Rokosh (2007). "Stromal cell derived factor-1 alpha confers protection against myocardial ischemia/reperfusion injury: role of the cardiac stromal cell derived factor-1 alpha CXCR4 axis." *Circulation* **116**(6): 654-663.
- Hunt, S. A., W. T. Abraham, M. H. Chin, A. M. Feldman, G. S. Francis, T. G. Ganiats, M. Jessup, M. A. Konstam, D. M. Mancini, K. Michl, J. A. Oates, P. S. Rahko, M. A. Silver, L. W. Stevenson and C. W. Yancy (2009). "2009 focused update incorporated into the ACC/AHA 2005 Guidelines for the Diagnosis and Management of Heart Failure in Adults: a report of the American College of Cardiology Foundation/American Heart Association Task Force on Practice Guidelines: developed in collaboration with the International Society for Heart and Lung Transplantation." *Circulation* **119**(14): e391-479.
- Jackson, G., C. R. Gibbs, M. K. Davies and G. Y. Lip (2000). "ABC of heart failure. Pathophysiology." *BMJ* **320**(7228): 167-170.
- Jiang, Y., B. N. Jahagirdar, R. L. Reinhardt, R. E. Schwartz, C. D. Keene, X. R. Ortiz-Gonzalez, M. Reyes, T. Lenvik, T. Lund, M. Blackstad, J. Du, S. Aldrich, A. Lisberg, W. C. Low, D. A. Largaespada and C. M. Verfaillie (2002).

- "Pluripotency of mesenchymal stem cells derived from adult marrow." Nature **418**(6893): 41-49.
- Kajstura, J., A. Leri, N. Finato, C. Di Loreto, C. A. Beltrami and P. Anversa (1998). "Myocyte proliferation in end-stage cardiac failure in humans." Proc Natl Acad Sci U S A **95**(15): 8801-8805.
- Kajstura, J., M. Rota, B. Whang, S. Cascapera, T. Hosoda, C. Bearzi, D. Nurzynska, H. Kasahara, E. Zias, M. Bonafe, B. Nadal-Ginard, D. Torella, A. Nascimbene, F. Quaini, K. Urbanek, A. Leri and P. Anversa (2005). "Bone marrow cells differentiate in cardiac cell lineages after infarction independently of cell fusion." Circ Res **96**(1): 127-137.
- Kang, P. M. and S. Izumo (2000). "Apoptosis and heart failure: A critical review of the literature." Circ Res **86**(11): 1107-1113.
- Kawabata, K., M. Ujikawa, T. Egawa, H. Kawamoto, K. Tachibana, H. Iizasa, Y. Katsura, T. Kishimoto and T. Nagasawa (1999). "A cell-autonomous requirement for CXCR4 in long-term lymphoid and myeloid reconstitution." Proc Natl Acad Sci U S A **96**(10): 5663-5667.
- Kawamoto, A., H. C. Gwon, H. Iwaguro, J. I. Yamaguchi, S. Uchida, H. Masuda, M. Silver, H. Ma, M. Kearney, J. M. Isner and T. Asahara (2001). "Therapeutic potential of ex vivo expanded endothelial progenitor cells for myocardial ischemia." Circulation **103**(5): 634-637.
- Kehat, I., D. Kenyagin-Karsenti, M. Snir, H. Segev, M. Amit, A. Gepstein, E. Livne, O. Binah, J. Itskovitz-Eldor and L. Gepstein (2001). "Human embryonic stem cells can differentiate into myocytes with structural and functional properties of cardiomyocytes." J Clin Invest **108**(3): 407-414.
- Kinnaird, T., E. Stabile, M. S. Burnett, M. Shou, C. W. Lee, S. Barr, S. Fuchs and S. E. Epstein (2004). "Local delivery of marrow-derived stromal cells augments collateral perfusion through paracrine mechanisms." Circulation **109**(12): 1543-1549.
- Koch, K. C., W. M. Schaefer, E. A. Liehn, C. Rammos, D. Mueller, J. Schroeder, T. Dimassi, T. Stopinski and C. Weber (2006). "Effect of catheter-based transendocardial delivery of stromal cell-derived factor 1alpha on left ventricular function and perfusion in a porcine model of myocardial infarction." Basic Res Cardiol **101**(1): 69-77.
- Kocher, A. A., M. D. Schuster, M. J. Szabolcs, S. Takuma, D. Burkhoff, J. Wang, S. Homma, N. M. Edwards and S. Itescu (2001). "Neovascularization of ischemic myocardium by human bone-marrow-derived angioblasts prevents cardiomyocyte apoptosis, reduces remodeling and improves cardiac function." Nat Med **7**(4): 430-436.
- Kucia, M., B. Dawn, G. Hunt, Y. Guo, M. Wysoczynski, M. Majka, J. Ratajczak, F. Rezzoug, S. T. Ildstad, R. Bolli and M. Z. Ratajczak (2004). "Cells expressing early cardiac markers reside in the bone marrow and are mobilized into the peripheral blood after myocardial infarction." Circ Res **95**(12): 1191-1199.
- Kucia, M., K. Jankowski, R. Reza, M. Wysoczynski, L. Bandura, D. J. Allendorf, J. Zhang, J. Ratajczak and M. Z. Ratajczak (2004). "CXCR4-SDF-1 signalling, locomotion, chemotaxis and adhesion." J Mol Histol **35**(3): 233-245.
- Kucia, M., J. Ratajczak, R. Reza, A. Janowska-Wieczorek and M. Z. Ratajczak (2004). "Tissue-specific muscle, neural and liver stem/progenitor cells reside in the bone marrow, respond to an SDF-1 gradient and are mobilized into peripheral blood during stress and tissue injury." Blood Cells Mol Dis **32**(1): 52-57.

- Lapidot, T., A. Dar and O. Kollet (2005). "How do stem cells find their way home?" Blood **106**(6): 1901-1910.
- Lapidot, T. and I. Petit (2002). "Current understanding of stem cell mobilization: the roles of chemokines, proteolytic enzymes, adhesion molecules, cytokines, and stromal cells." Exp Hematol **30**(9): 973-981.
- Laugwitz, K. L., A. Moretti, J. Lam, P. Gruber, Y. Chen, S. Woodard, L. Z. Lin, C. L. Cai, M. M. Lu, M. Reth, O. Platoshyn, J. X. Yuan, S. Evans and K. R. Chien (2005). "Postnatal isl1+ cardioblasts enter fully differentiated cardiomyocyte lineages." Nature **433**(7026): 647-653.
- Leone, A. M., S. Rutella, G. Bonanno, A. M. Contemi, D. G. de Ritis, M. B. Giannico, A. G. Rebuzzi, G. Leone and F. Crea (2006). "Endogenous G-CSF and CD34+ cell mobilization after acute myocardial infarction." Int J Cardiol **111**(2): 202-208.
- Leri, A., J. Kajstura and P. Anversa (2005). "Cardiac stem cells and mechanisms of myocardial regeneration." Physiol Rev **85**(4): 1373-1416.
- Levesque, J. P., J. Hendy, Y. Takamatsu, P. J. Simmons and L. J. Bendall (2003). "Disruption of the CXCR4/CXCL12 chemotactic interaction during hematopoietic stem cell mobilization induced by G-CSF or cyclophosphamide." J Clin Invest **111**(2): 187-196.
- Levesque, J. P., J. Hendy, Y. Takamatsu, B. Williams, I. G. Winkler and P. J. Simmons (2002). "Mobilization by either cyclophosphamide or granulocyte colony-stimulating factor transforms the bone marrow into a highly proteolytic environment." Exp Hematol **30**(5): 440-449.
- Levesque, J. P., F. Liu, P. J. Simmons, T. Betsuyaku, R. M. Senior, C. Pham and D. C. Link (2004). "Characterization of hematopoietic progenitor mobilization in protease-deficient mice." Blood **104**(1): 65-72.
- Levesque, J. P., Y. Takamatsu, S. K. Nilsson, D. N. Haylock and P. J. Simmons (2001). "Vascular cell adhesion molecule-1 (CD106) is cleaved by neutrophil proteases in the bone marrow following hematopoietic progenitor cell mobilization by granulocyte colony-stimulating factor." Blood **98**(5): 1289-1297.
- Liles, W. C., H. E. Broxmeyer, E. Rodger, B. Wood, K. Hubel, S. Cooper, G. Hangoc, G. J. Bridger, G. W. Henson, G. Calandra and D. C. Dale (2003). "Mobilization of hematopoietic progenitor cells in healthy volunteers by AMD3100, a CXCR4 antagonist." Blood **102**(8): 2728-2730.
- Lusso, P. (2006). "HIV and the chemokine system: 10 years later." EMBO J **25**(3): 447-456.
- Luster, A. D. (1998). "Chemokines--chemotactic cytokines that mediate inflammation." N Engl J Med **338**(7): 436-445.
- Ma, Q., D. Jones, P. R. Borghesani, R. A. Segal, T. Nagasawa, T. Kishimoto, R. T. Bronson and T. A. Springer (1998). "Impaired B-lymphopoiesis, myelopoiesis, and derailed cerebellar neuron migration in CXCR4- and SDF-1-deficient mice." Proc Natl Acad Sci U S A **95**(16): 9448-9453.
- Ma, Q., D. Jones and T. A. Springer (1999). "The chemokine receptor CXCR4 is required for the retention of B lineage and granulocytic precursors within the bone marrow microenvironment." Immunity **10**(4): 463-471.
- Maltsev, V. A., J. Rohwedel, J. Hescheler and A. M. Wobus (1993). "Embryonic stem cells differentiate in vitro into cardiomyocytes representing sinusnodal, atrial and ventricular cell types." Mech Dev **44**(1): 41-50.
- McMurray, J. J. and M. A. Pfeffer (2005). "Heart failure." Lancet **365**(9474): 1877-1889.

- Menendez, P., M. D. Caballero, F. Prosper, M. C. Del Canizo, J. A. Perez-Simon, M. V. Mateos, M. J. Nieto, M. Corral, M. Romero, J. Garcia-Conde, M. A. Montalban, J. F. San Miguel and A. Orfao (2002). "The composition of leukapheresis products impacts on the hematopoietic recovery after autologous transplantation independently of the mobilization regimen." Transfusion **42**(9): 1159-1172.
- Misao, Y., G. Takemura, M. Arai, T. Ohno, H. Onogi, T. Takahashi, S. Minatoguchi, T. Fujiwara and H. Fujiwara (2006). "Importance of recruitment of bone marrow-derived CXCR4+ cells in post-infarct cardiac repair mediated by G-CSF." Cardiovasc Res **71**(3): 455-465.
- Morimoto, H., M. Takahashi, Y. Shiba, A. Izawa, H. Ise, M. Hongo, K. Hatake, K. Motoyoshi and U. Ikeda (2007). "Bone marrow-derived CXCR4+ cells mobilized by macrophage colony-stimulating factor participate in the reduction of infarct area and improvement of cardiac remodeling after myocardial infarction in mice." Am J Pathol **171**(3): 755-766.
- Morrison, S. J., D. E. Wright and I. L. Weissman (1997). "Cyclophosphamide/granulocyte colony-stimulating factor induces hematopoietic stem cells to proliferate prior to mobilization." Proc Natl Acad Sci U S A **94**(5): 1908-1913.
- Mouquet, F., O. Pfister, M. Jain, A. Oikonomopoulos, S. Ngoy, R. Summer, A. Fine and R. Liao (2005). "Restoration of cardiac progenitor cells after myocardial infarction by self-proliferation and selective homing of bone marrow-derived stem cells." Circ Res **97**(11): 1090-1092.
- Murdoch, C. (2000). "CXCR4: chemokine receptor extraordinaire." Immunol Rev **177**: 175-184.
- Murphy, P. M., M. Baggiolini, I. F. Charo, C. A. Hebert, R. Horuk, K. Matsushima, L. H. Miller, J. J. Oppenheim and C. A. Power (2000). "International union of pharmacology. XXII. Nomenclature for chemokine receptors." Pharmacol Rev **52**(1): 145-176.
- Murry, C. E., M. H. Soonpaa, H. Reinecke, H. Nakajima, H. O. Nakajima, M. Rubart, K. B. Pasumarthi, J. I. Virag, S. H. Bartelmez, V. Poppa, G. Bradford, J. D. Dowell, D. A. Williams and L. J. Field (2004). "Haematopoietic stem cells do not transdifferentiate into cardiac myocytes in myocardial infarcts." Nature **428**(6983): 664-668.
- Nagasawa, T., S. Hirota, K. Tachibana, N. Takakura, S. Nishikawa, Y. Kitamura, N. Yoshida, H. Kikutani and T. Kishimoto (1996). "Defects of B-cell lymphopoiesis and bone-marrow myelopoiesis in mice lacking the CXC chemokine PBSF/SDF-1." Nature **382**(6592): 635-638.
- Nagasawa, T., T. Nakajima, K. Tachibana, H. Iizasa, C. C. Bleul, O. Yoshie, K. Matsushima, N. Yoshida, T. A. Springer and T. Kishimoto (1996). "Molecular cloning and characterization of a murine pre-B-cell growth-stimulating factor/stromal cell-derived factor 1 receptor, a murine homolog of the human immunodeficiency virus 1 entry coreceptor fusin." Proc Natl Acad Sci U S A **93**(25): 14726-14729.
- Nygren, J. M., S. Jovinge, M. Breitbach, P. Sawen, W. Roll, J. Hescheler, J. Taneera, B. K. Fleischmann and S. E. Jacobsen (2004). "Bone marrow-derived hematopoietic cells generate cardiomyocytes at a low frequency through cell fusion, but not transdifferentiation." Nat Med **10**(5): 494-501.
- Oh, H., S. B. Bradfute, T. D. Gallardo, T. Nakamura, V. Gausson, Y. Mishina, J. Pocius, L. H. Michael, R. R. Behringer, D. J. Garry, M. L. Entman and M. D. Schneider (2003). "Cardiac progenitor cells from adult myocardium: homing,



- differentiation, and fusion after infarction." Proc Natl Acad Sci U S A **100**(21): 12313-12318.
- Onai, N., Y. Zhang, H. Yoneyama, T. Kitamura, S. Ishikawa and K. Matsushima (2000). "Impairment of lymphopoiesis and myelopoiesis in mice reconstituted with bone marrow-hematopoietic progenitor cells expressing SDF-1-intrakin." Blood **96**(6): 2074-2080.
- Orlic, D., J. Kajstura, S. Chimenti, I. Jakoniuk, S. M. Anderson, B. Li, J. Pickel, R. McKay, B. Nadal-Ginard, D. M. Bodine, A. Leri and P. Anversa (2001). "Bone marrow cells regenerate infarcted myocardium." Nature **410**(6829): 701-705.
- Papayannopoulou, T. (2000). "Mechanisms of stem-/progenitor-cell mobilization: the anti-VLA-4 paradigm." Semin Hematol **37**(1 Suppl 2): 11-18.
- Papayannopoulou, T. (2004). "Current mechanistic scenarios in hematopoietic stem/progenitor cell mobilization." Blood **103**(5): 1580-1585.
- Papayannopoulou, T. and B. Nakamoto (1993). "Peripheralization of hemopoietic progenitors in primates treated with anti-VLA4 integrin." Proc Natl Acad Sci U S A **90**(20): 9374-9378.
- Papayannopoulou, T., G. V. Priestley, H. Bonig and B. Nakamoto (2003). "The role of G-protein signaling in hematopoietic stem/progenitor cell mobilization." Blood **101**(12): 4739-4747.
- Papayannopoulou, T., G. V. Priestley and B. Nakamoto (1998). "Anti-VLA4/VCAM-1-induced mobilization requires cooperative signaling through the kit/mkit ligand pathway." Blood **91**(7): 2231-2239.
- Peled, A., O. Kollet, T. Ponomaryov, I. Petit, S. Franitza, V. Grabovsky, M. M. Slav, A. Nagler, O. Lider, R. Alon, D. Zipori and T. Lapidot (2000). "The chemokine SDF-1 activates the integrins LFA-1, VLA-4, and VLA-5 on immature human CD34(+) cells: role in transendothelial/stromal migration and engraftment of NOD/SCID mice." Blood **95**(11): 3289-3296.
- Pelus, L. M., D. Horowitz, S. C. Cooper and A. G. King (2002). "Peripheral blood stem cell mobilization. A role for CXC chemokines." Crit Rev Oncol Hematol **43**(3): 257-275.
- Penn, M. S., M. Zhang, I. Deglurkar and E. J. Topol (2004). "Role of stem cell homing in myocardial regeneration." Int J Cardiol **95 Suppl 1**: S23-25.
- Percherancier, Y., Y. A. Berchiche, I. Slight, R. Volkmer-Engert, H. Tamamura, N. Fujii, M. Bouvier and N. Heveker (2005). "Bioluminescence resonance energy transfer reveals ligand-induced conformational changes in CXCR4 homo- and heterodimers." J Biol Chem **280**(11): 9895-9903.
- Petit, I., M. Szyper-Kravitz, A. Nagler, M. Lahav, A. Peled, L. Habler, T. Ponomaryov, R. S. Taichman, F. Arenzana-Seisdedos, N. Fujii, J. Sandbank, D. Zipori and T. Lapidot (2002). "G-CSF induces stem cell mobilization by decreasing bone marrow SDF-1 and up-regulating CXCR4." Nat Immunol **3**(7): 687-694.
- Phillips, R. J., M. D. Burdick, K. Hong, M. A. Lutz, L. A. Murray, Y. Y. Xue, J. A. Belperio, M. P. Keane and R. M. Strieter (2004). "Circulating fibrocytes traffic to the lungs in response to CXCL12 and mediate fibrosis." J Clin Invest **114**(3): 438-446.
- Pitchford, S. C., R. C. Furze, C. P. Jones, A. M. Wengner and S. M. Rankin (2009). "Differential mobilization of subsets of progenitor cells from the bone marrow." Cell Stem Cell **4**(1): 62-72.
- Pittenger, M. F. and B. J. Martin (2004). "Mesenchymal stem cells and their potential as cardiac therapeutics." Circ Res **95**(1): 9-20.
- Pool, P. E. (1998). "Neurohormonal activation in the treatment of congestive heart failure: basis for new treatments?" Cardiology **90**(1): 1-7.

- Proulx, C., V. El-Helou, H. Gosselin, R. Clement, M. A. Gillis, L. Villeneuve and A. Calderone (2007). "Antagonism of stromal cell-derived factor-1alpha reduces infarct size and improves ventricular function after myocardial infarction." *Pflugers Arch* **455**(2): 241-250.
- Pyo, R. T., J. Sui, A. Dhume, J. Palomeque, B. C. Blaxall, G. Diaz, J. Tunstead, D. E. Logothetis, R. J. Hajjar and A. D. Schecter (2006). "CXCR4 modulates contractility in adult cardiac myocytes." *J Mol Cell Cardiol* **41**(5): 834-844.
- Rafii, S., B. Heissig and K. Hattori (2002). "Efficient mobilization and recruitment of marrow-derived endothelial and hematopoietic stem cells by adenoviral vectors expressing angiogenic factors." *Gene Ther* **9**(10): 631-641.
- Ratajczak, M. Z., E. Zuba-Surma, M. Kucia, R. Reza, W. Wojakowski and J. Ratajczak (2006). "The pleiotropic effects of the SDF-1-CXCR4 axis in organogenesis, regeneration and tumorigenesis." *Leukemia* **20**(11): 1915-1924.
- Sasaki, T., R. Fukazawa, S. Ogawa, S. Kanno, T. Nitta, M. Ochi and K. Shimizu (2007). "Stromal cell-derived factor-1alpha improves infarcted heart function through angiogenesis in mice." *Pediatr Int* **49**(6): 966-971.
- Saxena, A., J. E. Fish, M. D. White, S. Yu, J. W. Smyth, R. M. Shaw, J. M. DiMaio and D. Srivastava (2008). "Stromal cell-derived factor-1alpha is cardioprotective after myocardial infarction." *Circulation* **117**(17): 2224-2231.
- Schuh, A., E. A. Liehn, A. Sasse, M. Hristov, R. Sobota, M. Kelm, M. W. Merx and C. Weber (2008). "Transplantation of endothelial progenitor cells improves neovascularization and left ventricular function after myocardial infarction in a rat model." *Basic Res Cardiol* **103**(1): 69-77.
- Segers, V. F. and R. T. Lee (2008). "Stem-cell therapy for cardiac disease." *Nature* **451**(7181): 937-942.
- Segers, V. F., T. Tokunou, L. J. Higgins, C. MacGillivray, J. Gannon and R. T. Lee (2007). "Local delivery of protease-resistant stromal cell derived factor-1 for stem cell recruitment after myocardial infarction." *Circulation* **116**(15): 1683-1692.
- Shen, H., T. Cheng, I. Olszak, E. Garcia-Zepeda, Z. Lu, S. Herrmann, R. Fallon, A. D. Luster and D. T. Scadden (2001). "CXCR-4 desensitization is associated with tissue localization of hemopoietic progenitor cells." *J Immunol* **166**(8): 5027-5033.
- Shiba, Y., M. Takahashi, T. Hata, H. Murayama, H. Morimoto, H. Ise, T. Nagasawa and U. Ikeda (2009). "Bone marrow CXCR4 induction by cultivation enhances therapeutic angiogenesis." *Cardiovasc Res* **81**(1): 169-177.
- Shiels, H. A. and E. White (2008). "The Frank-Starling mechanism in vertebrate cardiac myocytes." *J Exp Biol* **211**(Pt 13): 2005-2013.
- Shirozu, M., T. Nakano, J. Inazawa, K. Tashiro, H. Tada, T. Shinohara and T. Honjo (1995). "Structure and chromosomal localization of the human stromal cell-derived factor 1 (SDF1) gene." *Genomics* **28**(3): 495-500.
- Shizuru, J. A., R. S. Negrin and I. L. Weissman (2005). "Hematopoietic stem and progenitor cells: clinical and preclinical regeneration of the hematolymphoid system." *Annu Rev Med* **56**: 509-538.
- Sierro, F., C. Biben, L. Martinez-Munoz, M. Mellado, R. M. Ransohoff, M. Li, B. Woehl, H. Leung, J. Groom, M. Batten, R. P. Harvey, A. C. Martinez, C. R. Mackay and F. Mackay (2007). "Disrupted cardiac development but normal hematopoiesis in mice deficient in the second CXCL12/SDF-1 receptor, CXCR7." *Proc Natl Acad Sci U S A* **104**(37): 14759-14764.

- Smart, N. and P. R. Riley (2008). "The stem cell movement." Circ Res **102**(10): 1155-1168.
- Spiegel, A., O. Kollet, A. Peled, L. Abel, A. Nagler, B. Biorai, G. Rechavi, J. Vormoor and T. Lapidot (2004). "Unique SDF-1-induced activation of human precursor-B ALL cells as a result of altered CXCR4 expression and signaling." Blood **103**(8): 2900-2907.
- Strauer, B. E., M. Brehm, T. Zeus, M. Kosterling, A. Hernandez, R. V. Sorg, G. Kogler and P. Wernet (2002). "Repair of infarcted myocardium by autologous intracoronary mononuclear bone marrow cell transplantation in humans." Circulation **106**(15): 1913-1918.
- Sun, Y., Z. Cheng, L. Ma and G. Pei (2002). "Beta-arrestin2 is critically involved in CXCR4-mediated chemotaxis, and this is mediated by its enhancement of p38 MAPK activation." J Biol Chem **277**(51): 49212-49219.
- Sweeney, E. A., H. Lortat-Jacob, G. V. Priestley, B. Nakamoto and T. Papayannopoulou (2002). "Sulfated polysaccharides increase plasma levels of SDF-1 in monkeys and mice: involvement in mobilization of stem/progenitor cells." Blood **99**(1): 44-51.
- Tang, J., J. Wang, H. Song, Y. Huang, J. Yang, X. Kong, L. Guo, F. Zheng and L. Zhang (2009). "Adenovirus-mediated stromal cell-derived factor-1 alpha gene transfer improves cardiac structure and function after experimental myocardial infarction through angiogenic and antifibrotic actions." Mol Biol Rep **37**(4): 1957-1969.
- Tang, Y. L., W. Zhu, M. Cheng, L. Chen, J. Zhang, T. Sun, R. Kishore, M. I. Phillips, D. W. Losordo and G. Qin (2009). "Hypoxic preconditioning enhances the benefit of cardiac progenitor cell therapy for treatment of myocardial infarction by inducing CXCR4 expression." Circ Res **104**(10): 1209-1216.
- Tavor, S., I. Petit, S. Porozov, A. Avigdor, A. Dar, L. Leider-Trejo, N. Shemtov, V. Deutsch, E. Naparstek, A. Nagler and T. Lapidot (2004). "CXCR4 regulates migration and development of human acute myelogenous leukemia stem cells in transplanted NOD/SCID mice." Cancer Res **64**(8): 2817-2824.
- To, L. B., D. N. Haylock, P. J. Simmons and C. A. Juttner (1997). "The biology and clinical uses of blood stem cells." Blood **89**(7): 2233-2258.
- Tomita, S., R. K. Li, R. D. Weisel, D. A. Mickle, E. J. Kim, T. Sakai and Z. Q. Jia (1999). "Autologous transplantation of bone marrow cells improves damaged heart function." Circulation **100**(19 Suppl): II247-256.
- Townson, D. H. and A. R. Liptak (2003). "Chemokines in the corpus luteum: implications of leukocyte chemotaxis." Reprod Biol Endocrinol **1**: 94.
- Vaday, G. G. and O. Lider (2000). "Extracellular matrix moieties, cytokines, and enzymes: dynamic effects on immune cell behavior and inflammation." J Leukoc Biol **67**(2): 149-159.
- van Empel, V. P., A. T. Bertrand, L. Hofstra, H. J. Crijns, P. A. Doevendans and L. J. De Windt (2005). "Myocyte apoptosis in heart failure." Cardiovasc Res **67**(1): 21-29.
- Vandervelde, S., M. J. van Luyn, R. A. Tio and M. C. Harmsen (2005). "Signaling factors in stem cell-mediated repair of infarcted myocardium." J Mol Cell Cardiol **39**(2): 363-376.
- Vasa, M., S. Fichtlscherer, K. Adler, A. Aicher, H. Martin, A. M. Zeiher and S. Dimmeler (2001). "Increase in circulating endothelial progenitor cells by statin therapy in patients with stable coronary artery disease." Circulation **103**(24): 2885-2890.

- Verfaillie, C. M. (2002). "Hematopoietic stem cells for transplantation." Nat Immunol **3**(4): 314-317.
- Vila-Coro, A. J., J. M. Rodriguez-Frade, A. Martin De Ana, M. C. Moreno-Ortiz, A. C. Martinez and M. Mellado (1999). "The chemokine SDF-1alpha triggers CXCR4 receptor dimerization and activates the JAK/STAT pathway." FASEB J **13**(13): 1699-1710.
- Wong, D. and W. Korz (2008). "Translating an Antagonist of Chemokine Receptor CXCR4: from bench to bedside." Clin Cancer Res **14**(24): 7975-7980.
- Wright, D. E., E. P. Bowman, A. J. Wagers, E. C. Butcher and I. L. Weissman (2002). "Hematopoietic stem cells are uniquely selective in their migratory response to chemokines." J Exp Med **195**(9): 1145-1154.
- Yamaguchi, J., K. F. Kusano, O. Masuo, A. Kawamoto, M. Silver, S. Murasawa, M. Bosch-Marce, H. Masuda, D. W. Losordo, J. M. Isner and T. Asahara (2003). "Stromal cell-derived factor-1 effects on ex vivo expanded endothelial progenitor cell recruitment for ischemic neovascularization." Circulation **107**(9): 1322-1328.
- Yamani, M. H., N. B. Ratliff, D. J. Cook, E. M. Tuzcu, Y. Yu, R. Hobbs, G. Rincon, C. Bott-Silverman, J. B. Young, N. Smedira and R. C. Starling (2005). "Peritransplant ischemic injury is associated with up-regulation of stromal cell-derived factor-1." J Am Coll Cardiol **46**(6): 1029-1035.
- Yu, L., J. Cecil, S. B. Peng, J. Schrementi, S. Kovacevic, D. Paul, E. W. Su and J. Wang (2006). "Identification and expression of novel isoforms of human stromal cell-derived factor 1." Gene **374**: 174-179.
- Zamilpa, R. and M. L. Lindsey "Extracellular matrix turnover and signaling during cardiac remodeling following MI: Causes and consequences." J Mol Cell Cardiol **48**(3): 558-563.
- Zaruba, M. M., H. D. Theiss, M. Vallaster, U. Mehl, S. Brunner, R. David, R. Fischer, L. Krieg, E. Hirsch, B. Huber, P. Nathan, L. Israel, A. Imhof, N. Herbach, G. Assmann, R. Wanke, J. Mueller-Hoecker, G. Steinbeck and W. M. Franz (2009). "Synergy between CD26/DPP-IV inhibition and G-CSF improves cardiac function after acute myocardial infarction." Cell Stem Cell **4**(4): 313-323.
- Zelis, R., L. I. Sinoway, U. Leuenberger, B. S. Clemson and D. Davis (1991). "Time-constant adaptations in heart failure." Eur Heart J **12 Suppl C**: 2-7.
- Zhang, M., N. Mal, M. Kiedrowski, M. Chacko, A. T. Askari, Z. B. Popovic, O. N. Koc and M. S. Penn (2007). "SDF-1 expression by mesenchymal stem cells results in trophic support of cardiac myocytes after myocardial infarction." FASEB J **21**(12): 3197-3207.
- Zhao, T., D. Zhang, R. W. Millard, M. Ashraf and Y. Wang (2009). "Stem cell homing and angiomyogenesis in transplanted hearts are enhanced by combined intramyocardial SDF-1alpha delivery and endogenous cytokine signaling." Am J Physiol Heart Circ Physiol **296**(4): H976-986.
- Zou, Y. R., A. H. Kottmann, M. Kuroda, I. Taniuchi and D. R. Littman (1998). "Function of the chemokine receptor CXCR4 in haematopoiesis and in cerebellar development." Nature **393**(6685): 595-599.

## 8. Appendix

### 8.1. Abbreviations

Ang II	Angiotensin II
ANP	Atrial natriuretic peptide
AP	Alkaline phosphatase
APS	Ammonium persulfate
ASCs	Adult stem cells
BAC	Bacterial Artificial Chromosome
BM	Bone marrow
BMSCs	Bone marrow derived stem cells
BNP	Brain natriuretic peptide
BSA	Bovine serum albumin
cDNA	Complementary DNA
cKO	Cardiac knock out
CMV	Cytomagalovirus
CSCc	Cardiac stem cells
Cy	Cyclophosphamide
DEPC	Diethylpyrocarbonate
DMSO	Dimethyl sulfoxide
DNA	Deoxyribonucleic acid
DNase	Deoxyribonuclease
dNTP	Deoxynucleotide triphosphate
ECHO	Echocardiography
ECL	Enhanced chemiluminescence
EDTA	Ethylenediamine-tetraacetic acid
EF	Ejection fraction
EPCs	Endothelial progenitor cells
ESCs	Embryonic stem cells
FS	Fractional shortening
GAPDH	Glyceraldehyde 3-phosphate dehydrogenase
G-CSF	Granulocyte colony stimulating factor
GFP	Green Fluorescence Protein
G-PCR	G protein–coupled receptor

G418	Geneticin
HGF	Hepatocyte growth factor
HIF-1 $\alpha$	Hypoxia inducing factor-1 alpha
HRP	Horseradish Peroxidase
HPCs	Hematopoietic stem cells
IGF-1	Insulin growth factor-1
IL	Interleukin
IVS	Intraventricular septal thickness
KO	Knock out
LV	Left ventricular
LVd	Left ventricular diastole
LVPWd	Left ventricular posterior wall in diastole
MCP-1	Monocyte chemoattractant protein-1
MI	Myocardial Infarction
MIP-1	Macrophage inflammatory protein
MLC2	Myosin light chain-2
MMPs	Matrix metalloproteinases
mRNA	Messenger RNA
MSCc	Mesenchymal stem cells
NILV	Non-infracted left ventricular hypertrophy
PAGE	Polyacrylamide gel electrophoresis
PB	Peripheral blood
PBS	Phosphate buffered saline
PCR	Polymerase chain reaction
PFA	Paraformaldehyde
rpm	Rotations per minute
RT	Room temperature
RT-PCR	Reverse transcription polymerase chain reaction
SCF	Stem cell factor
SEM	Standard error of the mean
SDF-1 $\alpha$	Stromal cell derived factor-1 alpha
SDS	Sodium dodecyl sulfate
Taq	Thermus aquaticus

TAE	Tris/Acetate/EDTA
TE	Tris EDTA buffer
TEMED	N,N,N',N'-Tetramethylethylenediamine
Tris	Tris(hydroxymethyl)aminomethane
UV	Ultraviolet light
VCAM	Vascular cell adhesion molecule-1
VEGF	Vascular endothelial growth factor
WB	Western blot
WT	Wild type

-

## **9. Curriculum Vitae**

For reasons of data protection,  
the curriculum vitae is not included in the online version



## **Publications**

Ghadge SK, Mühlstedt S, Ozcelik C, Bader M. SDF-1 $\alpha$  as therapeutic stem cell homing factor in myocardial infarction. *Journal of Pharmacology & Therapeutics*, Oct 2010.

Panek AN, Posch MG, Alenina N, Ghadge SK, Erdmann B, Popova E, Perrot A, Geier C, Dietz R, Morano I, Bader M, Ozcelik C. Connective tissue growth factor overexpression in cardiomyocytes promotes cardiac hypertrophy and protection against pressure overload. *PLoS One*. 2009 Aug 25;4(8):e6743.

Posch MG, Panek A, Kersten A, Ghadge SK, Geier C, Richter S, Perrot A, Gailani M, Dietz R, Lüftner D, Ozcelik C. Plasma HER2 levels are not associated with cardiac function or hypertrophy in control subjects and heart failure patients. *Int J Cardiol*. 2009 Jun 18.

## 10. Acknowledgements

I take this opportunity to acknowledge my deep sense of gratitude and indebtedness towards those who have helped me in this project. First and foremost, I sincerely thank to my mentors Dr. Cemil Özcelik and Prof. Michael Bader for trusting me with the PhD work and introducing me especially in the field of cardiovascular science. Their systematic guidance, excellent technical support, criticism and invaluable inputs were making this project possible and successful.

I would like to thank Prof. Udo Heinemann for agreeing to be the head of my PhD thesis at the Free University of Berlin.

I owe my heartfull thanks to Fatimunnisa Qadri for performing the immunohistological work for my doctoral studies.

I am grateful to Larissa Vilianovitch, who has been helpful in generating a knockout mouse model.

I am gratefull to Tanja Schalow, Astrid Schiche, Martin Taube, Ariane Giese, Sina Wohlfart for providing excellent technical help throughout my PhD work.

I also thank my fellow colleagues Anna Panek, Silke Mühlstedt, Andreas Perrot, Maximilian Posch, who have been helpful and their enthusiastic encouragement in doing things in the best possible way.

I thank to all the staff members of Prof. Michael Bader and Dr. Cemil Özcelik for the fun-time and pleasant working environment at MDC.

I thank to every soul who has helped in one or the other ways in making this project a great success.

I am indebted to my wife, Sandhya Dilip Kumar, for believing in my abilities and encouraging me in the time of need. You have been a source of constant strength in my life.

Although it's not possible to express in words, finally I thank my parents and my family from the bottom of my heart for their unconditional love and constant support. Without your support and belief I wouldn't have been able to succeed in my studies.

## **11. Eidesstattliche Erklärung**

Hiermit versichere ich, die vorliegende Dissertation selbstständig und ohne unerlaubte Hilfe angefertigt zu haben.

Bei der Verfassung der Dissertation wurden keine anderen als die im Text aufgeführten Hilfsmittel verwendet.

Ein Promotionsverfahren wurde zu keinem früheren Zeitpunkt an einer anderen Hochschule oder bei einem anderen Fachbereich beantragt.

**Berlin, Dec, 2010**